DEVELOPMENT OF A SOLAR AIR-CONDITIONING SYSTEM IN SAUDI ARABIA

BY

ALI ABDULAZIZ AL-UGLA

A Dissertation Presented to the

DEANSHIP OF GRADUATE STUDIES

KING FAHD UNIVERSITY OF PETROLEUM & MINERALS

DHAHRAN, SAUDI ARABIA

In Partial Fulfillment of the
Requirements for the Degree of

DOCTOR OF PHILOSOPHY

In

Mechanical Engineering

DECEMBER 2015

In the name of Allah, the Most Gracious and the Most Merciful

KING FAHD UNIVERSITY OF PETROLEUM AND MINERALS

DHAHRAN 31261, SAUDI ARABIA

DEANSHIP OF GRADUATE STUDIES

This thesis, written by Ali Abdulaziz Al-Ugla under the direction of his thesis advisor and approved by his thesis committee, has been presented to and accepted by the Dean of Graduate Studies, in partial fulfillment of the requirements for the degree of DOCTOR OF PHILOSOPHY IN MECHANICAL ENGINEERING.

Maged El-Shaarawi 9th December, 2015

Dr. Maged A. I. El-Shaarawi (Advisor)

Dr. Zuhair M. Gasem

(Department Chairman)

Dr. Syed A.M. Said (Member)

Dr. Salam A. Zummo

(Dean of Graduate Studies)

20/12/15

Date

Dr. Amro M. Al-.Qutub (Member)

Dr. Habib Abulhamayel (Member)

Dr. Mohamed A. Antar (Member)

This Dissertation is

Dedicated to

My Beloved Parents and

My Wife for their prayers,

encouragement and

patience

ACKNOWLEDGMENTS

All praise and thanks are due to Allah, my creator, for his immense beneficence and endless blessings to complete this work. Subsequently, I would like to extend my thanks to KFUPM for the extensive support I received during my program through university extraordinary facilities and for the opportunity I granted to pursue my graduate studies and for providing excellent research opportunities and a healthy academic environment.

Thereafter, with deep appreciation and gratitude, I acknowledge the valuable time, the inspiration, encouragement, continuous guidance, suggestions and motivation given to me by my dissertation advisor, Dr. Maged A.I. El-Shaarawi. Moreover, Dr. Maged A.I. El-Shaarawi powerful support towards this study was a major achievement to me. I am also thankful to my Committee member, Dr. Syed A. M. Said, Dr. Amro Al-Qutub, Dr. Habib Abulhamayel and Dr. Mohamed A. Antar for their positive direction, suggestions support and motivation.

My sincere gratitude is due to my parents for their guidance, moral support and prayers during my educational time. Their advice, to strive for excellence has enabled all this research achievable. I am also grateful to my wife who supported me through the last stage of completing my research.

Special thanks are due to my senior colleague, Dr. Fahad Al-Amri, for his usual support and motivation to complete this program. My thanks are also extended to my colleagues in the Mechanical Engineering Department for their help and prayers.

TABLE OF CONTENTS

LIST OF TABLES

LIST OF FIGURES

LIST OF SYMBOLS AND ABBREVIATIONS

A	:	Area (m^2)
COP	:	Coefficient of Performance
COP_s	:	Solar Coefficient of Performance
kW_p	:	kilowatt-peak (peak output of a photovoltaic system)
h	:	enthalpy (kJ/kg)
I	:	Incident Solar radiation, (kWh/m^2) on horizontal surface
m	:	mass (kg)
$\dot{m}$	:	mass flow rate (kg/s)
NPV	:	net present value ($)
PBP	:	payback period (Year)
PV	:	photovoltaic
Q_{CS}	:	Cold thermal energy stored in the cold storage tank (kWh)
Q_E	:	heat added to refrigerant in evaporator (kWh)
Q_{ED}	:	heat added to refrigerant in evaporator at daytime for cold storage system (kWh)
Q_G	:	heat input to generator (kWh)
Q_{Gd}	:	heat input to generator at daytime for heat storage system (kWh)
Q_{Gn}	:	heat input to generator at nighttime from heat storage system (kWh)
Q_{hs}	:	heat storage tank (kWh)

Q_{rf}	:	thermal energy stored in the refrigerant tank (kWh)
RCECS	:	Ratio of cooling effect for nighttime by cold storage (%)
RCEHS	:	Ratio of cooling effect for nighttime by heat storage (%)
T	:	temperature (°C)
VC	:	Vapor Compression
W	:	pump work (kWh)
x	:	mass concentration of water (refrigerant) in the solution per unit mass of solution; kg_{H2O} / $kg_{solution}$
y	:	mass concentration of LiBr (absorbent) in the solution per unit mass of solution; y = 1-x, $kg_{LiBr}/kg_{solution}$

Greek symbols

ε	:	effectiveness
η	:	efficiency

Subscripts

c	:	collector
cond	:	condenser
cs	:	cold storage
E	:	environment
e	:	evaporator
ex	:	exit from the excess heat storage tank
f	:	solar collectors' working fluid exit temperature
g	:	generator
gn	:	generator at nighttime

HE	:	heat exchanger
hs	:	heat storage
II	:	second law
in	:	inlet to the excess heat storage tank
n	:	night time
P	:	pump
r	:	refrigerant
rch	:	refrigerant/cold hybrid system
rhch	:	refrigerant/heat/cold hybrid system
rhh	:	refrigerant/heat hybrid system
rs	:	refrigerant storage
rsc	:	refrigerant storage for hybrid cold-refrigerant storage system
rsh	:	refrigerant storage for hybrid heat-refrigerant storage system
rshc	:	refrigerant storage for hybrid heat-cold-refrigerant storage system
ss	:	strong refrigerant-absorbent solution (strong solution)
ws	:	weak refrigerant-absorbent solution (weak solution)
1-10	:	system state points

ABSTRACT

NAME: **ALI ABDULAZIZ AL-UGLA**

TITLE: **DEVELOPMENT OF A SOLAR AIR-CONDITIONING SYSTEM IN SAUDI ARABIA**

MAJOR FIELD: **MECHANICAL ENGINEERING**

DATE OF DEGREE: **DECEMBER 2015**

The air-conditioning systems in Saudi Arabia consume around 65% of the electrical energy of the building sector. The conventional (vapor-compression) air-conditioning types are the most used systems in Saudi Arabia. Solar energy can be used to power such systems to save a large amount of electrical/mechanical energy which can be employed in the industry and production sectors. This research focuses on the design of solar air-conditioning application in buildings in Saudi Arabia to accommodate a 24-hour uninterrupted daily cooling load. It includes an in-depth review of novel alternative solar-powered LiBr-water absorption designs of three storage systems and four hybrid storage systems. This review is followed by the unsteady analysis of hybrid storage (cold plus refrigerant) system for 5 kW absorption chiller. Moreover, techno-economic analysis for three systems: conventional vapor-compression, solar absorption and solar photovoltaic vapor-compression for commercial buildings are investigated. The techno-economic results showed that solar absorption system is more feasible than solar photovoltaic vapor-compression system. The thermodynamic results revealed that the best designs are the refrigerant storage system and the cold and refrigerant hybrid storage system. Finally, the results indicated that the coefficient of performance decreases at the start and end of the effective sunlight.

ARABIC ABSTRACT

ملخص الرسالة

الاسم: علي عبدالعزيز العقلا

عنوان الرسالة: تطوير نظام تكييف الهواء عن طريق الطاقه الشمسيه في المملكه العربيه السعوديه

التخصص: الهندسة الميكانيكية

تأريخ التخرج: ديسمبر 2015

أنظمة تكييف الهواء في المملكة العربية السعودية تستهلك ما يقرب من ٦٥٪ من الطاقة الكهربائية في قطاع المباني. معظم أنظمة تكييف الهواء المستخدمة في المملكة العربية السعودية هي من النوع التقليدي (ضغط البخار). استخدام الطاقة الشمسية لتشغيل هذه النظم سوف يعمل على حفظ كمية كبيرة من الطاقة (الكهربائيه / الميكانيكية) التي يمكن استخدامها من قبل القطاعات الصناعية والإنتاجية. يركز هذا البحث على تصميم أنظمة تكييف الهواء بالطاقة الشمسية في المباني في المملكة العربية السعودية لاستيعاب حمولة التبريد اليومي على مدار 24 ساعة دون انقطاع. يشمل هذا البحث على دراسه متعمقة لتطوير تصاميم جديدة بديلة تعمل بالطاقة الشمسية عن طريق ثلاثة أنظمة تخزين وأربعة أنظمة تخزين مجتمعه. يلي ذلك تحليل متعمق لتصميم ٥ كيلو واط طاقة تبريد لنظام التخزين المجتمع عند حالة تباين الاوضاع الحراريه. تم في هذا البحث دراسة التحاليل الفنيه والاقتصاديه لثلاثة أنظمة: نظام ضغط البخار التقليدي، ونظام الامتصاص بالطاقة الشمسية ونظام ضغط البخار الكهروضوئي في المباني التجاريه. أظهرت النتائج الفنية والاقتصادية ان نظام الامتصاص بالطاقة الشمسية هو أكثر جدوى من ضغط البخار الكهروضوئي. كشفت النتائج الحرارية أن أفضل التصاميم هي نظام التخزين المكثف و نظام التخزين المجتمع البارد مع المكثف . وأخيرا ، أشارت النتائج أن معامل الأداء ينخفض في بداية و نهاية أشعة الشمس.

CHAPTER 1

INTRODUCTION

The extreme cooling demand in Saudi Arabia is a direct outcome of hot weather conditions. The ambient temperature in Saudi Arabia reaches 46 ∘C at night in summer [1], hence, it is essential to use air-conditioning in all life fields; mainly in the building sector such as residential, commercial and industrial buildings. Currently, almost all the air-conditioning generated in Saudi Arabia is by means of conventional, vapor-compression, systems. These systems are driven by the electrical energy which is produced by burning fossil fuel. If this electrical energy is saved, it can be effectively used in other sectors such as industrial application. The non-industrial sector consumes nearly 81% of the total electrical energy produced in Saudi Arabia as shown in figure 1-1 [2]. Approximately 65% of this energy is consumed by air conditioning systems [3]. Hence, air conditioning systems alone are consuming 53% of the total electrical energy produced by Saudi Electrical Company SEC.

At the current growth rate, the future domestic power demand is predicted to increase to 71 GW and 120 GW by 2020 and 2030 respectively as shown in figure 1-2 [4]. The projected electricity demand in the next two decades will require an increase in fossil fuel local consumption to about 8.3 Million Barrel/Day [4]. Therefore, it is critical to consider the utilization of innovative solutions such as solar cooling as almost all the air-conditioning systems in Saudi Arabia are vapor-compression.

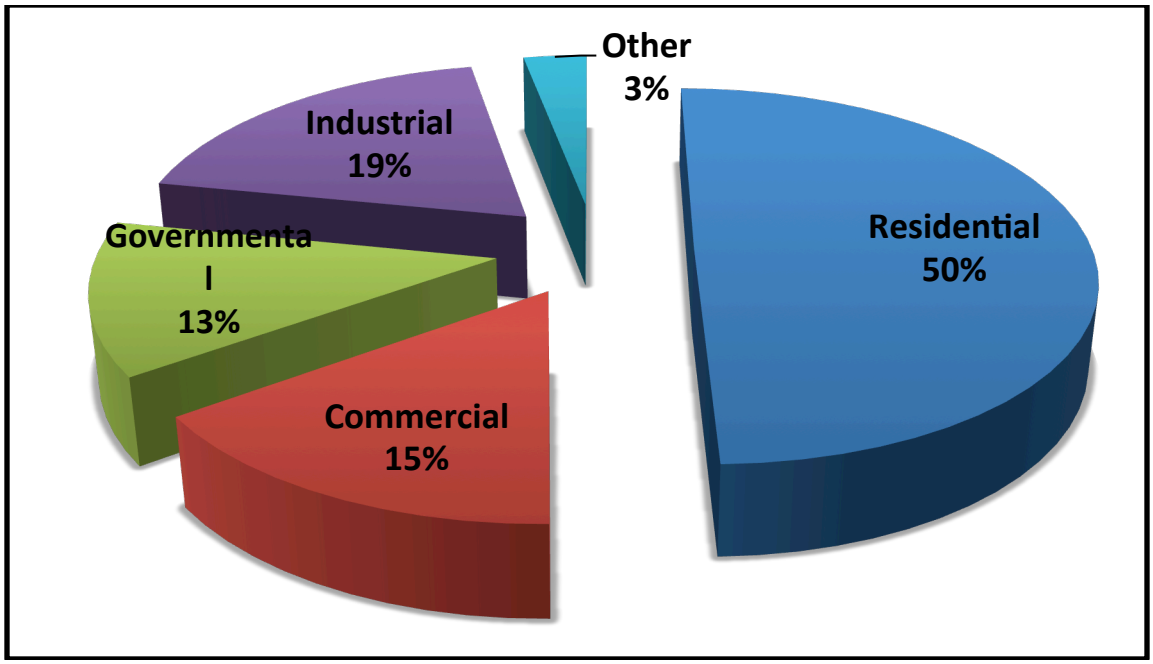

Figure 1-1 Saudi Arabia Electrical Power Demand Distribution [2]

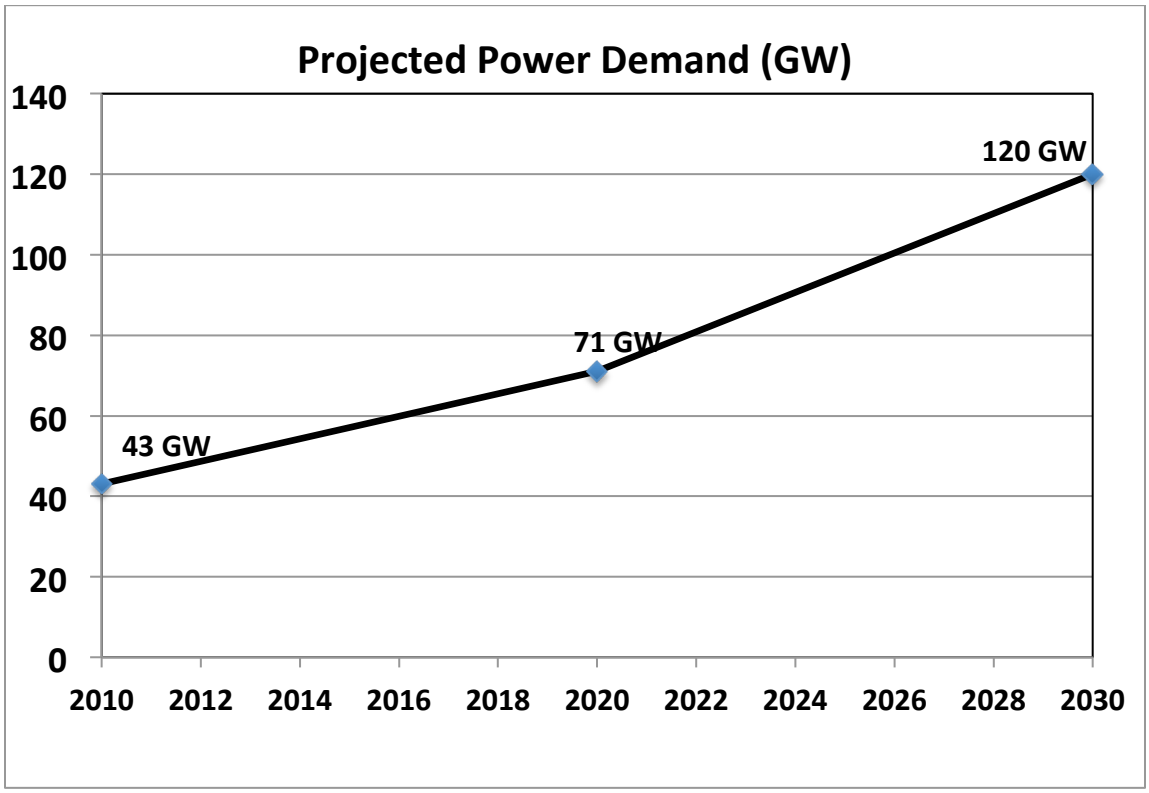

Figure 1-2 Projected Growth in Saudi Arabia Domestic Power Demand [4]

The environmental effects of carbon dioxide are currently of significant interest. Energy consumption in various sectors is the main source of CO_2 emission. The increase of carbon dioxide emission has major negative impact on the environment. According to the World Bank, Saudi Arabia emits close to 1.4 % of the world CO_2 emission as shown in Table 1-1 [5, 6]. The table shows that the rate of CO_2 emissions is high. The use of solar air-conditioning system will reduce the emission of carbon dioxide which will have positive impact on the environment. The average amount of CO_2 emission that can be reduced when using solar energy is about 392 CO_2/kWh of electricity [7].

Table 1-1 CO2 emissions in Saudi Arabia [5, 6]

Country	**Annual CO2 Emissions (kt)**	**Per Capita (t)**	**% of World Total**
Saudi Arabia	464,481	17.04	1.38%

The development for a technology of alternative source of energy to run air-conditioning systems is highly recommended in order to utilize the electrical energy generated from the fossil fuels in the production sector, industry, rather than the consumption sector such as comfort conditioning. These air-conditioning systems can assist in the reduction of CO_2 carbon emission which will reduce the global warming effects and the environmental pollution. Moreover, these air-conditioning systems can considerably share the load of electrical-energy produced by burning fossil fuel. Out of various renewable sources of energy, solar energy can be the greatest candidate for air-conditioning due to the coincidence of the greatest solar radiation input with the period of maximum cooling load.

Solar energy has other main benefits such as its purity and natural availability. The total solar radiation transmitted to the earth is approximately 1.74 x 10^{17} W [8]. On the other hand, the total consumed energy of the world is approximately 1.84 x 10^{13} W [9]. Thus, solar energy can be effectively utilized as potential renewable energy source for the total world energy. Solar energy can be used to generate air-conditioning system in two methods. In the first method, solar energy can be converted into electricity using photo-voltaic modules which can be used to operate a conventional, vapor-compression, air-conditioning system. In the second method, solar energy can be used to provide heat in the generator, working-fluid, of a vapor sorption (absorption or adsorption) system. In the absorption system, the waste heat rejected to the surrounding or the heat gained by solar collectors (solar energy) can be used by the generator of absorption refrigeration systems. This research will analyze in-depth on Solar Absorption Air Conditioning Systems.

1.1 Solar Energy Projects in Saudi Arabia

Saudi Arabia has invested in several solar energy projects in the recent years as shown in Table 1-2. Table 1-2 shows the completed projects, its size, owner and completion date. On other hand, there are still ongoing projects as shown in Table 1-3. As shown in both tables, the total size of completed and under construction projects are approximately 160 MW.

Table 1-2 Completed Solar Energy Projects in Saudi Arabia [10]

No.	Project Name	Project Size	Owner	Completed
1	Saudi Aramco Solar Car Park	10.5 MW	Saudi Aramco	2012
2	Princess Noura Bint Abul Rahman University	25 MWth	Princess Noura Bint Abdulrahman University for Women	2012
3	King Abdulaziz International Airport Development Project	5.4 MW	General Authority of Civil Aviation (GACA)	2013
4	KAPSARC project	3.5 MW	Saudi Aramco	2013
5	KAUST Solar Park	2 MW	Saudi Aramco	2010
6	Pilot project	500 kW	Saudi Electricity Company (SEC) and Showa Shell Sekiyu	2011
7	King Abdullah Financial District project	200 kW	KAUST	2012

Table 1-3 Ongoing Solar Energy Projects in Saudi Arabia [10]

No.	Project Name	Project Size	Owner	Date
1	Solar Energy Project	100 MW	Makkah	2018
2	Al Khafji plant	10 MW	-	2015
3	KAPSARC II project	1.8 MW	Saudi Aramco	2014

The main issues that may have impact on the development of solar energy system in Saudi Arabia are the extreme high ambient temperature that could decrease the efficiency of PV cells, dust which may have a drop of system performance, and water cleaning for collectors which require water consumption which is limited in Saudi Arabia.

1.2 Solar Absorption Systems

In the absorption air conditioning system, a heat source drives the cooling process. Absorption cooling can be considered an alternative to conventional air conditioning if excess heat is available, such as heat from the sun which is applicable in Saudi Arabia. Absorption air conditioning systems are commercially available and used in air conditioning applications since the 1950s. It can reduce the peaks in a building's electric load and can be designed for cooling loads ranging on the residential scale of a few kilowatts to the megawatt industrial scale.

The main difference between vapor compression and absorption system is that the compressor is replaced by absorber, generator and pump. In term of performance, absorption systems can be categorized into one of the following three types:

- Single Effect: COP 0.6 to 0.8
- Double Effect: COP 1.0 to 1.2
- Triple Effect COP 1.4 to 1.6

The coefficient of performance (COP) is used to measure the performance of cooling systems. The main benefits of absorption systems are:

- Vibration-free
- Longer life-time
- High reliability
- Low maintenance
- Energy Saving

The major working refrigerant pairs employed for solar absorption systems are LiBr-H_2O and H_2O-NH_3. Most researches confirm that the coefficient of performance (COP) is higher for Lithium-bromide water compared to other working fluids. The cost of LiBr-H_2O is low and its performance is high which make it the favorable candidate for use in solar air conditioning cycles. However, it cannot be used in sub-zero cooling application. The ammonia-water system has the following disadvantages when compared to Lithium-bromide water system [11].

- The coefficient of performance (COP) for the ammonia-water system is lower than that for the Lithium-bromide water system.
- Ammonia-water requires a higher generator inlet temperature which results in the H_2O-NH_3 cooling systems achieving a lower COP.
- Ammonia-water requires higher pumping power and pressures.
- Ammonia-water is a more complex system to separate ammonia and water vapor at the generator outlet using a rectifier.
- It causes hazards associated which results in the restrictions in-building applications of cooling units.

From the above points, the lithium bromide-water system is considered the suitable working fluid for solar absorption air-conditioning applications. The major components of Lithium-bromide water solar air-conditioning systems are chillers and solar collectors.

An overview of the available technologies, such as open cooling cycles and closed thermal driven cooling cycles (e.g., adsorption, absorption) future developments, was described in [12]. The up to date of application and installations of solar assisted air-conditioning in Europe were presented [12]. If the systems are properly designed, solar assisted air conditioning can lead to extraordinary primary energy savings. It is essential to maximize the use of solar thermal energy by supplying other services that require heat such as domestic hot water systems with the solar heat as far as possible in order to optimize the economics. Improvements in the performance of thermally driven chillers and open cooling cycles play a key role in order to approach economic feasibility.

Storage can be used in absorption cooling systems to increase the effectiveness of the system and meet continuous operation (24-hour a day). The two common strategies exist for the storage are [12]:

1. Heat storage tank that stores excess solar heat, which is then used later if needed.

2. Cold storage tank stores the excess cooling potential and is used if the present cold production of the chiller is insufficient to meet the cooling load.

These two methods can be used in combination or individually. The average coefficient of performance (COP) of LiBr-water chiller, single-effect, is below 1.0, which means that storage downstream of the chiller (cold tank) is necessarily smaller than an equivalent storage upstream of the chiller (hot tank). This indicates that the hot storage tank must be larger than the cold storage tank to provide corresponding cooling energy storage.

The hot water storage tank is used in the heat storage system to order to decrease the losses in the exchange of thermal energy. The hot storage tank helps in addressing the fluctuating heat availability by allowing the storage of excess heat for later use when heat is not sufficient [12].

The cold storage can be incorporated, similarly to the addition of the hot storage tank, in order to store cooling effect at the period of high radiation for use at the period when the available solar energy is insufficient to meet the cooling demand. The cooling load reaches a peak in the afternoon or evening times while solar intensity reach a peak in the solar noon time. Thus, the storage system is designed to meet the cooling load for numbers of hours [12].

CHAPTER 2

LITERATURE REVIEW

This chapter presents the comprehensive assessment on the latest researches in the field of solar air-conditioning. The literature review is presenting mainly the techno-economic comparison of different solar air-conditioning systems, techno-economic analysis of solar thermal air-conditioning systems, technical analysis and simulation of solar absorption air-conditioning systems and experimental work done for solar absorption air-conditioning systems.

2.1 Techno-economic Comparison of Different Solar Air-Conditioning Systems

In the field of the economic and technical comparison of different solar air-conditionings, there are several studies that have been done. Enibe [13] highlighted that the system cost is the main barrier for PV-powered refrigeration. The solar cell efficiencies have increased recently from 7 to 13%, and the unit costs have decreased, however, the overall system cost of the vapor-compression refrigeration is still below the overall system cost of the PV-powered refrigeration. Therefore, solar absorption refrigeration systems are candidate selection in the development of small communities particularly those are away from the electrical net. Fong et al. [14] conducted comparative study for subtropical city for five solar cooling systems types: solar absorption refrigeration, solar PV-vapor compression refrigeration, solar mechanical

compression refrigeration, solar adsorption refrigeration and solar solid desiccant cooling. The results showed that the energy saving is higher for solar PV-vapor compression refrigeration and solar absorption refrigeration in the subtropical Hong Kong.

Karagiorgas et al. [15] performed the analysis for five renewable energy technologies: solar PV, solar thermal, solar passive, geothermal energy and biomass. The analysis conducted in parallel for five Europe regions: Sicily, East Attica, Alpes-Andalusia, Maritimes and Madeira. The project HOTRES aimed outlook enormous applications of the renewable energy developments in industry. The objective of this study is to show the technical–economic results attained of the applicable broad technical support project in 200 hotels. The shortest payback period refers to the solar thermal. The payback period varies from 1.7 years in Greece up to 19 years in France for the solar thermal. On the other hand, it varies from 6 years in Spain up to 43 years in Greece for the solar PV. Kim and Ferreira [16] presented the comparison analysis of solar thermal refrigeration and solar Photo-voltaic refrigeration systems in term of energy efficiency and economic feasibility. The results indicated that solar Photo-voltaic refrigeration systems are more expensive than solar thermal systems.

Mokhtar et al. [17] analyzed several technologies of solar cooling. The methodology is based on assessing the performance of each solar cooling technology as a system taking into account cost, performance parameters and weather and cooling demand. The assessment was applied to 25 solar cooling technologies based on the

climatic conditions and cooling demand time series of Abu Dhabi, UAE. The results showed that large-scale cooling plant options are the most economical. On a smaller scale, Fresnel concentrators and thin film PV cells are the most economically viable. However, in terms of overall efficiency, the multi-crystalline PV cells with vapor compression chillers were the most efficient option of all. Kohlenbach and Dennis [18] showed the current and future outlook of solar cooling in Australia. The current potential of energy by using alternative solar air-conditioning systems was discussed. The lifetime cost is lower for solar thermal cooling system than the solar photovoltaic cooling system. However, both systems have higher lifetime costs than a conventional vapor-compression system. The solar thermal cooling is more economic than the solar photovoltaic cooling if the electricity rate is below $0.28/kWh. The solar photovoltaic system becomes the most economic cooling alternative if the electricity rate exceeds $0.54/ kWh. The solar thermal system becomes more economic than a conventional system for electricity rate above of $0.67/kWh. Hartmann et al. [19] presented a comparison of solar thermal and solar electric cooling for a typical small office building exposed to two different European climates (Freiburg and Madrid). A parametric study on collector and storage size was carried out for the solar thermal system to reach achieve the minimal cost per unit of primary energy saved. The grid coupled PV system led to lower costs of primary energy savings than the solar thermal system at both locations. The presumed macroeconomic advantages of the solar thermal system, due to the non-usage of energy during peak demand, can be confirmed for Madrid.

Arias-Varela et al. [20] presented a system design of absorption refrigeration to conserve sea food to communities lack the source of conventional energy using evacuated tube solar collectors. Initially, solar energy refrigeration is more expensive, however, they have the same cost at twenty three years of operation. When the lifetime exceeds twenty-three years, the conventional refrigeration will be more expensive. Florides et al. [21] developed TRNSYS simulation of an absorption solar cooling system that consists of 15 m^2 (CPC) compound parabolic solar-collector, LiBr–water absorption refrigerator of 11 kW, storage tank and boiler. The total life cycle cost for 20 years of the complete system will be £13,380. The cost of the absorption system will be £4800. The results showed that the absorption system is economically competitive compared to conventional cooling systems when its capital cost is below £2000.

Zettel [22] provided a framework for public power utilities that are interested in alternatives to conventional HVAC systems. The review focused on the reduction of peak demand while simultaneously deriving the majority of the energy needed to operate the HVAC system from a renewable resource, the sun. The initial installation costs of the SAAC (Solar-Assisted Absorption Chilling) system are nearly 9 times that of a conventional system. The small SAAC systems are being installed for approximately $9,000/ton without gas fired backup, while the conventional packaged units are installed for approximately $1,000/ton. As evident by the 15 year net present value (NPV) of both systems, the SAAC is not cost competitive on a life cycle basis. This is mainly due to the high cost of initial installation. In order to break even with the conventional technology, the installed cost of the above SAAC system would need to equal approximately

$4,300/ton. At this price level, the savings realized from reduced electricity, natural gas, and capacity usage render SAAC as a commercially competitive product. Shekarchiana et al. [23] investigated the energy cost per unit area and the required energy for cooling per unit area for air conditioning systems in Iran. Also they investigated the impact of the coefficient of performance (COP) of absorption systems on cost saving. It was found that using absorption systems will increase the energy usage per unit area; however, the energy cost per unit area will decrease. For each 0.1 increment in COP of absorption systems, there is at least $ 50/m^2 saved cost.

Pietruschka et al. [24] compared different solar thermal cooling systems to a PV driven and a net connected compression chiller in hot and dry southern climate for an office building project in Cairo Egypt. Four different systems are studied: single-effect, double-effect and triple-effect absorption systems and a PV driven compression chiller. The single effect reaches efficiency of 40% where double and triple effects reach to 31% and 27%. The COP is 0.7, 1.31 and 1.83 for single, double and triple effects. The triple effect has the highest primary energy ratio of 1.6 while the single effect has the lowest ratio of 1.43. Chemisana et al. [25] presented a comparison between two cooling systems for a specific three-floor building, with and without solar concentration. The first is a conventional system which consists of evacuated tube collectors feeding a single-effect absorption system. On the other hand, a Fresnel reflective solar concentrating system is coupled to a double-effect absorption system. The results showed an important reduction of the solar collectors' absorber area in the concentrating system compared with the standard solar thermal installation. However, the solar concentrating system requires a

large aperture area. The rejected heat in the double-effect chiller is lower which lead to significant reduction of the investment and operation costs of the solar concentrating cooling system.

Otanicar et al. [26] described an economical comparison of thermally and electrically solar cooling driven. It was discussed the comparison of the initial costs of each technology and future costs of solar electric and solar thermal systems. The system cost for solar photovoltaic cooling is highly dependent on the system coefficient of performance (COP) when photovoltaic (PV) prices remain at the current levels, however, when prices are lowered the effect of the coefficient of performance (COP) becomes diminished. The cost of solar collection for solar thermal cooling is much lower as overall cost percentage while the cost of the refrigeration system often represents a higher percentage of the cost. The cost of the PV cooling is projected to be decreased much more than the solar thermal cooling over the next 20 years due to the relatively stable cost of collection and storage of the solar thermal cooling. Fong et al. [27] analyzed the performance of solar cooling systems with building integrated (BI) solar-collectors. Two types (flat-plate collectors for absorption refrigeration and the PV panels for DC-driven vapor compression refrigeration) were used in the analysis. It was found that in both cases, the adoption of BI solar collectors resulted in a higher primary energy consumption even though the zone loads were reduced. If energy saving potential considered, the system performance with the BI flat-plate type collectors made them technically infeasible. The use of BI solar collectors in solar cooling systems should be restricted only to situations where the availability of the roof was limited or insufficient when

applied in sub-tropical regions like Hong Kong. Asdrubali et al. [28] conducted comparative analysis, by the University of Perugia, of solar cooling systems to assess their potentialities, and to indicate the qualities and limitations of each system for market introduction. The analysis showed that the solar cooling technology is mature to become a replacement to the high level of electric consumption due to the high summer cooling demand.

Abdulateef et al. [29] performed an economical assessment for a solar cooling system based on life-cycle savings for Malaysia and similar regions. The system consists of 70 m^2 evacuated tube solar collectors and ammonia-water absorption unit. The prospects of solar cooling are expected to further improve with the growth of solar industry and the escalation of fuel cost. Thomas and Andre [30] built a simulation that can analyze precisely the energy consumption of an air conditioning system using a solar driven absorption chiller, the rejection system, solar panels field, storage devices, heater, pumps, heating-cooling, networks, emission system and building. The simulation features were defined closely to real-life operation (typical European office building); almost all air-conditioning devices have their parameters taken in manufacturers' data sheets.

Casals [31] analyzed the first commercial solar heating and cooling implemented recently in Spain. Limited effective storage capacity should be compensated as far as possible with appropriate design choices. The operating strategies with this objective, like maintaining building air conditioning in non working days to store cooling energy in the building structure should be also considered. The solar absorption cooling may be loosing

its market chance because of the long time that it is taking to give an appropriate answer to its costs and its technical limitations. Centralized solar cooling is close to become available and present significant cost and other advantages.

Shahin [32] investigated the effect of dust on solar photovoltaic systems in Saudi Arabia. It was indicated that the dust led to 10 – 15 % efficiency loss in one month in case there is no cleaning. Moreover, it was illustrated that the dust has effect by 5 - 7.5% unavoidable energy loss of power plant. The decrease in solar energy efficiency due to dust storms was measured to be 60%. It was concluded that the dust effect on performance varies per location and per technology. It was recommended that photovoltaic systems in Saudi Arabia need models for frequency of cleaning.

Concentrator photovoltaic (CPV) uses lenses and curved mirrors to direct sunlight onto small multi-junction solar cells. CPV systems use solar trackers to increase the system efficiency. This technology requires less photovoltaic material, has higher efficiency and its optical system comprises standard materials [33]. However, in 2013 CPV installations accounted for only 0.1% or 50 megawatts (MW) of the annual global PV market of nearly 39,000 MW. The main challenge of CPV is to compete with flat-plate PV modules on cost, in light of the recent drop in flat-plate PV module prices. CPV companies expect that this technology can compete with flat-plate PV when installed in sunny areas, but the road to scale has been difficult [34].

2.2 Techno-economic Analysis for Solar Thermal Air-conditioning Systems

Several techno-economic studies have been conducted for solar thermal air-conditioning systems. Tsoutsos et al. [35] conducted an economic analysis for solar absorption cooling system and solar adsorption system. The study showed that absorption system is cheaper than adsorption system by 50 % in term of capital cost. The analysis demonstrated that solar cooling systems are better suited to replacing conventional air-conditioners in remote areas, where there is no connection with the electricity grid and where the conventional fuel used is gas. Younes et al. [36] studied a Lithium-Bromide absorption machine viewing the amount of fuel used in the last years for air-conditioning systems. The effect of absorption machine in saving a large amount of fuel was discussed. The results showed that the absorption machine requires 6 years and eight month to retain its costs with an annual payback of $120,000. However, the absorption machine and its equipment are more expensive than the centrifugal machine and its equipment. The time back decreases as the absorption machine power increases.

Calise [37] presented dynamic modeling of a solar heating and cooling system and studied detailed optimization of its thermo-economic performance. A detailed case study was developed and discussed, in which hourly, monthly and yearly results are presented. The system under investigation, designed to provide 20% of the maximum cooling load by of solar source. It was capable to achieve a significant primary energy saving of 64.7%. In order to get a satisfactory economic performance of the SHC system, a possible public feed-in tariff was considered. The Payback is approximately 12 years.

Obviously, without any economic public contribution, the Pay Back periods would be much longer than the system operating life. Cleveland et al. [38] provided a model to outline financial options for commercial solar thermal investments and provide a analysis of system costs, escalation of energy costs, and renewable energy credit prices. The net present value (NPV) of conventional and solar system turn out to be approximately equivalent between years 13 and 14 of the project. The results showed that the solar system have an incrementally better NPV in the remaining years. The net present value (NPV) for the solar system improves with higher energy price escalation and with longer evaluation time frames and.

Tsoutsos et al. [39] studied the performance and the economical evaluation of a solar heating and cooling system of a hospital in Crete using the transient simulation program (TRNSYS). The results proved that LiBr–H_2O has a higher coefficient of performance (COP) than that of the other working fluids. The payback time without funding subsidies is 11.5 years. In the case that there is a funding of 40%, the payback time reduced to 6.9 years. Koroneos et al. [40] presented the cost analysis of a 70 kW solar-powered LiBr-H_2O absorption chiller. Their results pointed out that the cost of this system is 138,000 Euro which is 107,640 Euro higher than the cost of the conventional, vapor-compression, system. The payback time of this system is approximately 24 years.

Hang et al. [41] presented a methodical economical, energetic, and environmental assessment on a solar cooling system for a medium-sized office building in Los Angeles, California using system modeling. The studied system consists of evacuated-tube solar

collectors and single-effect LiBr-H_2O absorption chiller at 120 kW working with both a hot tank in the solar collection loop and cold storage tanks in the load loop. As the solar collector area increases, the solar cooling system becomes increasingly expensive, mainly due to the high initial cost of the solar collectors and absorption chiller. It showed that when considering government subsidies, the simple year payback of the optimized solar cooling system case becomes 13.8 years, which is 40% less than the case without government subsidies. Al-Alili et al. [42] evaluated the feasibility of a solar powered absorption cycle under Abu Dhabi's climate conditions. The proposed system uses evacuated-tube collectors to drive a 10 kW ammonia–water absorption chiller. The solar air conditioner system has a specific collector area of 6 m^2/ kW and a specific tank volume of 0.1 m^3/kW. The selected system size requires about 47% less electrical energy than the widely spread vapor-compression cycles of the same cooling capacity. The ammonia–water system has the advantage that it can be operated at very low temperatures. The solar absorption air conditioners are less attractive when the electricity prices are low due to longer payback period (PBP).

Eicker and Pietruschka [43] showed a design of solar thermal absorption systems. A comprehensive simulation model was presented for absorption cooling systems, combined with a stratified storage tank under steady state condition or dynamic collector model and hourly resolved building loads. The simulation was verified with experimental data from various solar cooling plants. The cost analysis of solar powered LiBr-H_2O absorption system was also conducted. The total system costs are between 180 and 270 Euro MWh^{-1}. The costs can rise as high as 680 Euro MWh^{-1} for commercially available

solar cooling systems for a more moderate climate with low cooling energy demand. The results of the cost analysis showed that for long operation hours in the locations of Southern European, cooling costs are around 200 Euro MWh^{-1} and about 280 Euro MWh^{-1} for buildings with lower internal gains and shorter cooling periods. Florides et al. [44] presented the simulation of LiBr-water system performance equipped with $15m^2$ compound parabolic collectors and a 600 Liter hot water storage tank. The cost optimization for Cyprus was also performed. The results of cost optimization showed that the life cycle savings are £1,376 without subsidized fuel cost. Florides and Kalogirou [45] studied the optimization of the major components of Lithium-Bromide water (LiBr-H_2O) absorption solar cooling system. The studied components and parameters are the solar collector type, slope and area and the storage tank size. The analyzed collector types are the flat plate, evacuated tube and compound parabolic collectors. The optimization was established based on the life cycle cost of the solar system versus the amount of useful energy collected. The analysis indicated that using approximately 28,100 kWh of boiler heat can meet the annual load. The results showed that it was economically feasible to replace approximately 10,000 kWh with solar energy collected with 15 m^2 of compound parabolic collector (CPC). It was found that the life cycle savings of this system were € 320. The increase of the cost of fuel compels consumers to move to other energy forms in order to meet their needs. Renewable energy forms can economically replace part of the fuel energy as the fuel price increases.

Moreno et al. [46] studied variables that have effect on solar cooling of a building air-conditioning system to resolve the external conditions of temperature and radiation in order to achieve the required room temperature. The results showed that as the surface of solar collectors' area increases, the slope of the solar supply curve decreases due to the average temperature increase of water in the collectors, which makes the performance to decrease. The yearly cost of gas boiler increase increases as the storage tank volume increases. This confirms that the increase that is caused by losses as a result of the bigger contact surface with the outside, in this case, is more significant than the increase of the capacity of heat storage connected to the bigger volume. Calise et al. [47] investigated the optimal thermo-economic configuration of Solar Heating and Cooling systems (SHC). A case study is referred to an office building located in Naples (south Italy); for such building, three different SHC configurations were analyzed. A zero-dimensional transient simulation model, developed in TRNSYS, was used to analyze each layout from both thermodynamic and economic points of view. The results were presented on weekly and monthly, were paying a special attention to the financial flows and energy in the optimal configurations. The thermo-economic analysis and optimization showed that a good funding policy for the promotion of such technologies should combine a feed-in tariff with a slight Capital Cost Contribution, allowing to achieve satisfactory Pay-Back Periods. Moya et al. [48] determined the efficiency and viability of the performance of an advanced tri-generation system that consists of a micro gas turbine in which the exhaust gases heat hot thermal oil to produce cooling with an air cooled absorption chiller and hot water. The modeling performance of the tri-generation system and the electrical modeling of the micro gas turbine were presented and compared with experimental results. The

primary energy saving and the economic analysis showed the advantages and drawbacks of this tri-generation configuration.

Sumathy et al. [49] presented a design of an integrated solar cooling and heating system using two-stage absorption chiller, cooling capacity 100 kW. The results showed that the system (two-stage chiller) can achieve around the same total COP as of the conventional cooling system (single-stage chiller) with a cost reduction of about 50%. Edem et al. [50] studied absorption and adsorption for long-term solar energy storage. Even though there is no mature long-term sorption or thermo-chemical energy storage yet, primarily, as the cost of the materials is still high, the suitability of this technology to long-term storage remains its main power of attracting. The study has demonstrated the feasibility of such systems but has ended up in chemical heat pumps or short-term storage machines for those with highest performances. The materials that have been studied are essentially the same that are used for conventional absorption/adsorption machines, i.e. chemical heat pumps and absorption chillers. The study interested in closed adsorption has led unsatisfying results but those that used closed absorption seem to be promising.

Kizilkan et al. [51] performed thermo-economic optimization of a LiBr absorption refrigeration system. Thermo-economic optimization technique combines thermodynamic analysis with economic constraints to obtain an optimum configuration of a thermal system. Different components like condenser, absorber, generator and evaporator were analyzed. This study determined the optimum heat exchanger areas with optimum operating temperatures. The optimization specified a cost function for the optimum

conditions. Rosen [52] conducted the economic analysis based on exergy rather than energy analysis of the LiBr absorption system components. He reviewed different relations based on exergo-economics, thermodynamics, and capital cost and thermodynamic.

Farshi et al. [53] conducted the energy-economic analysis of the absorption cooling system (double-effect). The analysis results showed that the cost decreases as the evaporator and the generator temperatures increases, the condenser temperature decreases, and the solution heat exchanger effectiveness decreases. Massimo and Filippo [54] applied the theory of exergetic cost on a refrigeration plant. This methodology reduced the global problem into a locally optimized system in which costs of all internal flows were evaluated. A simplified cost minimization methodology is applied to evaluate the economic costs of all the internal flows and products of the installation. The results showed that that a design configuration not far from the real global optimum can be obtained by means of a sequential, local optimization of the system, carried out unit by unit, that is, breaking down the global problem into a sequence of simpler problems. The results showed acceptable accuracy when compared with the conventional optimization methodology.

Jerko et al. [55] presented the cost of the absorption system. The average cost sharing for small scale solar cooling systems showed that 35% of the total cost is mainly of storage tanks, fans, pumps, and other type of auxiliary equipment costs; absorption chiller shares approximately 30% of total cost; solar collectors make 20%; control system

around 10% and 5% are other costs. The costs of two systems (US installation and Italian installation) are compared per kW of produced cooling capacity. The US installation with 2886 €/kWc seems to be twice cheaper compared to 6537 €/kWc of the Italian installation. The cost of solar collectors and storage could be lowered by 10% in the next 2-3 years while the cost reduction potential for absorption chillers is around 20%.

2.3 Technical Review, Thermal Analysis and Simulation Studies for Solar Absorption Air-conditioning Systems

Absorption systems have gained considerable attention among researchers. Several studies have been conducted for solar absorption air-conditioning systems. Chung et al. [56] built a solar air conditioner by using lithium bromide-water as the working fluid during the summer of 1962. The solar air conditioner was used to cool part of the Laboratory of Solar Energy of the University of Wisconsin. Wang et al. [57] presented various solar cooling typical systems, small scale, for potential residential applications. The system suitability for solar cooling, working principals, maintenance and performance have been also presented. This work helps in addressing detailed options and guidelines of solar cooling for residential applications.

Ullah et al. [58] presented the review of different solar thermal refrigeration systems within various working fluids. The review focuses mainly on solar adsorption refrigeration systems and solar absorption refrigeration systems. The different working pairs are demonstrated by taking into consideration the coefficients of performance (COP), cooling capacity, minimum and maximum working temperatures and specific cooling power. The review indicates optimum operating conditions and performance of those systems. Zhai et al. [59] introduced the review of the existing experimental and theoretical investigations of solar single effect absorption cooling systems. They showed some new design options related to auxiliary energy systems, cooling modes and solar collectors. The review indicated that the flat-plate and the evacuated tubular solar collectors are still the major preferred selections for solar absorption cooling systems in

the near future. Most of the solar cooling systems available in the market are mainly single effect absorption systems, with a demonstrated technology employing LiBr-H_2O as the working fluid pair. The review summaries the coefficient of performance (COP) of the exiting single-effect absorptions cooling systems; COP: 0.33-0.7 and collectors efficiency; 35%-50%.

Shwarts and Shitzer [60] investigated thermodynamically the feasibility to operate the solar absorption refrigeration system for the application of air-conditioning purposes. The results illustrated that the system was applicable for air-conditioning domestic use. Sun [61] demonstrated a thermodynamic design of the absorption refrigeration processor for water-ammonia, and lithium bromide-water. An optimization of absorption refrigeration system was performed in order to map the most common cycles. The results can be utilized to achieve a maximum coefficient of performance (COP) from the system by selecting the optimum operating conditions. Antonio et al. [62] conducted a thermodynamic simulation of a solar single absorption refrigeration cycle (ammonia-water) that uses solar energy as a primary source. The simulation is used to analyze the effect of the heat exchanger effectiveness and the generator temperature on the Coefficient of Performance (COP) and mass flux. The simulation results showed that the system Coefficient of Performance (COP) decreases as the generator temperature increases. The simulation results indicated that for constant heat exchanger effectiveness, there is an optimum generator temperature to be used.

Karamangil et al. [63] presented a review on the absorption refrigeration systems (ARSs), the currently used refrigerant–absorbent pairs and their alternatives. The thermodynamic analysis of ARS using commonly encountered solution pairs was carried out, and a software package including visual components was developed. The effects of operating temperatures, the effectiveness of solution, refrigerant and solution–refrigerant heat exchangers (SHE, RHE, SRHE), and selection of working fluid pair on the system performance were examined by using the developed package. It was concluded that the coefficient of performance (COP) of the cycles improve with the increase of the generator and the evaporator temperatures. However, the coefficient of performance (COP) decreases with the increase of the condenser and absorber temperatures. Gomri [64] conducted both the first law and second law of thermodynamic analysis of LiBr-H_2O system. The analysis conducted for the single effect, the double effect and the triple effect systems. The analysis results showed that the maximum efficiency of the second law for the single effect, the double effect & the triple effect systems are as follows: 0.125-0.232, 0.143-0.251 & 0.177-0.252 respectively.

Kaushik & Arora [65] presented the first law and second law of thermodynamic analysis of single effect and double effect LiBr- H_2O absorption system. The first law analysis results showed that the coefficient of performance (COP) of double effect absorption system is 60 to 70% higher than the single effect absorption system. The most favorable coefficient of performance (COP) is achieved when the generator temperature is equal to 91°C for single effect system and 150°C for double effect system. Correspondingly, the second law analysis results showed that the optimal exergetic

efficiency is achieved when the generator temperature is equivalent to 80°C for single effect system and 130°C for double effect system. Kilic & Kaynakli [66] conducted also the first law and second law of thermodynamic analysis of LiBr- H_2O absorption system. The results demonstrated that irrespective of the working conditions, the generator has the highest exergy loss component such as 45.6% of the overall exergy loss of the system. On the other hand, the pump and refrigerant heat exchanger have the lowest exergy loss component of the system.

Rosiek and Batlles [67] presented the solar powered, single effect, absorption cooling system of cooling capacity of 70 kW installed in the Center of Solar Energy Research in Spain which consists of 160 m^2 flat-plate solar collectors to cover the energy demands whichever for cooling in summer or heating in winter. The solar powered cooling absorption system performance was observed and measured by data acquisition system. The results showed that, the cooling demand and heating demand during the entire year were 13,255 kWh and 8,124 kWh, respectively. Moreover, the results indicated that the solar collectors were capable to provide satisfactory energy supply to meet the total heating demand and cover the absorption system requirements during the summer mode during one year of operation. For summer months, the cooling capacity and the average coefficient of performance (COP) values are found 40 kW and 0.6, correspondingly. Pongsid et al. [68] provided the review of different types of absorption systems. Different absorption cycles are compared to invent new efficient cycles. Multi effect systems with increased COP have shown a great potential to be used for large scale industries. They also discussed the ways by which the increased COP of the system can

be achieved without increasing the complexities. A combined ejector-absorption system can provide the COP as high as a double effect system and it can be used for domestic refrigeration.

Gomri [69] investigated the potential for the application of single effect system, double effect system and triple effect system absorption cooling cycles for production chilled water. For the three systems identical cold output of 300 kW was used. The simulation results used to analyze effect of various operating parameters on the coefficient of performance (COP), the efficiency and the refrigerant mass flow rate ratio required to the three systems heat supplied. When operating under the same conditions, the results showed that, for double effect system, the coefficient of performance (COP), 1.22-1.42, is roughly double the coefficient of performance (COP) of single effect system, 0.73-0.79. Also, it indicated that, for triple effect system, the coefficient of performance (COP) is almost triple the coefficient of performance (COP) of single effect system. Maintaining the exergy to its minimum, the applicable generator temperature for varying condenser and evaporator temperatures was determined. The efficiency of double effect system and triple effect system increase slightly compared to the efficiency of single effect system. Triple effect system generated more vapor refrigerant per unit heat supplied as compared with single effect and double effect systems. Alizadeh [70] performed a technical study of multi pressure absorption cooling systems. The study showed that double effect absorption refrigeration has almost twice the COP at the optimum generator temperature as compared to the single effect refrigeration system. The effective electrical COP for different chiller configurations was also compared. It

concluded that the maximum effective electrical COP for ideal single effect refrigeration system was achieved.

Balghouthi et al. [71] presented a solar cooling absorption chiller, 16 kW LiBr-water double effect, installation located at the Center of Researches and Energy Technologies (CRTEn), in Bordj-Cédria, Tunisia. The system composed mainly of parabolic trough solar collectors, associated with a cooling tower, a backup heater, two tanks for storage and drain-back storage and a set of fan-coils installed in the building to be conditioned. It was found that the coefficient of performance COP was ranged between 0.8 and 0.91 during the installation running while the solar coefficient of performance (COPs) was between 0.1 and 0.43. The maximum output of the absorption chiller was around 12 kW. Lecuona et al. [72] determined the temperature of the hot water that increases the total instantaneous efficiency of a solar cooling facility, single-effect lithium bromide–water absorption systems. They developed a model for a modified characteristic equation for small capacity air conditioning machines of small buildings and homes.

Kim and Ferreira [73] theoretically investigated an air-cooled LiBr–H_2O absorption chiller with low temperature-driven for solar air-conditioning applications in dry and hot regions. The system is developed for a combination with low-cost flat solar collectors. The investigation covered directly and indirectly air-cooled chillers that were modeled and solved with an algebraic equation solver by properly combining component models and boundary conditions in a matrix system. The results of the simulation found

that the chillers can supply chilled water approximately at 7.0 ºC and coefficient of performance (COP) of 0.37 from 90 ºC hot water for 35 ºC ambient conditions. Compared with the directly air-cooled chiller, the indirectly air-cooled chiller presented a cooling power performance reduction of about 30%. Gordon and Choon [74] analyzed mini-dish systems that can supply high-temperature heat at high efficiencies of solar-to-thermal conversion. The mini-dish systems were able to provide coefficient of performance (COP) about 1.0 to double-stage absorption chillers.

Berhane et al. [75-77] considered the exergy destruction of half, single, double and triple effect LiBr-H_2O absorption cycles. The half effect absorption system configuration is the same as the double effect absorption except the heat flow directions are different. In the half effect system, the high temperature heat from an external source transfers to both generators. The coefficient of performance (COP) of the half effect absorption system is relatively low as it rejects more heat than a single effect absorption cycle around 50%. However, it can be operated with the relatively low temperature heat source. In the tripe effect absorption system, three generators are used in total (high-temperature, medium temperature, and low-temperature). The heat of high temperature generated in the high temperature generator is sequentially used in the generators of lower temperatures. An increase in COP from double to triple effect absorption cycles was investigated. Largest energy destruction was obtained at generator and absorber components. The effect of coefficient of 25 structural bonds on the heat exchanger area was considered. This proposed approach could be used for alternative design cycles rather than a single design. Kayankli & Kilic [78] presented a parametric study, variation of operating parameters,

over the coefficient of performance (COP) of the LiBr-H_2O system. The results showed that the coefficient of performance (COP) increases by 44% by the solution heat exchanger while the COP increases by 2.8% by the refrigerant heat exchanger.

Kundu et al. [79] analyzed the impact of different solar collectors' types on the performance of solar powered absorption systems. The results showed that the concave parabolic shape collectors turn to be the most excellent design for the absorption system. Yang and Wang [80] investigated the effect of the collector's types on the performance of the chiller. It was concluded that the double-glazed forced convection collector has a higher system performance than the single-glazed natural convection collector.

Tubb [81] presented the design of solar power refrigerated 13.5 meter trailers, resulting in a cost effective solution which will enable the concept to be accepted as a commercial reality. Also, further objective set to operate the trailer temperature at +3 C whereas the original design operated at +7 C. The work was achieved by evolving the design from the prototype with a strong input from Sainsburys Plc. The results showed that during its operation there had been sufficient solar energy to sustain the refrigeration system. It showed that during the Autumn months, the difference between the solar energy and the refrigeration demand for energy is the smallest, but still positive. In the spring months, the difference is a it's maximum. This is due to the spring temperatures being lower than those in Autumn for the same sun positions. Atmaca and Yigit [82] demonstrated a simulation of solar cooling absorption system at 10.5 kW constant cooling load for Antalya, Turkey. The simulation was developed to analyze solar energy

parameters and various cycle configurations. It was found that the storage tank mass 3750 kg and solar collector area of 50 m^2 appeared to be the best choice.

Qussai and Abdul-Ghafour [83] developed integrated transient simulation program (TRNSYS) for a solar cooling system, lithium bromide–water absorption chiller, for the Iraqi solar house cooling system and other solar cooling systems similar to the Iraqi solar house. Other computer programs were developed and used in parallel with (TRNSYS) in order to meet the complete the simulation of the system. The simulation results, using f-chart model, were used to develop a general design procedure for solar cooling systems. The simulation assists in simplifying the designers' task in predicting the long term cooling energy supplied from a solar collector array to operate absorption chilled water system. A correlation was developed from the simulation results to estimate the hot water storage size needed for the solar cooling system. Balghouthia et al. [84] presented a research project to assess the feasibility of solar-powered absorption cooling technology, lithium bromide- water, under Tunisian, the capital of Tunisia, conditions. The simulations used (EES) and (TRNSYS) programs with a meteorological year data file to select and size the different components of the solar system intended for installation. The system was optimized for a typical building of 150 m^2, 11 kW absorption chiller of capacity, 30 m^2 flat plate solar collectors' area tilted 35º from the horizontal and, 0.8 m^3 hot water storage tank. The simulation results show that absorption solar air-conditioning systems are suitable under Tunisian conditions. Despite their high first cost, these systems can help to minimize energy use generated by fossil fuel, reduce electrical energy at the period of peak demand in summer.

Ming et al. [85] studied a solar thermal cooling and heating system at Carnegie Mellon University. The study covered the design, modeling, installation and evaluation of 16 kW double effect, lithium bromide-water (LiBr-H_2O) absorption chiller with linear parabolic trough solar collectors to effectively supply energy by the means of solar energy for the operation of 52 m^2 building in Pittsburgh, PA. If the system built-in a appropriately sized storage tank and low, short diameter connecting pipes, the solar thermal system can potentially provide 39% of cooling and 20% of heating energy of the total building demand, Praene et al. [86] analyzed a solar-powered 30 kW LiBr-water absorption, single-effect, cooling system. The system was designed and installed at Institute University Technology of Saint Pierre. It was found that the solar loop can produce hot water to operate the absorption chiller from 8:00 AM to 5:00 PM. The system was capable to meet the required thermal comfort with the classrooms mean air temperature around 25 ◦C in accordance to the field test.

Molero-Villar et al. [87] analyzed the selection of the most suitable configuration for residential cooling systems with solar energy. In Spain, where cooling needs are usually higher than heating needs, the interest of a reversible heat pump as auxiliary system and a secondary cooling storage are analyzed. A complete TRNSYS model had been developed to compare a configuration with just hot storage and a configuration with both, hot and cool storages. As the collector area increases, the advantages of a cool storage vanish. The increase of the collector area tends to increase the temperature of the hot storage, leading to higher thermal losses in both the collector and the tank. The effect of other variables on the optimal configuration was also analyzed: collector efficiency

curve, COP of the absorption chiller, storage size, and temperature set-points of the chillers. Onan et al. [88] exploited (MATLAB) software to analyze the hourly performance of 106 kW solar powered LiBr-H_2O system in an environment of ambient temperature ranges from 13.2 °C to 40.3 °C. The results showed that the loss of the total exergy in the collector varies from 10-70% which has the highest loss compared to the other components of the system. Hong et al. [89] illustrated a proposal of an evaporator absorber exchange (EAX) absorption system. The system utilizes the heat of condensation of the vapors that is produced from the high temperature generator. The results of the simulation showed that the coefficient of performance (COP) of this system is 40% higher than the conventional single-effect system. However, the coefficient of performance (COP) of this system is lower than the conventional double-effect system when the generator temperatures operate between 127.5°C to 150 °C.

Somers et al. [90] conducted a comparison between the results of the simulation software (EES) and (ASPEN) software. The comparison focused on the performance of solar powered LiBr-H_2O system, single-effect and double-effect. The comparison results of the (ASPEN) software when compared to EES results, showed that there are an error of around 3% for the single effect system and 5% for the double-effect system. Cascales et al. [91] utilized the artificial neural networks (ANN) software to simulate a solar-operated LiBr-H_2O system. The simulation of the (ANN) code was validated using the experimental data of the period of two years. The simulation results showed that (ANN) predicted roughly accurate the outlet temperatures of the absorber and condenser. However, the prediction of the coefficient of performance (COP) was not accurate most

likely due to the high inconsistent experimental results. Calise et al. [92] developed transient simulation model (TRNSYS) software for solar assisted heating and cooling systems (SHC) for three different configurations using single-stage LiBr–H_2O absorption chiller. For the three different configurations, the (SHC) system is coupled with evacuated solar collectors and gas-fired boiler for auxiliary heating for the usage of winter season only. The developed economic model assesses the capital and the operating costs of the systems under analysis. The economic model results indicated that the (SHC) systems are still not economically feasible.

Ortiz et al. [93] developed (TRANSYS) simulation model to evaluate the performance of the solar powered LiBr-H_2O system. The results of the simulation showed that this system could minimize the total external cooling energy demand by ranges of 33% to 43%. Eicker et al. [94] applied dynamic simulation models for 15 kW single effect of solar powered LiBr- H_2O system. The results of the simulation showed that the maximum primary energy ratio of 88% for solar fraction that is approximately triple than the electrical conventional system, vapor-compression. Gonzalez-Gil et al. [95] described new direct air-cooled, single-effect, LiBr-H_2O absorption prototype for solar cooling application. The solar facility comprised of a 48 m^2 flat-plate collectors to examine the operation of the single-effect mode of the prototype. The prototype worked efficiently, with COP values around 0.6 and the system was capable to meet 65% of the cooling demand corresponding to a room of 40 m^2.

Solar energy can be successfully exploited for air-conditioning applications by using a vapor-absorption system, lithium bromide-water. However, the greatest challenge in using solar energy for continuous cooling is the un-availability of solar energy during the period of nighttime. In order to achieve such continuous cooling demand from the solar energy, it is required to be coupled with a storage system that will compensate for these needs at the periods of the nighttime and low solar intensity. The temperature range for most of the available phase change materials (PCMs) is from −5 °C to 190 °C which is applicable for the energy storage of the absorption air-conditioning system. Zalba et al. [96] conducted a review of energy storage of phase change materials (PCM) and heat transfer analysis and its applications. The review discussed 45 (PCMs) materials commercially available in the market and 150 (PCMs) materials under research. Koca et al. [97] analyzed the latent heat storage of a phase change material (PCM): $CaCl_2.6H_2O$ for solar collectors. The analysis used special heat transfer fluid to carry the heat energy gained from the solar collectors to (PCM) phase change material. The results indicated that the average efficiencies of exergy and energy are 2.2 % and 45 %, respectively. Patrice et al. [98] presented the review of the available methods for seasonal storage of solar thermal energy. The review mainly focuses on the systems of residential scale and those that store sensible forms of energy. The review indicated that chemical and latent principles are still present difficulties due to the identification of suitable, cheap materials that could offer thermal stability.

Chidambaram et al. [99] reviewed researches that discussed storage techniques, solar cooling methods and solar collectors. The review covered the improvement of the performance of the solar cooling systems, integration using cascaded thermal storage systems and thermal stratification systems. The review confirmed that thermal storage is necessary in the solar cyclr, in order to take greatest advantage of the solar supply and control differences between the solar radiation availability and the cooling requirements. The review confirmed indicated that the integration of the thermal storage with solar cooling systems increases the overall performance and the cooling capacity as well improves the cooling availability. Li and Sumathy [100] analyzed the performance of a 4.7 kW solar-powered absorption LiBr-H_2O air conditioning system with a 2.75 m^3partitioned, into two parts, hot water storage tank and a 38 m^2 flat-plate collectors. The analysis confirmed that the solar cooling effect can be realized almost 2 hours earlier for the system operating in partitioned mode. Moreover, the experimental results indicated that the system cannot provide a cooling effect during the days of cloudy when driven conventionally. However, in the partitioned mode-driven system the chiller, using solar energy as heat source, can be energized.

Salgado et al. [101] presented a numerical model of the multiple purpose solar thermal facility installed at Universidad Carlos III de Madrid using the TRNSYS tool. The simulation results show that there is a hot storage tank capacity that optimizes the facility in terms of COP, SCOP and total cold produced. Even with no storage at all, the facility still improves its behavior from current operating conditions. Tang and Gerstler [102] proposed novel LiBr based absorption chiller with cold storage to improve

absorption chiller operating at high ambient temperatures that may result in performance degradation, crystallization in the absorber, and high water consumption for heat rejection to the ambient. The cold storage includes tanks for storing liquid water and LiBr solution, associated piping, and control devices. The proposed system is designed to allow the LiBr solution to crystallize in the absorber. The proposed system is evaluated at a representative climate condition and cooling load profile for small buildings with in-house thermodynamic models and consistent fluid properties and assumptions. The performance, size of the storage tank, and the water consumption of the proposed system is compared to those of a conventional LiBr-based absorption chiller.

Lazzarin [103] reported some schemes of operating cooling plants by analyzing the role of the storage and the sizing of solar section and absorption chiller together with recorded results. The results showed that the solar collector performance can be optimized and absorption chiller capacity can be reduced when using well sized storage system with a cold and hot section. Hamza et al. [104] presented the performance assessment of an integrated cooling plant in operation since August 2002 in Oberhausen, Germany. The integrated cooling plant consists of free cooling system and 35.17 kW solar powered lithium bromide–water absorption, single-effect, chiller. The plant consists of 108 m^2 vacuum tube collectors, 1.5 m^3 cold water storage capacity, 6.8 m^3 hot water storage tank size and 134 kW cooling tower. In certain cooling months, the free cooling can be up to 70% while it is around 25% during the period of five years of the plant operation. The coefficient of performance (COP) of the chiller ranges from 0.37 to 0.81and the efficiency of collectors varies from 0.352 to 0.492. It was found that, the

solar energy system support of the institute heating system for the duration from August 2002 to November 2007 is 8,124 kWh and the specific collector area ratio is 4.23 (m^2/kW).

Said et al. [105] developed three alternative designs for a continuous (24 hours) operating solar powered aqua ammonia absorption refrigeration technology. The designs includes thoroughly review of the operation of the conventional and solar-assisted absorption refrigeration systems. The objective of such review is to develop new alternate designs with detailed thermodynamic analysis of those new alternative designs in order to select the most suitable alternative design. The results of the analysis indicated that continuously operating solar powered aqua ammonia absorption system with refrigerant storage is the most suitable alternative design for a continuous supply of cooling effect. Al-Ugla et al. [106] developed three designs for a 24-hours operating solar powered LiBr-H_2O absorption air-conditioning system technology. The results showed that the refrigerant storage is the best choice for continuous operating solar-powered LiBr- H_2O absorption air-conditioning system.

The hybrid storage design for solar absorption system has several benefits related to performance improvement, maintenance processes optimization and collector size reduction. El-Shaarawi et al. [107] developed a hybrid-storage design for solar aqua-ammonia absorption refrigeration system. The system includes thermal collector, generator, condenser, evaporator, cold storage tank, absorber, weak solution tank, strong solution tank, refrigerant storage tank, refrigerant heat exchanger and solution heat

exchanger. El-Shaarawi et al. [108] analyzed the dual storage design for solar aqua-ammonia absorption refrigeration. The storage system consists of one ammonia tank, an ice tank and two aqua-ammonia tanks. The results showed that the coefficient of performance is lower in summer than winter. However, the required solar collector field area is smaller in summer than in winter.

2.4 Experimental Works for Solar Absorption Air-conditioning

Several experimental works have been conducted for solar absorption air-conditioning systems. Sozen et al. [109] investigated experimentally an aqua–ammonia absorption heat pump system (AHP) prototype, in Ankara in Turkey, by means of solar energy. The system was designed to be coupled with a parabolic type collector to receive the required temperatures where the high temperature water needed for the generator was provided from the collector. The thermodynamic analysis indicated that both losses and irreversibility have an impact on absorption system performance. The analysis showed the components that need thermal improvement. The components of the evaporator and absorber of the system had a higher exergy loss than the other components. Pongtornkulpanich et al. [110] designed and installed a solar-driven 10-ton LiBr-H_2O single-effect absorption cooling system at the School of Renewable Energy Technology (SERT). The system includes 72m^2 evacuated tube solar collector supplied an annually average solar fraction of 81%, however, the remaining 19% of thermal energy required by the system was supplied by the LPG-fired backup heating unit.

Sumathy et al. [111] designed a 100 kW double stage solar powered LiBr-H_2O absorption chiller in south China. The results of the experimental test showed that the system can be operated when the generator temperature varies from 60 °C to 75 °C. Syed et al. [112] reported experimental results for typical Spanish houses in Madrid during the summer period of 2003 derived through field testing of a part load solar energized cooling system. Solar hot water was delivered by 49.9 m^2 flat-plate collectors to operate

35 kW (LiBr-H_2O) absorption, single effect, chiller. The results indicated that measured daily average, period average and maximum instantaneous coefficient of performance (COP) were 0.42, 0.34 and 0.60 (at maximum capacity), respectively. The results clearly demonstrated that this system works best in hot and dry weather conditions as the large daily differences in relative humidity and dry bulb temperature prevail. To improve the system performance, it was recommended that thicker tank insulating material be used. The steel pipes can be replaced with UPVC in primary and tertiary circuits.

Izquierdo et al. [113] conducted experimental research to determine the performance of a 4.5-kW air-cooled chiller, single effect LiBr-H_2O absorption unit (Rotartica 045v). The experiments were run at the Eduardo Torroja Institute Heat Pump and Absorption Chiller Laboratory at La Poveda, Arganda del Rey, Madrid, in August 2005 where the measurements were recorded over the period of 20 days. The hot water inlet temperature in the generator ranged throughout the day from 80 ºC to 107 ºC. The total energy supplied to the generator came to 1,085.5 kWh and the heat removed in the evaporator to 534.5 kWh. The average COP for the period as a whole was 0.49. When the electric power used by auxiliary equipment was factored into the equation, primary energy based COP came to 0.37.

Agyenim et al. [114] presented a domestic-scale prototype experimental solar cooling system, 4.5 kW LiBr-H_2O absorption chiller. The system consisted of a 12 m^2 vacuum tubular solar collector, a 6 kW fan coil and a 1000 Liter cold storage tank. The experimental results indicated that the average coefficient of performance (COP) of the

system was 0.58. The results confirmed the feasibility of the cold storage for cooling in domestic scale buildings with low chilled water temperatures as 7.4 ^{O}C. Moreover, the experimental results indicated that solar powered, single-effect, absorption cooling systems were able of working in the driving temperature range of 65 ^{O}C ‑100 ^{O}C. Berlitz et al. [115] presented an experimental setup of high efficient absorption chiller which facilitates the supply of a constant load of coldness at constantly high COP in spite of periodically available driving heat.

Hu et al. [116] conducted an experimental study for 40 W micro absorption heat pump. The absorption system was constructed of micro-condenser, micro-evaporator, and expansion channel. The experimental results showed that the coefficient of performance (COP) varying from 0.465 to 0.511 when the generator temperature operates at 100°C and the evaporator operates at a temperature varying from 11 °C to 19 °C. Bermejo et al. [117] developed a 174 kW gas/solar powered double effect LiBr-water absorption chiller in Spain using 352 m^2 linear concentrating Fresnel collectors. Their experimentation results indicated the solar energy contributed 75% of the total heat input to the generator producing a COP of 1.1-1.25 when operated at the evaporator temperature of 8°C.

Hidalgo et al. [118] conducted an experimental research on solar absorption cooling. The facility is based on an on-Campus field of 50 m^2 flat plate solar collectors driving a single-effect commercial LiBr-H_2O absorption machine through a hot-water storage tank. The results showed that absorption machine cooling power reaches 6–10 kW, with a generator driving power input of 10–15 kW, achieving a mean cooling period

of 6.5 h of complete solar autonomy on a seasonal average day. Salgado et al. [119] demonstrated experimental results for two basic configurations of a thermal storage tank (Stratification and Well-mixed) in a solar cooling facility. The results show that for solar cooling applications, having a well-mixed temperature in the thermal storage tank produce more daily cooling energy than in a stratified one, although the solar field efficiency is lower. The effects on the facility produced by Well-mixed configuration are: efficiency reduction on the solar collector's field, 0.27, higher daily COP's, 0.33, and extended solar cooling time of about two hours.

Rosiek and Garrido [120] presented the performance of solar-assisted air-conditioning system with two chilled water storage tanks installed in the Solar Energy Research Center building. The system consists mainly of solar collectors' array, a hot-water driven absorption chiller, a cooling tower, two hot storage tanks, an auxiliary heater as well as two chilled storage tanks. The results demonstrate that 20% of the total energy consumption and about 30% of water consumption can be saved, which takes into account the chilled water tanks action. Moreover, it was demonstrated that the integration of chilled water storage tanks allows to reduce the sudden absorption chiller on/off cycles, thereby improving the efficiency of the solar-assisted system. Darkwa et al. [121] presented the experimental analysis of a LiBr-water absorption system operated by evacuated tubular and flat plate solar collectors. The system is coupled with four hot water storage tanks. The results of the experimental showed that the coefficient of performance (COP) of 0.69 can be reached when the heated water at 96.3°C is supplied by the solar collectors.

Marcos et al [122] discussed the experimental results of using a solar facility with a net collector area of 42 m^2 to meet the heating and cooling needs of an 80-m^2 laboratory energetically similar to the average Spanish home. They found that the absorption chiller would be payback in 34 years, if the electrical consumption is not taken into account. The experiments proved that approximately 10 m^2 of solar panels are needed to produce 1 kW of cooling capacity with an air-cooled LiBr/water absorption chiller.

The following conclusions can be made based on the literature review:

- Both solar thermal air-conditioning system and solar photovoltaic-vapor compression air-conditioning system have better feasibility when the fuel price increases.

- Thermal (absorption & adsorption) air-conditioning system is the most suitable option to be powered by solar energy compared to solar photovoltaic-vapor compression air-conditioning system.

- Solar absorption system is more feasible than solar adsorption system based on techno-economical evaluation.

- LiBr-water absorption system presents so far best proven absorbent-refrigerant working pair for air-conditioning application.

- The thermal storage has advantages over solar thermal air-conditioning systems in terms of system performance improvement and energy saving.

- Several simulations and technical analysis researches have been conducted on absorption systems.

- Several experimental researches have also been conducted on absorption systems.

None of the researches in the preceding survey investigated the comparison of the three air-conditioning systems (conventional vapor compression, PV- vapor compression and solar absorption) for commercial buildings in Saudi Arabia. Moreover, none of the researches studied the solar-powered absorption LiBr-H_2O system for a continuous supply (24-hours a day operation) of cooling effect. Hence, in the present research, several designs for a continuously (24 hours a day) operating solar-powered absorption LiBr-H_2O air-conditioning technology are discussed in detail.

CHAPTER 3

OBJECTIVES AND METHODOLOGY

This chapter shows the objectives of the dissertation and the description of methodology to achieve the objectives.

3.1 Objectives

The overall objective of the present dissertation is to design solar air-conditioning system for buildings in Saudi Arabia. The specific objectives include:

1. Techno-economic evaluation comparison of solar LiBr-water absorption air-conditioning systems, solar photovoltaic vapor compression air-conditioning systems and conventional vapor compression air-conditioning systems.

2. Design of a continuous operation (24-hour a day) solar LiBr-water absorption air-conditioning system.

3. Design of hybrid storage for continuous operation (24-hour a day) solar LiBr-water absorption air-conditioning system.

4. Thermodynamic analysis of the continuous operation (24-hour a day) system designed in 2.

5. Thermodynamic analysis of the hybrid storage system designed in 3.

6. Unsteady analysis of a hybrid storage (cold storage and refrigerant storage) system under the climatic conditions of Dhahran, Saudi Arabia.

3.2 Methodology

To achieve the above listed objectives, the following methodology was adopted:

- A comprehensive literature review of solar air-conditioning systems. This includes a thorough study of absorption systems and their utilization in air-conditioning application.

- Techno-economic investigation to evaluate the technical feasibility of several solar air-conditioning systems to be used in buildings in Saudi Arabia. The study focuses on photovoltaic vapor compression systems, solar absorption systems and conventional (vapor compression) systems.

- Development of different designs for continuously operated (24-hour a day) totally solar powered absorption air-conditioning systems using lithium-bromide water as the working fluid. The designs include the arrangements required to facilitate the solar powered system.

- Development of hybrid storage designs for continuously totally solar powered absorption lithium-bromide water air-conditioning system. These designs allow uninterrupted operation and achieve maintenance process optimization. The designs include arrangements required to facilitate the solar powered system.

- Thermodynamic analysis of continuous operation designs using EES Software. Thermodynamic analysis for these designs will be performed to provide a conceptual formulation of each design. The thermodynamic analysis assists in defining the controlling parameters that affect the performance of each design and finally determine the efficiency of each design.

- Analysis of continuous operation designs based on system performance and storage tanks size using EES Software. The parametric thermodynamic analysis will enable the selection of the best suitable design.

- Thermodynamic analysis of hybrid storage designs using EES Software. Thermodynamic analysis for these designs will be conducted to provide a theoretical formulation of each design. The thermodynamic analysis supports in defining the controlling parameters that affect the performance of each design and finally determine the efficiency of each design.

- Analysis of hybrid storage designs based on system performance and storage tanks size using EES Software. The parametric thermodynamic analysis will enable the selection of the best suitable design.

- Unsteady analysis of hybrid storage (cold storage and refrigerant storage) system under Dhahran ambient conditions using EES Software.

CHAPTER 4

TECHNO-ECONOMIC ANALYSIS OF SOLAR-ASSISTED AIR-CONDITIONING SYSYTEMS FOR COMMERICAL BUILDINGS IN SAUDI ARABIA

A techno-economic analysis of three air-conditioning systems (conventional vapor-compression, solar LiBr-H_2O absorption and solar photovoltaic vapor-compression) was carried out. It was assumed that each air-conditioning system can meet a constant cooling load of a typical large-size commercial building in Khobar City in Saudi Arabia. The analysis utilizes two economical methodologies: Payback Period (PBP) and Net Present Value (NPV).

4.1 Cooling Load and Solar Radiation Energy Comparison

This section shows the comparison of the cooling load and the solar radiation energy between Saudi Arabia and USA. Table 4-1 shows the comparison of the cooling load per area between one commercial building in Khobar, Saudi Arabia and office building in Los Angles, California, USA. The table indicates that the cooling load in Saudi Arabia is higher than in USA by approximately 22% due to the extreme high ambient conditions in Saudi Arabia. This increase justifies the significance to investigate and study new innovative cooling system in Saudi Arabia.

Table 4-1 Cooling Load Comparison

Country	Cooling Load (W/m2)
Saudi Arabia	32
USA [41]	25

On the other hand, the solar radiation between Saudi Arabia and USA was compared as shown in Table 4-2. Table 4-2 shows that Saudi Arabia has higher solar intensity than USA. This data should lead to an implantation strategy in Saudi Arabia for solar energy utilization in cooling applications compared to other countries.

Table 4-2 Solar Radiation Energy Comparison

Country	Solar Radiation (W/m2)
Saudi Arabia	1048
USA [41]	905

4.2 Building Characteristics

In order to provide a consistent baseline of comparison between the three air-conditioning systems; Table 4-3 shows the building information for the selected commercial building. The building consists of hypermarket and residential apartments. Khobar city has the same weather and solar data of Dhahran city which is used in the analysis.

Table 4-3 Building Data [123]

Characteristic	Description
Type	Three floors (Two floors residential apartments: 12,200 m^2, One floor Hypermarket: 16,616 m^2)
Plan Shape	Court Yard Shape: 1^{st} & 2^{nd} floors. Rectangular shape: Ground floor
Total Height	14.7 m
Gross Floor Area	41,016 m^2
Gross Wall Area	9937.2 m^2
Window Area	1350.03 m^2
Window to Wall Ratio	13.59%
Lighting heat flux	Residential area 12.91 W/m^2 and Hyper Market area 36.59 W/m^2
Equipment heat flux	Assumed 2.7 W/m^2
Thermal Transmittance (U-value)	
Glazing	5.6 $W/m^2 K$
External Walls	5.1 $W/m^2 K$
Internal Core Wall	1.930 $W/m^2 K$
Roof	0.539 $W/m^2 K$

4.3 Systems Description

This section describes the three air-conditioning systems and associated major components used in the techno-economic analysis. Figure 4-1 shows the three systems basic configuration and the descriptions are as follows:

- Conventional vapor-compression system: uses conventional vapor-compression air-cooled chiller.

- Solar absorption system: uses flat plate collectors, hot water tank and single-effect lithium bromide/water absorption air-cooled chiller. The flat-plate collectors are cheaper and has simpler design compared to the evacuated-tube collectors. The single-effect system as it is cheaper than the double-effect and triple-effect systems.

- Solar photovoltaic vapor-compression system: uses photovoltaic (PV) panels to generate electricity connected to a conventional vapor-compression air-cooled chiller. The photovoltaic system consists of modules, arrays, controller, inverter and battery.

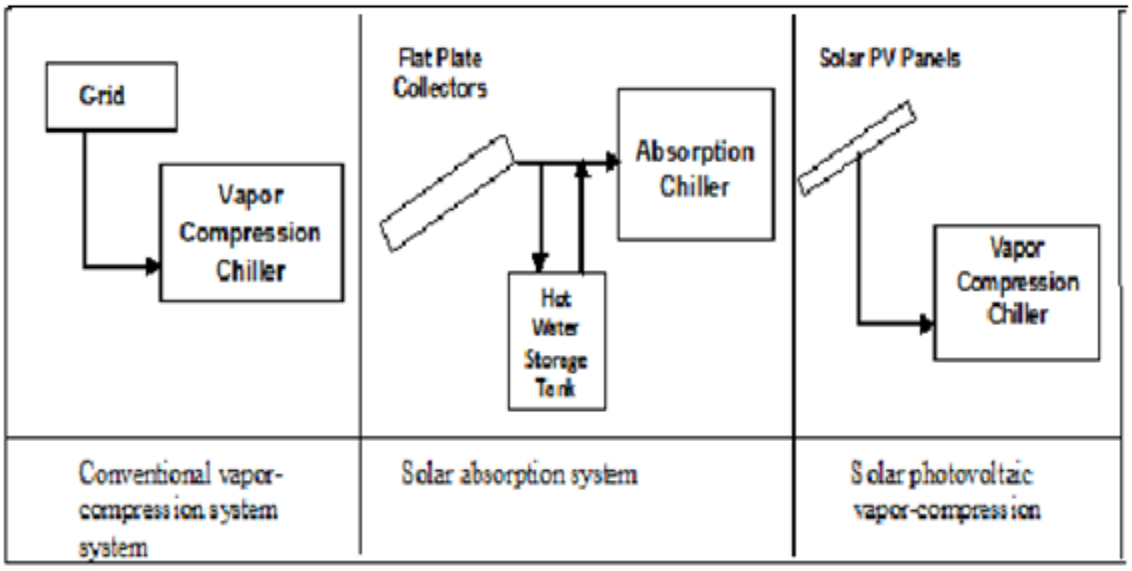

Figure 4-1 Three Systems Basic Layout Configuration

4.4 Systems Design

The three systems are designed to meet building constant hourly average cooling load (940 kWh) during daytime operation (10 hours operation: 7 AM to 5 PM) with the objective to cover peak solar energy for solar absorption and solar photovoltaic systems in order to mitigate electricity peak load during the summer time. Moreover, the three systems have the same nominal chiller capacity needed for building cooling load. All the cooling generated is used during the daytime operation and there is no thermal or electrical storage to be used for nighttime operation as the solar absorption and PV systems are solar-assisted systems for only daytime operation.

The economical evaluation is conducted based on the sizing of the main components for the three systems (flat plate collectors, absorption chiller, hot water tank, vapor compression chiller and PV system). Flat plate collectors have a lower cost and simpler design compared to evacuated tube collectors. The collectors design is based on an assumed efficiency of 50 %, yearly average daily solar radiation in Dhahran of 5.84 kWh/m^2 and an assumed solar absorption chiller COP = 0.7 [112, 124, 125]. The actual COP will be discussed in the results and discussion chapter to obtain the actual PBP and NPV for solar absorption system. The hot water tank of the solar absorption system is used to store the excess hot water after meeting the cooling load during daytime operation. This excess heat is utilized when the solar insolation is insufficient to provide heat to the system during the daytime operation. This is also applicable for the electrical storage "Battery" of the PV system. The optimal designing size ratio of the tank volume

to the collector area is 0.04 m^3/m^2 [41]. It is note of worth that the recent change of the air-conditioning standards in Saudi Arabia can increase the lifespan of the AC machines used in the economic analysis. However, to be more on the conservative side, it was not considered in this analysis.

The flat plate collectors' area is calculated using the following equation:

$$A_c = \frac{\text{Hourly Average Cooling Load} \,.\, \text{Solar Avaliable Time}}{\text{COP} \,.\, \text{Average Daily Solar Radiation Energy} \,.\, \eta c} \quad (4.1)$$

The absorption chiller for the solar absorption system is designed to receive the greatest solar energy during noontime. It has been designed with a maximum power of 1500 kW to meet the highest required cooling load. This maximum power would be obtained at the solar peak intensity in Dhahran which is 3.349 MJ/m^2 [126]. The chiller size for conventional vapor-compression and photovoltaic vapor-compression systems is the same as for solar absorption system since the building-cooling load is constant for the three systems. Moreover, the size of the chiller should be the same in order to have accurate economical comparison between the two systems. The COPs values of both systems are different in order to have a better and near to practical values of the required heating energy for each system. The chiller power is sized based on the following formula:

$$\text{Chiller Power} = \text{COP}_{(\text{absorption})} \,.\, A_c \,.\, \eta c \,.\, \text{Maximum Solar Radiation Intensity} \quad (4.2)$$

The PV system, module efficiency of 15 % [127], is designed for 940 kW_p based on COP of 2.5 for the vapor-compression chiller and conservative daily sun hours in Dhahran = 4 hr/day [127, 128]. The cooling demand during daytime outside the

conservative daily sun hours would be obtained from the electric battery storage system for daytime operation. Table 4-4 shows the three systems design parameters.

Table 4-4 Systems design parameters

	Conventional VC	**PV-VC**	**Solar Absorption**
Flat Plate Collectors (m^2)	-	-	4,600
PV System (kWp)	-	940	-
Hot Water Tank (m^3)	-	-	184
Chiller Cooling Power (kW)	1,500	-	1,500

4.5 Economic Assessment

There are many available methods to evaluate the economic performance, to analyze the economic consequences of particular design decisions and evaluate alternative approaches fairly. The economic analysis of the three systems will determine the feasibility and identify the economic advantages and disadvantages. Using the initial investment cost and the annual operating costs (maintenance and electricity costs), the payback period (PBP) and the net present value (NPV) are determined for each system.

The payback period (PBP) is the simplest method of examining one or more investment projects. It measures the time required to recover investment costs, therefore, it can be determined by dividing the investment cost by the savings made per year as follows.

$$\text{PBP} = \frac{IC}{ACF} \tag{4.3}$$

IC is the investment cost (initial capital) and ACF is the annual cash flow (saving or revenue). The annual cash flow is the difference in amount of cash available at the beginning of a year (opening balance) and the amount at the end of that year (closing balance). However, this method has some limitations:

- Ignores the benefits that occur after the payback period, which are recommended for consideration as the solar air-conditioning system could still be working reliably for up to 25 years.

- Ignores the changing value of money over time. The change of money value could be due to the inflation and/or the discounted cash flow.

The Net Present Value (NPV) is a traditional analytical method used to describe time adjusted economic benefits or savings between competing alternatives. It is the difference between the sum of discounted cash flow which is expected from the investment, and the amount that is initially invested. In this study, the net present value methodology analysis is conducted using the economical concept of the solar engineering field [129] which is expressed as:

$$\text{NPV} = \frac{A*(1+i)^{N-1}}{(1+d)^{N}} \tag{4.4}$$

A is the investment cost, i is the inflation rate, d is the discount rate and N is the total number of periods. In financial concept, if there is a choice between two alternatives, the one yielding the higher NPV should be selected. If NPV > 0, the investment would add value and the project is feasible to be accepted. If NPV < 0, it means the investment is not feasible and the project should be rejected.

The operating cost (electricity and maintenance) is one of the major elements in the economical analysis. In Saudi Arabia, the electricity rate is classified into three categories by Saudi Arabia Electricity & Cogeneration Regulatory Authority rate based on monthly consumption as shown in Table 4-5. The building under study consumes more than 8,000 kWh per month. Therefore, the electricity cost is $0.0693/kWh.

Table 4-5 Saudi Electricity Rates for Commercial Sector [130]

Monthly Consumption Range (kWh)	**Rate (SR/kWh)**	**Rate ($/kWh)**
0- 4,000	0.12	0.0320
4,001-8,000	0.20	0.0533
More than 8,000	0.26	0.0693

The electric consumption of the absorption chiller due to electrical pump consumption is assumed 10% of the vapor compression chiller consumption [31]. The actual consumption of the pump is calculated and discussed in the results and discussion chapter. For PV-vapor compression chiller, there is no electricity consumed from the grid

and there is no electrical operating cost subjected to this system**.** The annual maintenance cost for vapor compression system is assumed to be 4% of the investment cost [35]. For the solar absorption system, the annual maintenance cost is 0.1% of the investment cost [35]. The key parameters used for economical analysis are shown in Table 4-6.

Table 4-6 Key parameters of economical analysis

	Unit	**Rate**
Collectors [125]	$\$/m^2$	230
Absorption Chiller, COP=0.7 [125]	\$/kW	516
Hot Water Tank [41]	$\$/m^3$	1000
VC Chiller, COP=2.5 [125]	\$/kW	400
PV System [131]	$\$/kW_p$	1,776
Electricity Rate [130]	\$/kWh	\$0.0693
Discount Rate [132]	-	3%
Inflation [133]	-	4%
VC Chiller Life Cycle [18]	Years	12
Absorption Chiller Life Cycle [18]	Years	20

4.6 Thermodynamic Analysis of Solar Absorption System

The analysis in section 4.2 to 4.5 was carried out based on the assumption of COP and electric pump consumption. In order to evaluate the actual PBP and NPV based on actual COP and pump electric consumption, the thermodynamic analysis of the solar absorption system is performed to find the required inlet and outlet thermodynamic states of the refrigerant and refrigerant-absorption solution for each stage of the absorption cycle in steady-state operation. The thermodynamic analysis is based on the first law of thermodynamics and the appropriate property relations.

The second law efficiency "exergy" is obtained by determining the maximum coefficient of performance as expressed by equations 4.5 and 4.6.

The second law efficiency is given as:

$$\eta_{II} = COP/COP_{max} \quad (4.5)$$

where the $$COP_{max} = (T_g - T_E / T_g) * (T_e/T_E - T_e) \quad (4.6)$$

The performance of the system based on varying parameters of the design is analyzed using Engineering Equation Solver (EES).

Since heat rejection to the environment is required in condenser and absorber, they need to operate at higher temperature than ambient temperature. The initial assumed temperature difference between the condenser/absorber and the ambient is 10 ºC. The

maximum summer hourly average ambient temperature in Dhahran (Khobar) is 41ºC [1] Table 4-7 shows the assumed design temperatures.

Table 4-7 Design Temperature Variables

Component	Generator	Condenser	Evaporator	Absorber
Temperature (ºC)	105	51	7.5	51

CHAPTER 5

DESIGNS FOR CONTINUOUS OPERATION (24-HOUR A DAY) SOLAR LIBR-WATER ABSORPTION AIR-CONDITIONING SYSYEM

This chapter presents the proposed alternative designs of a continuous operation (24-hour a day) solar-powered LiBr-water absorption air-conditioning system. Solar-powered LiBr-H_2O air-cooled absorption air-conditioning systems can achieve continuous operation (day and night) based on different types of thermal energy storage systems. The use of air-cooled absorption systems with no cooling tower saves water, reduces maintenance cost and space, which are major key considerations for the residential sector. The cooling tower needed for the water-cooled system increases the operation cost and the initial cost of the system. It might cause the growth of bacteria. The main disadvantage of water cooling system is the associated water consumption, ranging from 2 kg and 5 kg kWh^{-1} of cooling [134]. Those drawbacks make water-cooled systems have lower feasibility compared to the air-cooled systems for small scale cooling applications, especially in regions where water is scarce such as in Saudi Arabia. The continuous operation designs for 24-hour solar-powered LiBr-water absorption air-conditioning systems are categorized based on the storage techniques in use, as heat storage, or cold storage or refrigerant storage.

In this chapter, chapter 7 and chapter 8, the following major definitions are used:

Weak solution: low refrigerant (water) content, weak-in-refrigerant while the absorbent (LiBr) has high concentration.

Strong solution: high refrigerant (water) content, strong-in-refrigerant while the absorbent (LiBr) has low concentration.

5.1 Heat Storage System

The stored hot thermal energy is supplied to the generator when the incident solar radiation is insufficient to produce the required generator temperatures. This is the most common storage method in solar cooling systems. The main advantage of the heat storage system is the employment of heat storage unit for continuous (day and night) cooling requirements using a LiBr-H_2O vapor absorption air-conditioning system.

The heat storage system stores heat during the day when the solar energy is sufficient and utilizes the stored heat during both nighttime (when solar energy is not available) and when solar insolation is not sufficient to produce the required generator temperature for operating the system. Figure 5-1 shows a continuous operating solar-powered LiBr-water vapor absorption air-conditioning system with heat storage. As shown in figure 5-1, this system requires two sets of solar collectors. The first set of

collectors, flat plate type, provides solar energy to the generator for daytime operation, and the second set of collectors, evacuated tube type, provides energy to the heat storage tank at a relatively much higher temperature for nighttime operation and when the solar insolation is insufficient. The second set of collectors operates at much higher temperature due to the heat storage temperature requirements which make the cost more expensive compared to the first set of collectors. The designs of two sets of collectors will results in cost saving as the first set that provides solar energy to the generator will be decrease the overall solar collecting cost.

The refrigerant-absorbent solution is heated in the generator where refrigerant (water) is released from the absorbent (LiBr). The weak refrigerant-absorbent solution travels to the absorber while the refrigerant vapor travels to the condenser. The weak solution is throttled through the first expansion valve (EV1) in order to reduce the pressure of the solution. The refrigerant experiences a throttling process through the second expansion valve (EV2) to decrease the pressure of the refrigerant and then it passes to the evaporator and then to the absorber, where it is reabsorbed by the weak solution to create a strong refrigerant-absorbent solution. This solution is then pumped to the generator, thus completing the cycle. The heat exchanger between the generator and absorber is used to increase the performance of the system.

During the night, both sets of collectors come to an end to operate and the heat storage tank is directly connected through valves to the generator to provide the required heat. The heat from the absorber and the condenser can be rejected to the environment by

natural convection or forced fan. The whole electrical energy requirement for the entire heat storage system is limited to that required by the solution pump. The valves: V1, V2, V5 and V6 are in open mode during daytime operation and closed in the nighttime operation. However, the valves V3 and V4 are in closed mode during daytime operation and opened in the nighttime operation and at the period of low solar insolation.

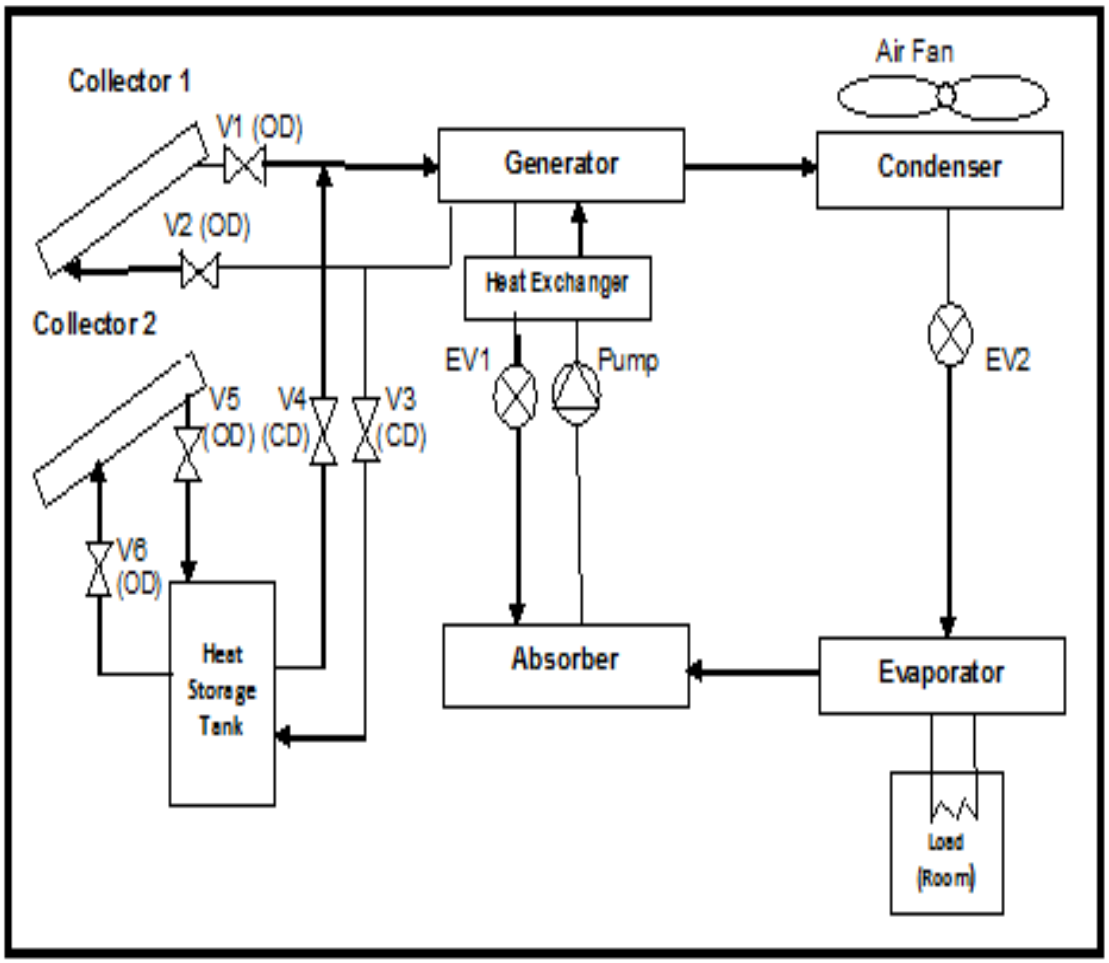

Figure 5-1 Continuous Operated Solar-powered LiBr-Water Absorption Air-conditioning System with (Heat Storage).
(CD): Closed Daytime
(OD): Open Daytime
EV: Expansion Valve

5.2 Cold Storage System

The cold storage tank is introduced after the evaporator, as shown in figure 5-2. Losses to the environment in this system can be expected to be lower than in hot thermal energy storage because of the lower temperature difference between working and ambient temperatures. Working with cold thermal energy storage, the cooling effect is produced during the day, and excess over the daytime load is stored for later use when the heat input is not sufficient to separate the refrigerant from the solution in the generator.

Figure 5-2 shows a solar powered LiBr-water vapor absorption air-conditioning system with cold storage. During the day, solar energy gained by the solar collector provides heat to the refrigerant-absorbent solution in the generator and refrigerant (water) is released from the absorbent (LiBr) as a vapor. The refrigerant travels to the condenser, expansion valve, evaporator, and absorber, where it is reabsorbed by the weak solution to create a strong refrigerant solution. This solution is then pumped to the generator, and the heat exchanger between the generator and absorber is used to increase the performance of the system as a heat storage system. The required amount of cooling for nighttime requirements is stored in the cold storage tank.

Similar to the heat storage system, the heat from the absorber and condenser can be rejected to the environment by natural convection or forced fan. The total electricity requirement for the whole cold storage system is limited to that needed by the solution

pump. The three-way valve is used to enhance the system performance by regulating the storage of the daytime load and nighttime load for later use when the heat input is not sufficient to separate the refrigerant from the solution in the generator.

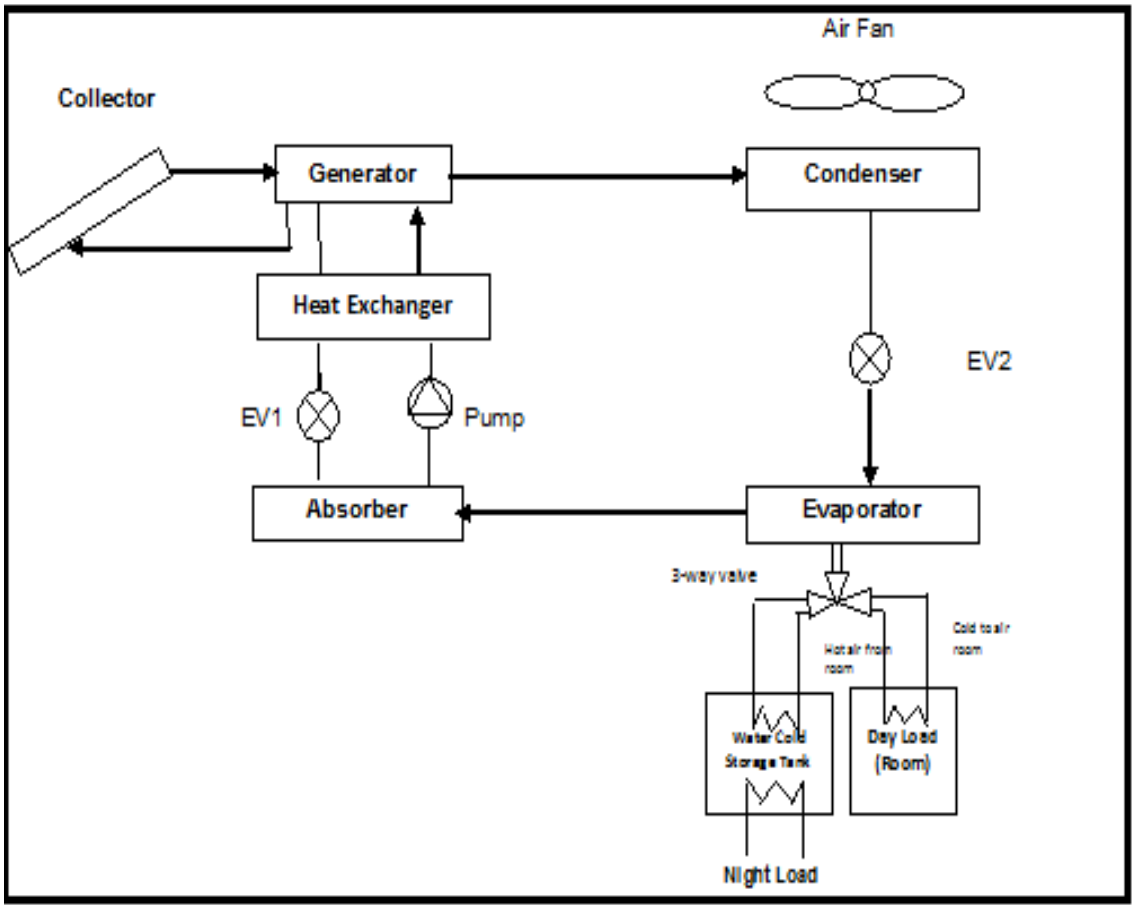

Figure 5-2 Continuous Operated Solar-powered LiBr-Water Absorption Air-conditioning System with (Cold Storage). (EV: Expansion Valve).

5.3 Refrigerant Storage System

The LiBr-water vapor absorption system with refrigerant storage is one of the primary designs under consideration. The storage for this system is associated with the condenser where the storage tank accumulates the refrigerant during the hours of high solar insolation. Then, this stored liquid refrigerant can be regulated at other times (e.g., nighttime) to meet the required cooling loads [135]. Figure 5-3 shows a continuous operated solar powered lithium bromide-water absorption air-conditioning system with refrigerant storage.

In this system, the storage temperature occurs at or near room temperature. The valves: V1 and V3 are in open mode in day operation and closed for night operation while valve V2 is in close mode in the day operation and open for nighttime operation and low solar insolation.

The advantages and disadvantages for each of these system designs are summarized in Table 5-1.

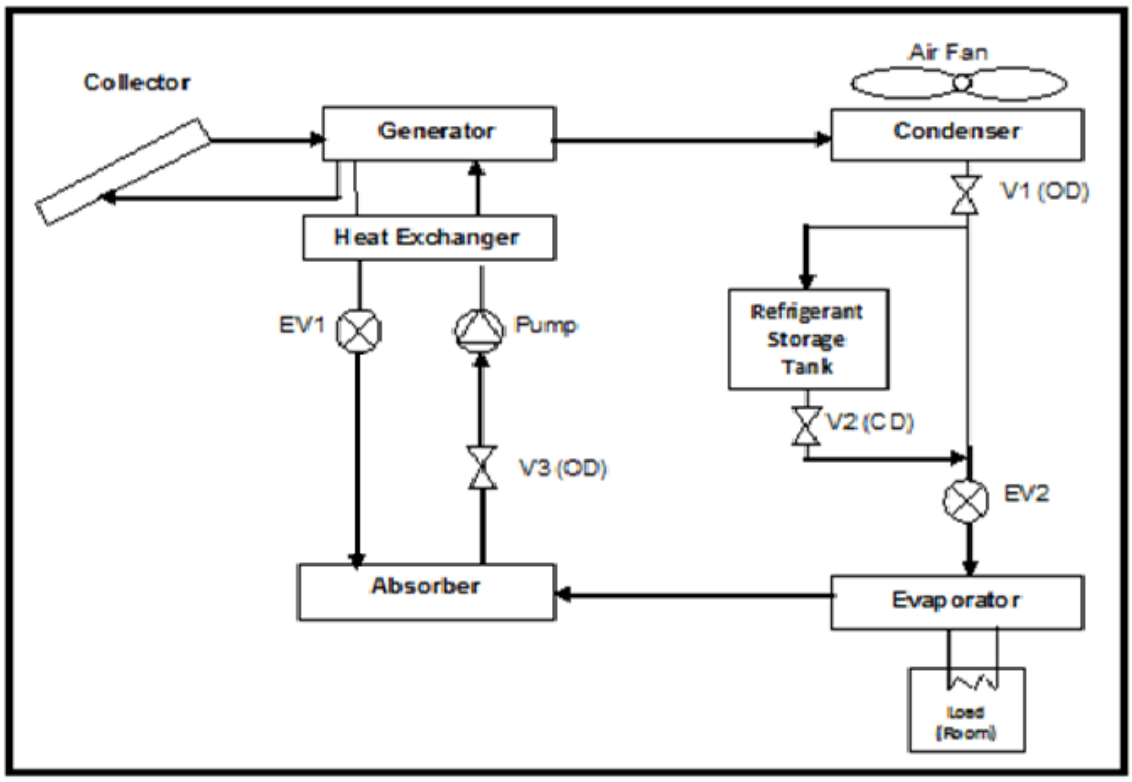

Figure 5-3 Continuous Operated Solar-powered LiBr-Water Absorption Air-conditioning System with (Refrigerant Storage).
(OD): Open Daytime
(CD): Closed Daytime
EV: Expansion Valve

Table 5-1 Comparative Analysis of Continuous Operation Designs

Design	Advantages	Disadvantages
Heat Storage	• COP of this system is relatively higher for nighttime operation.	• Two sets of solar collectors are required. • Components of the absorption system operate at daytime and nighttime. • Storage tank requires thicker insulation. • Evaporator works continuously.
Cold Storage	• Components of the absorption system operate at daytime only. • Less complexity in the control requirements due to less number of closing and opening daytime valves. • Evaporator works during daytime only.	• Larger evaporator size. • Larger generator size.
Refrigerant Storage	• Comparatively smaller solar collector size than heat and cold storages. • Storage pressure is low which makes the strength requirements of the storage tank not critical. • Storage tank has thinner insulation.	• Evaporator operates at daytime and nighttime as the heat storage design.

CHAPTER 6

HYBRID STORAGE SOLAR LIBR-WATER ABSORPTION AIR-CONDITIONING SYSYEM

This chapter presents the proposed alternative designs of the hybrid storage solar-powered LiBr-water absorption air-conditioning system. The 24-hour storage design is an important parameter that determines the performance of the system and optimizes its components. Introducing hybrid storage designs can improve system performance, reduce collector size, lower storage tank capacity, and hence makes the system more feasible. Moreover, hybrid storage designs will ensure 24-hour a day operation through uninterrupted operation in case of maintenance for one of the storage tank. Four hybrid storage designs (heat and refrigerant storage, cold and refrigerant storage, heat and cold storage, and heat, cold and refrigerant storage) are investigated.

The main features of hybrid storage systems instead of one storage tank are:

- Continuous uninterrupted operation even if one of the storage tanks is in maintenance.
- Storage tank size optimization which will reduce the overall cost of the system.

Solar-powered LiBr-H_2O absorption air-conditioning systems can meet continuous operation (daytime and nighttime) based on different types of thermal energy hybrid storage systems. The four alternative designs for 24-hour a day solar-powered LiBr-Water absorption air-conditioning systems are categorized based on the hybrid storage techniques used, as follows:

1) Heat and Refrigerant Storage

2) Cold and Refrigerant Storage

3) Heat and Cold Storage

4) Heat, Cold and Refrigerant Storage

6.1 Heat and Refrigerant Storage System

The stored hot thermal energy is supplied to the generator when the incident solar radiation is insufficient to produce the required generator temperatures. The heat storage tank will store heat during the daytime when the solar energy is sufficient and utilize the stored heat at both the nighttime when the solar energy is not available and when the solar insolation is not sufficient to produce the required generator temperature for the operation of the system.

The refrigerant storage is in association with the condenser where the storage tank accumulates the refrigerant during the hours of high solar insolation. Then, this stored liquid refrigerant can be throttled at other times (e.g. nighttime) when heat storage in not

sufficient to meet the required cooling loads. The storage temperature occurs at or near room temperature.

Figure 6-1 shows a continuous operated solar powered lithium bromide-water vapor absorption air-conditioning system with hybrid heat and refrigerant storage. The system requires two solar collectors' sets. The first set of solar collector supplies solar energy to the generator during the period of the daytime operation. However, the other set of solar collector provides energy to the heat storage unit. The refrigerant-absorbent solution is heated in the generator where refrigerant (water) is released from the absorbent (LiBr). The weak absorbent-refrigerant solution flows to the absorber while the refrigerant vapor flows to the condenser. The refrigerant goes through a throttling process, the evaporator and then to the absorber where it is reabsorbed by the weak solution to create a strong refrigerant solution. The solution is then pumped to the generator thus completing the cycle and the heat exchanger between the generator and absorber is used to increase the performance of the system.

For the nighttime, both set of collectors come to an end to operate and the heat storage tank is then connected directly to the generator to provide the required heat at the period of nighttime in order to meet portion of the required cooling load. The refrigerant storage tank is connected to evaporator to provide the rest of required cooling load during nighttime operation. The heat rejection to the ambient can be by natural convection or forced convection using a fan. The whole electricity needed for the whole system is limited to that needed to drive the solution pump. Valves: V1, V2, V5, V6 and V7 are in

open mode during day operation and closed during night operation. Valves: V3, V4 and V8 are in close mode in during operation and open during night operation.

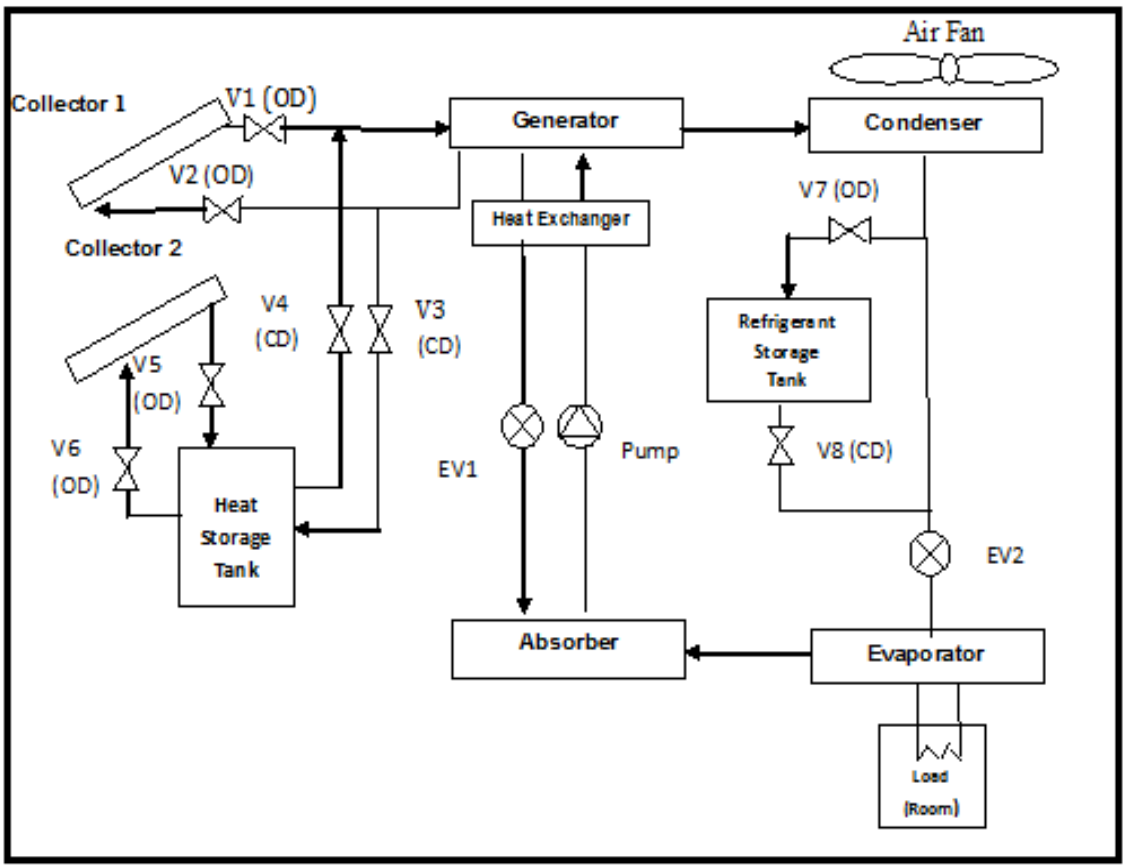

Figure 6-1 Continuous Operated Solar powered LiBr-Water Absorption Air-conditioning System with Hybrid Storage Heat and Refrigerant Storage.
(CD): Closed Daytime
(OD): Open Daytime
EV: Expansion Valve

6.2 Cold and Refrigerant Storage System

The cold storage tank is introduced after the evaporator as shown in figure 6-2. Losses to the environment in the cold storage can be expected to be lower than in hot thermal energy storage because of lower temperature difference between working temperatures and ambient. Working with cold thermal energy storage, cooling effect is produced during the day which exceeds the daytime load needs and hence the additional cooling effect is stored and used later when the heat input is not sufficient to separate refrigerant from the solution in the generator.

The refrigerant storage is in association with the condenser where the storage tank accumulates the refrigerant during daytime. Then, this stored liquid refrigerant can be throttled at nighttime to meet the required cooling loads in parallel with cold storage supply. The required amount of cooling effect for nighttime requirement is stored in the cold storage tank.

The heat rejection to the ambient and total electricity needed is similar to the hybrid heat and refrigerant storage system. Valves: V1, V3, V4 and V5 are in open mode during day operation and closed during night operation while valve V2, V6 and V7 is in close mode during day operation and open during night operation.

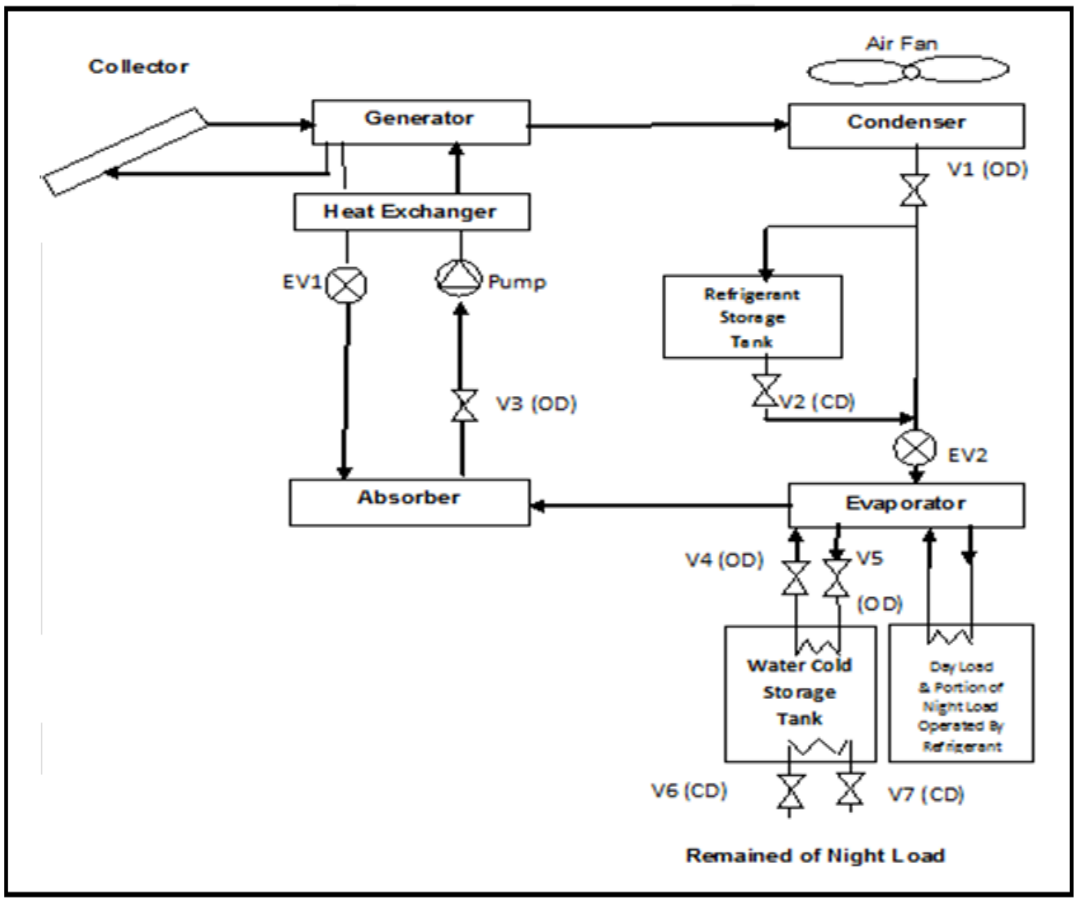

Figure 6-2 Continuous Operated Solar powered LiBr-Water Absorption Air-conditioning System with Hybrid Cold and Refrigerant Storage.
(CD): Closed Daytime
(OD): Open Daytime
EV: Expansion Valve

6.3 Heat and Cold Storage System

In this system, the heat storage is combined with cold storage as shown in figure 6-3. Solar energy obtained by the solar collector, during the period of daytime operation, provides heat to the refrigerant-absorbent solution in the generator and refrigerant (water) is released from the absorbent (LiBr) as a vapor. The required amount of cooling effect for nighttime requirement is stored in the heat and cold storage tanks.

The heat rejection to the ambient and total electricity needed is similar to the hybrid heat and refrigerant storage and cold and refrigerant storage systems. Valves: V1, V2, V5, V6, V7 and V8 are in open mode during day operation and closed during night operation. Valves: V3, V4, V9 and V10 are in close mode during day operation and open during night operation.

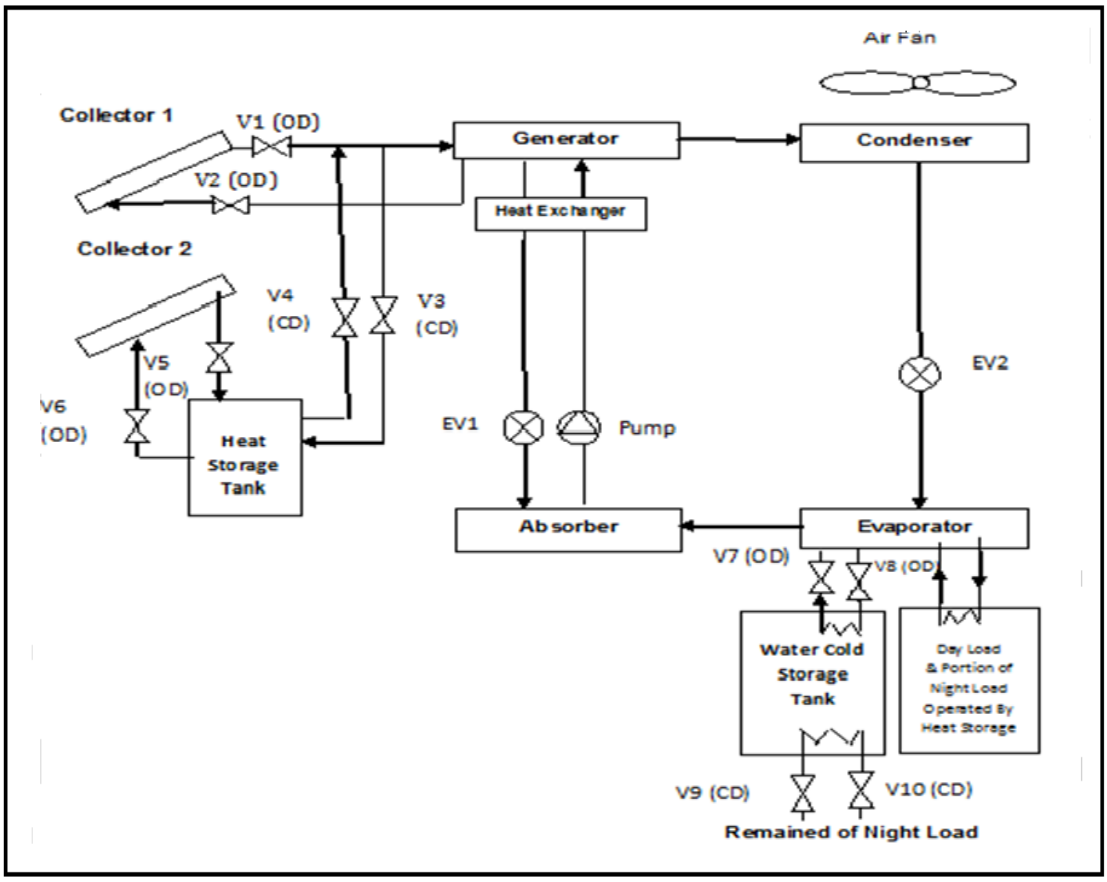

Figure 6-3 Continuous Operated Solar powered LiBr-Water Absorption Air-conditioning System with Hybrid Heat and Cold Storage.
(CD): Closed Daytime
(OD): Open Daytime
EV: Expansion Valve

6.4 Heat, Cold and Refrigerant Storage System

In this system, the heat storage is combined with cold and refrigerant storage as shown in figure 6-4. For the period of the daytime operation, solar energy obtained by the solar collector provides heat to the refrigerant-absorbent solution in the generator and refrigerant (water) is released from the absorbent (LiBr) as a vapor. The refrigerant flows to the condenser, the expansion valve, the evaporator and the absorber where it is reabsorbed by the weak solution to create a strong refrigerant solution. This solution is then pumped to the generator and the heat exchanger between the generator and absorber is used to increase the efficiency of the system as the heat storage system. The required amount of cooling effect for nighttime requirement is stored in the three storage tanks.

The heat rejection to the ambient and total electricity needed is similar to the other hybrid storage systems. Valves: V1, V2, V5, V6, V7, V9 and V10 are in open mode in during day operation and closed during night operation. The valves: V3, V4, V8, V11 and V12 are in close mode during day operation and open during night operation.

A comparative analysis based on the advantage and disadvantages for each of the four system designs is summarized in Table 6-1.

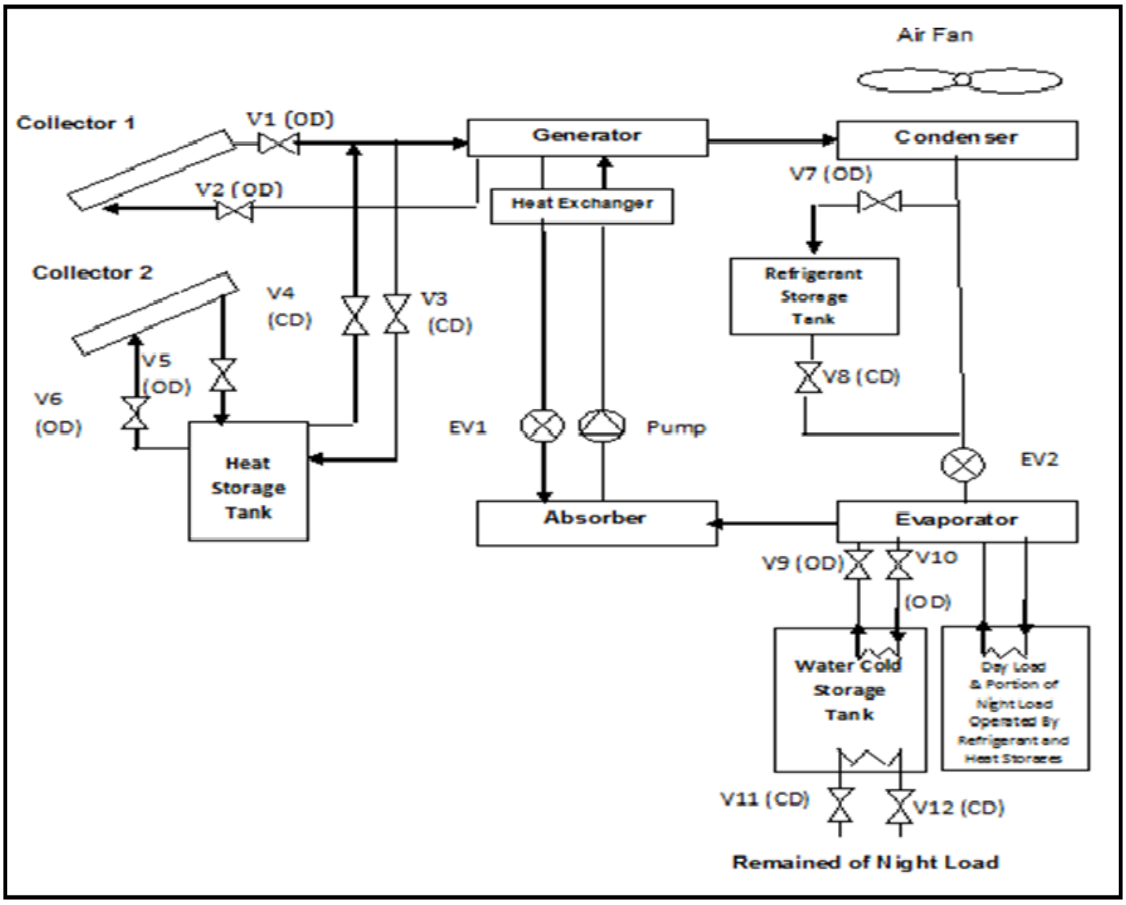

Figure 6-4 Continuous Operated Solar powered LiBr-Water Absorption Air-conditioning System with Hybrid Heat, Cold and Refrigerant Storage.
(OD): Open Daytime
(CD): Closed Daytime
EV: Expansion Valve

Table 6-1 Comparative Analysis of Hybrid Storage System Designs

Design	Advantages	Disadvantages
Heat and Refrigerant Storage	• COP of the system is comparatively higher than cold & refrigerant system for nighttime operation. • Refrigerant storage tank has thinner insulation.	• Two sets of solar collectors are required. • Components operate at daytime and nighttime. • Heat storage tank requires thicker insulation.
Cold and Refrigerant Storage	• Components, generator, condenser and absorber operate at daytime only. • Less complexity in the control requirements due to less number of closing and opening daytime valves. • Refrigerant storage tank has thinner insulation.	• Larger evaporator size. • Larger generator size. • Evaporator works continuously.
Heat and Cold Storage	• COP of the system is comparatively higher than cold & refrigerant system for nighttime operation.	• Two sets of solar collectors are required. • Components operate at daytime and nighttime. • Larger evaporator size. • Larger generator size.
Heat, Cold and Refrigerant Storage	• COP of the system is comparatively higher than cold & refrigerant system for nighttime operation. • Refrigerant storage tank has thinner insulation.	• Two sets of solar collectors are required. • Components operate at daytime and nighttime. • Larger evaporator size. • Larger generator size.

CHAPTER 7

THERMODYNAMIC ANALYSIS FOR CONTINUOUS OPERATION AND HYBIRD STORAGE DESIGNS

This chapter presents a detailed thermodynamic analysis based on mass and energy balance for each component for the developed designs for the continuous operation systems and the hybrid storage systems. The thermodynamic analysis has been used for solar absorption (LiBr-water) air-conditioning system for residential building application in order to have wider coverage of study for potential implementation as the commercial sector was studied in chapter 4.

7.1 Thermodynamic Analysis for Continuous Operation Designs

The thermodynamic analysis of the three designs is carried out to analyze the performance and capacity based on varying the design parameters. The cooling loads are estimated to fulfill the cooling requirements of a typical family living house in Dhahran to meet summer peak cooling load. A constant hourly average cooling of 5 kWh (Q_E = 5 kWh) is considered for the 24 hours of the day (day and night). This is equivalent to a total daily cooling load of 120 kWh. The systems are designed to meet a constant cooling load over the 24 hours. It is assumed that 10 hours of solar energy available for Dhahran,

Saudi Arabia, at a constant yearly average daily solar radiation of 5.84 kWh m^{-2} [124]. In this chapter, a steady-state model is used. The three systems have been designed to meet maximum summer temperature in Dhahran. The assumption of a constant cooling load for day and night can be acceptable in Dhahran (near Gulf) area since there is no great temperature difference between day and night ambient temperatures. Such assumption might not be acceptable for Riyadh city where there is large variation between day and night ambient temperatures. Accordingly, variation of solar radiation with time has not been taken into consideration and a daily average (constant) solar radiation was considered instead. The constant cooling load is assumed mainly to accommodate summer peak load.

The analysis is performed under ambient conditions in Dhahran. Based on Dhahran ambient temperatures, the daytime ambient temperature is assumed to be 41 ºC, the maximum summer yearly average temperature in Dhahran. The hourly average weather data used of 2012 to study the climate weather data for Dhahran, Saudi Arabia (latitude = 26.16) as presented in [1, 136]. The annual average ambient maximum temperature is presented in Table 7-1. From Table 7-1, it can be seen that the maximum summer annual average temperature in Dhahran is approximately 41 ºC. Thus, the three systems have been designed to meet such a maximum average summer temperature in Dhahran.

Table 7-1 Annual Average Temperature Data for Dhahran

Summer Temperature	Winter Temperature	Summer Temperature Range	Winter Temperature Range
41 ℃	10 ℃	10-12 ℃	7-8 ℃

The systems are designed to reject heat to the ambient, therefore, the absorber and condenser temperature are designed to operate 5 ℃ above the ambient temperature which is 41 ºC daytime and 33 º C nighttime. Thus, the daytime operating temperature of the condenser and absorber is maintained at 46 ºC, whereas their nighttime operating temperature is 38 ºC. The generator operating temperature is selected to be 100 ºC and 90 ºC for day and night operation, respectively. Selective-coated flat plate solar collectors are used in the cold storage system, the refrigerant storage system and for the first set of collectors in the heat storage system required for daytime operation. For the second set of collectors in the heat storage system, evacuated tube solar collectors are used to meet the high temperature requirements for the heat storage tank. The evaporator operating temperature is selected as 7.5 ºC (constant), which can be a suitable temperature for air-conditioning. The points of thermodynamic state (1-8) used in the analysis are shown in figure 7-1.

The formulation and consequent implementation under the following assumptions are made:

1. Steady-state operation
2. Only pure refrigerant flows through the condenser and evaporator
3. Refrigerant exiting the condenser is saturated liquid
4. Refrigerant exiting the evaporator is saturated vapor
5. Pump efficiency is 75%
6. Heat exchanger effectiveness is 70%
7. The efficiency for both selective flat plate collector and evacuated tube collector is 42% based on collector efficiencies curves developed by [136].

Figure 7-2 shows the enthalpy-concentration diagram for the steady-state LiBr-H_2O absorption cycle. State 3 has the lowest (evaporator) pressure value (P_{low}), which is constant and state 2 has the highest (condenser) pressure value. State 6 (after the pump) has the high solution pressure value and hence it is shown in the diagram above state 5. Since the throttling process is a constant enthalpy process, state 9 lie in the enthalpy-concentration diagram on top of state 10. However, state 9 is at the higher solution pressure (P_{high}) while state 10 is at the lower solution pressure (P_{low}).

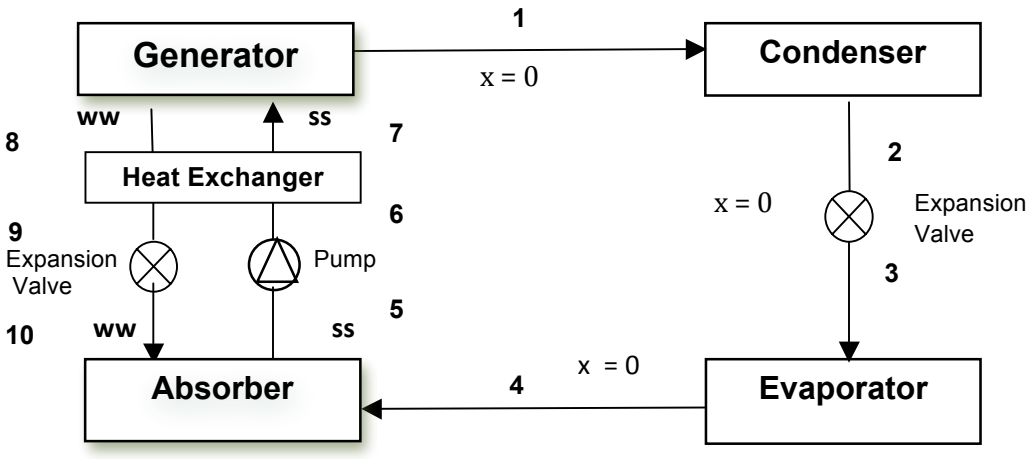

Figure 7-1 LiBr-H_2O Absorption Cycle

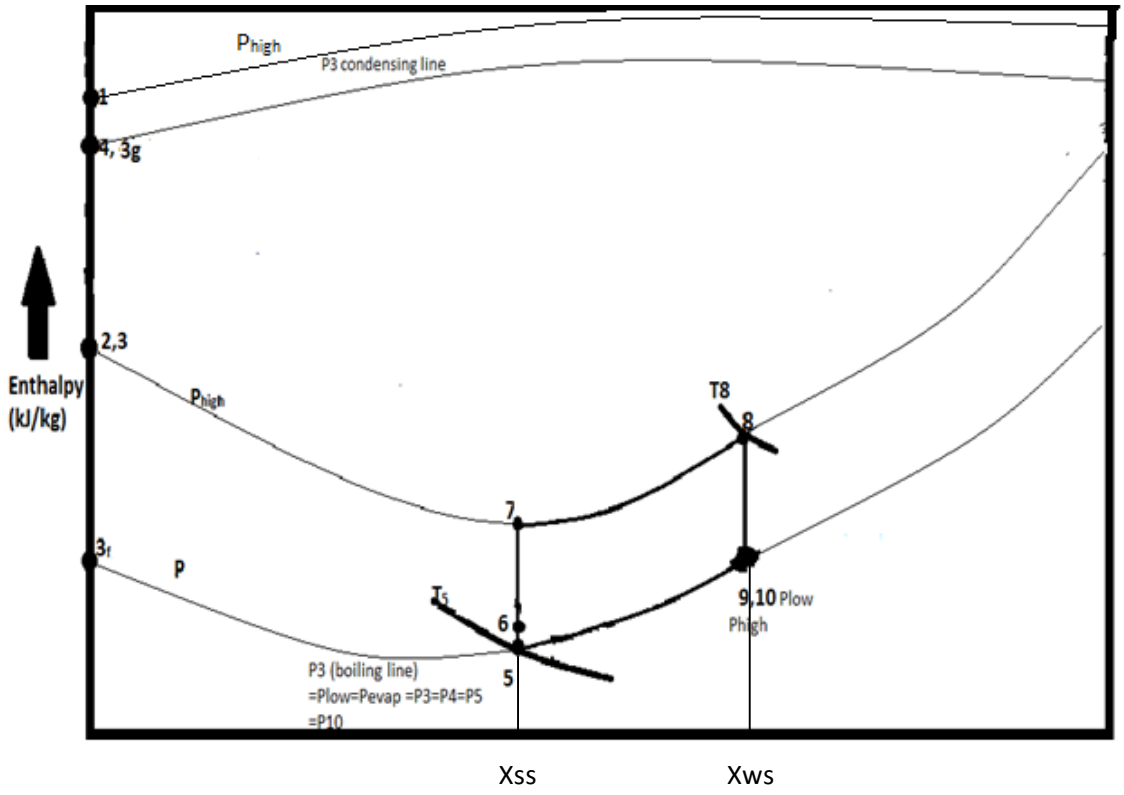

Figure 7-2 Enthalpy-Concentration Diagram of Steady-state LiBr-H_2O Absorption Cycle

Mass and energy balances are performed for the three systems:

Mass Balance

Figure 7-1 indicates that the mass flow rate of the weak solution is equal to the mass flow rate of thermodynamics states 8, 9 and 10. Hence;

$$\dot{m}_{ws} = \dot{m}_8 = \dot{m}_9 = \dot{m}_{10} \tag{7.1}$$

Also, figure 7-1 indicates that the mass flow rate of the strong solution is equal to the mass flow rate of thermodynamics states 5, 6 and 7 and written as:

$$\dot{m}_{ss} = \dot{m}_5 = \dot{m}_6 = \dot{m}_7 \tag{7.2}$$

Hence, the refrigerant (water) mass flow rate is written as:

$$\dot{m}_{r} = \dot{m}_{1} = \dot{m}_{2} = \dot{m}_3 = \dot{m}_4 \tag{7.3}$$

As the refrigerant is reabsorbed by the weak solution at the absorber, the mass flow rate of the strong solution is given as:

$$\dot{m}_{ss} = \dot{m}_r + \dot{m}_{ws} \tag{7.4}$$

Lithium Bromide-Water

The weak-in-water and strong-in-water refrigerant-absorbent solutions for lithium bromide-water are based on the mass fractions (concentrations) for weak-in-refrigerant and strong in-refrigerant solutions which are 65% and 60%, respectively [137]. The mass

flow rate of these solutions are written as:

$$\dot{m}_{ss} = \frac{Xws}{Xws - Xss}\dot{m}_r \quad (7.5)$$

$$\dot{m}_{ws} = \frac{Xss}{Xws - Xss}\dot{m}_r \quad (7.6)$$

Where Xws is the concentration of the solution weak-in-water and Xss is the strong-in-water solution in kg water/kg solution.

Energy Balance

Performing energy balance for the solution in the generator and the refrigerant in the evaporator; the heat transfer by the generator and the evaporator is expressed as:

$$\dot{Q}_G = (\dot{m}_r h_1 + \dot{m}_{ws} h_8 - \dot{m}_{ss} h_7) \quad (7.7)$$

$$\dot{Q}_E = (\dot{m}_r (h_4 - h_3)) \quad (7.8)$$

While the work needed to drive the pump is given as:

$$w_p = v (P_6 - P_5) = (h_6 - h_5) \quad (7.9)$$

$$\dot{W}_p = \frac{(\dot{m}ss\ (h6 - h5))}{\eta p} \quad (7.10)$$

Since the system operates in steady-state mode, $\dot{Q}_G = Q_{G,}\ \dot{Q}_E = Q_E$ and $\dot{W}_p = W_p$

Where the enthalpy $h_{(1\text{-}10)}$ is based on the thermodynamics states shown on figure 7-1.

For the cold storage system, the evaporator is working 24 hours per day and hence the evaporator heat transfer is given by:

$$Q_{ED} = \frac{QE\ .\ 24}{Solar\ Avaliable\ time} \quad (7.11)$$

Where Q_{ED} is the heat added to refrigerant in evaporator at daytime for cold storage system.

The enthalpies at the inlet and the exit of the expansion valve are equal:

$$h_3 = h_2 \quad (7.12)$$

$$h_{10} = h_9 \quad (7.13)$$

Heat exchanger effectiveness

The absorption system uses a heat exchanger between the generator and absorber to increase the performance and the effectiveness of the heat exchanger. The effectiveness of the heat exchanger is defined as the ratio of the actual heat transfer to the maximum possible heat transfer. The maximum heat transfer is the product of the solution minimum

mass flow rate and the enthalpy difference between the two heat exchanger inlet streams. Hence, the heat exchanger effectiveness is given as:

$$\varepsilon_{HE} = \frac{\dot{m}ss(h7 - h6)}{\dot{m}ws(h8 - h6)} \quad (7.14)$$

Coefficient of performance (COP)

The COP of an absorption system and the collector area can be expressed as follows:

$$COP = \frac{QE}{QG + Wp} \quad (7.15)$$

$$A_c = \frac{QG}{I \cdot \eta c} \quad (7.16)$$

The overall solar coefficient of performance that considers solar energy as the input source can be obtained as follows:

$$COP_s = \frac{QE}{Ac \cdot I} \quad (7.17)$$

For heat storage system, the generator, condenser, evaporator and absorber operate 24–hours in order to meet continuous day and night operation. The evaporator heat energy is constant at day and night times. The temperature values are designed according to the ambient conditions for day and night operations. The heat storage is obtained as:

$$Q_{hs} = Q_{Gn} \cdot \left[\frac{24 - Solar\ Avaliable\ Time}{Solar\ Avaliable\ Time}\right] \quad (7.18)$$

The mass storage for heat system is expressed as follows

$$m_{hs} = \frac{Qhs \cdot 3600 \cdot Solar\ Avaliable\ Time}{h\ in - h\ ex} \quad (7.19)$$

Where h_{in} is the enthalpy at the inlet of the heat storage tank and h_{ex} is the enthalpy at the exit of the heat storage tank.

For the heat storage system, the generator, condenser, evaporator and absorber operate 24 hours in order to meet continuous daytime and nighttime operation where the temperature values are designed according to the ambient conditions at day and night. The evaporator heat is constant at day and nighttime. Equations 7.1 to 7.15 are used for the analysis of heat storage system during the daytime operation and below equations used for the analysis during nighttime operation.

Mass Balance

Performing mass balance on the heat storage system during night operation**,** we get:

$$\dot{m}_{wsn} = \dot{m}_{8n} = \dot{m}_{9n} = \dot{m}_{10n} \quad (7.20)$$

The mass flow rate of the strong solution is equal to the mass flow rate of the thermodynamics states 5n, 6n and 7n as expressed below:

$$\dot{m}_{ssn}=\dot{m}_{5n}=\dot{m}_{6n}=\dot{m}_{7n} \quad (7.21)$$

Hence, the refrigerant mass flow rate is written as:

$$\dot{m}_{rn} = \dot{m}_{1n=} \dot{m}_{2n=} \dot{m}_{3n}= \dot{m}_{4n} \quad (7.22)$$

The mass flow rate of the strong solution is given as:

$$\dot{m}_{ssn}= \dot{m}_{rn}+\dot{m}_{wsn} \quad (7.23)$$

Lithium Bromide-Water

The strong and weak refrigerant-absorbent solutions are written as:

$$\dot{m}_{ssn}= \frac{Xws}{Xss-Xws} \dot{m}_{rn} \quad (7.24)$$

$$\dot{m}_{wsn}= \frac{Xss}{Xss-Xws} \dot{m}_{rn} \quad (7.25)$$

Performing energy balance on the heat storage system during night operation; we get

$$\dot{Q}_{Gn}= (\dot{m}_{rn}\, h_1n+ \dot{m}_{wsn}\, h_{8n}- \dot{m}_{ssn}\, h_{7n}) \quad (7.26)$$

$$\dot{Q}_{En} = (\dot{m}_{rn} (h_{4n} - h_{3n})) \quad (7.27)$$

The heat transfer by the evaporator during night operation is equal to the heat transfer by the evaporator during the day operation.

$$\dot{Q}_{En} = \dot{Q}_{E} \quad (7.28)$$

The work needed to drive the pump is given as:

$$w_{pn} = v\,(P_{6n} - P_{5n}) = v\,(P_{2n} - P_{4n}) = (h_{6n} - h_{5n}) \quad (7.29)$$

$$\dot{W}_{pn} = \frac{(\dot{m}ssn\,(h6n - h5n))}{\eta p} \quad (7.30)$$

Since the system operates in steady-state mode, $\dot{Q}_{Gn} = Q_{Gn,}\ \dot{Q}_{En} = Q_{En}$ and $\dot{W}_{pn} = W_{pn}$

The enthalpies at the inlet and the exit of the expansion valve are the same:

$$h_{10n} = h_{9n} \quad (7.31)$$

The heat exchanger effectiveness is given as :

$$\varepsilon_{HEn} = \frac{\dot{m}ssn(h7n - h6n)}{\dot{m}wsn(h8n - h6n)} \quad (7.32)$$

The COP of an absorption system and the collector area can be expressed as follows:

$$COP_{n} = \frac{Q En}{Q Gn + Wpn} \quad (7.33)$$

For cold storage system, the mass storage is given by:

$$m_{cs} = \frac{(24-\text{Hours Day}) \ . \ 3600 \ . \ QE}{h4 - h4f} \quad (7.34)$$

Where h_4 is the enthalpy of the vapor refrigerant (water) at the exit from the evaporator, h_{4f} is the enthalpy of the cold stored liquid refrigerant (water) in the cold storage tank.

The mass refrigerant storage can be obtained as follows:

$$m_{rs} = \dot{m}_r \ . \ 3600. \ (24\text{-Hours Day}) \quad (7.35)$$

where;

$$\dot{m}_r = \frac{QE}{(h4 - h3)} \quad (7.36)$$

For the three systems, engineering codes, Engineering Equation Solver (EES), have been simulated using the equations of the energy and mass balance. The software, Engineering Equation Solver (EES), is used to study the three systems performance based on variable design data for steady-state operation and to conduct the analysis of absorption cycles and produce all of the presented results. The EES has thermodynamic properties of LiBr-H_2O solutions that is a built-in procedure. Therefore, multiple iterations of the procedure are performed effectively to obtain the right solutions for the

problem under analysis. The iterative loop is carried out by EES using the mass and energy balance equations to determine the enthalpy (h) and mass flow rate ($\dot{m}$) values for each of the thermodynamics state to analyze the performance and storage capacity of the three systems based on the given design data related to the components temperature, heat exchanger effectiveness and pump efficiency.

7.2 Thermodynamics Analysis for Hybrid Storage Designs

The simulation of the four hybrid storage designs has been developed to analyze the performance and capacity based on varying the design parameters. The simulation is performed under ambient conditions in Dhahran and steady-state operation mode similar to the continuous operation designs. The daytime ambient temperature is assumed to be 41°C. Moreover, the cooling loads have been estimated to fulfill the cooling requirements of a typical family living house in Dhahran with constant cooling hourly average power of 5 kW (QE= 5 kWh) for a period of 24 hours (day and night) to meet a total daily cooling load of 120 kWh to cover mainly summer peak load.

It is assumed that 10 hours of solar energy available for Dhahran, Saudi Arabia, at constant yearly average daily solar radiation (I_H = 5.84 kWh/m^2 [124]). Based on the steady-state operation and the coincidence of the maximum cooling load with the period of maximum solar radiation input in Saudi Arabia, the average yearly average daily solar radiation is used. Accordingly, variation of solar radiation with time has not been taken into consideration and the average (constant) solar radiation was considered instead.

Based on Dhahran ambient temperatures, the daytime average ambient temperature is taken as 41 °C and the nightime average temperature is taken as 33 °C. Thus, the condenser and absorber daytime operating temperatures are kept as 46 °C to enable the system to reject heat to the ambient whereas their nighttime operating temperatures are kept as 38 °C. The generator operating temperature is selected as 100 °C at daytime

operation and 90 °C at nighttime operation. The evaporator operating temperature is selected as 7.5 °C, which can be a suitable temperature for air-conditioning or some vegitables and fruits cooling applications.

Selective-coated flat plate solar collectors are used in the four hybrid storage systems. For the second set of collectors in the three hybrid storage system (heat and refrigerant, heat and cold, heat-cold and refrigerant), evacuated tube solar collectors are used to meet the highly temperature requirements for the heat storage tank. The points of thermodynamic state (1-8) used in the analysis are shown in figure 7-1.

In order to simplify the formulation and the consequent implemetation, some assumptions are made:

1. Steady-state operation
2. Only pure refrigerant flows through the condenser and evaporator
3. Refrigerant exiting the condenser is saturated liquid
4. Refrigerant exiting the evaporator is saturated vapor
5. Pump efficiency is 75%
6. Heat exchanger effectiveness is 70%
7. The efficiency for the selective flat plate collector is 42% based on collector efficiencies curves developed by [136].
8. The efficiency for the evacuated tube collector is 42% based on collector efficiencies curves developed by [136].

In order to avoid crystallization, the weak and strong refrigerant-absorbent solutions for lithium bromide-water based on the mass fractions for weak and strong solutions assumed as 65% and 60%, respectively [137]. The mass flow rate of the strange and weak solutions can be found using equations (7.5 and 7.6).

Performing the energy balance for the solution in the generator and the evaporator; the heat transfer by the generator and the evaporator are given by equations (7.7, 7.8 and 7.10). The enthalpy h (1-10) is based on the thermodynamics state shown on figure 7-1.

The absorption system uses a heat exchanger between the generator and absorber to increase the effectiveness of the heat exchanger which is determined by equation (7.14). The collector area can be expressed using equation (7.16). The coefficient of performance (COP) and the overall solar coefficient of performance (COPs) that considers solar energy as the input source can be obtained from equations (7.15 and 7.17).

For the hybrid heat and refrigerant storage system, the generator, condenser, evaporator and absorber operate 24–hour in order to meet continuous day and night operation. As initial input for this system, both tanks store same amount of the cooling effect for nighttime operation. Thus, 50% of the required amount of cooling effect for nighttime operation is obtained by the stored thermal energy in the heat storage tank (RCEHS= 0.5, which is the ratio of cooling effect for nighttime by heat storage). The

optimum ratio of cooling effect for nighttime by heat storage for this system is discussed in details in the results and discussion chapter.

The evaporator cooling effect is constant during day and night. The temperature values are designed according to the ambient conditions for day and night operations. The heat and mass storage for the heat storage tank are obtained by using the following equations:

$$Q_{hs} = Q_{Gn} \cdot \left[\frac{24 - Solar\ Avaliable\ Time}{Solar\ Avaliable\ Time}\right] \quad (7.37)$$

$$m_{hs} = \frac{Qhs \cdot 3600 \cdot Solar\ Avaliable\ Time}{hin - hex} \quad (7.38)$$

where Q_{Gn} can be obtained from equation (7.26) and h_{in} is the enthalpy at the inlet of the heat storage tank and h_{ex} is the enthalpy at the exit of the heat storage tank. The refrigerant, strong solution and weak solution mass flow rate equations for the nighttime operation are expressed using equations (7.20, 7.21, 7.22, 7.23, 7.24 and 7.25)

The evaporator energy during the nighttime operation for the heat and refrigerant hybrid storage system can be found using the following equation.

$$Q_{\mathrm{En}} = Q_{\mathrm{E}} \,.\, \mathrm{RCEHS} \tag{7.39}$$

The refrigerant storage mass for the heat and refrigerant hybrid storage system can be obtained by equations (7.40 and 7.41):

$$m_{\mathrm{rsh}} = \dot{\mathrm{m}}_{\mathrm{rhh}}.\ 3600\ .\ (24\text{-Hours Day}) \tag{7.40}$$

$$\dot{\mathrm{m}}_{\mathrm{rhh}} = \frac{\mathrm{Q}E - \mathrm{Q}En}{(h4 - h3)} \tag{7.41}$$

For the hybrid cold and refrigerant storage system, as initial input, both storage tanks provide the cooling effect for nighttime operation equally, which means that 50% of the required amount of cooling effect for nighttime operation is stored in the cold storage tank (RCECS= 0.5, which is the ratio of cooling effect for nighttime by cold storage). The most favorable ratio of cooling effect for nighttime by cold storage for this system is discussed in details in the results and discussion chapter. The cold storage mass is obtained from equation (7.42):

$$m_{\mathrm{cs}} = \frac{(24\text{-Hours Day})\ .\ 3600\ .\ \mathrm{Q}CS}{h4 - h4f} \tag{7.42}$$

where;

$$Q_{CS} = Q_E . RCECS \quad (7.43)$$

The refrigerant storage mass for the cold and refrigerant hybrid storage system is obtained using equations (7.44 and 7.45):

$$m_{rsc} = \dot{m}_{rch}. 3600. (24\text{-Hours Day}) \quad (7.44)$$

$$\dot{m}_{rch} = \frac{Q_E - Q_{CS}}{(h4 - h3)} \quad (7.45)$$

For the initial input for the hybrid heat and cold storage system, the required amount of cooling effect for nighttime operation is stored equally in the heat and cold storage tanks (RCEHS = 0.5 and RCECS = 0.5). The ratio for both tanks is discussed in chapter 9. The heat and cold mass storages can be found for this system using equations (7.37, 7.39, 7.42 and 7.43).

For the hybrid heat, cold and refrigerant storages system, as initial input, 50% of the required amount of cooling effect for nighttime operation is stored in the heat and cold storage tanks (RCEHS = 0.25 and RCECS = 0.25). The ratio for the three storage tanks is investigated in the results and discussion chapter. The mass storages for this system are obtained from equation (7.37, 7.39, 7.42, 7.43, 7.46 and 7.47):

$$m_{rshc} = \dot{m}_{rhch}. 3600. \text{Hours Day} \quad (7.46)$$

$$\dot{m}_{rhch} = \frac{Q_E - Q_{En} - Q_{CS}}{(h4 - h3)} \quad (7.47)$$

The solar available time and components temperatures are given as initial design input for the simulation. The ratio of cooling effect for nighttime operation by heat storage tank, cold storage tank and refrigerant storage tank has been analyzed using EES. The engineering codes for these four hybrid storage systems have been developed by using Engineering Equation Solver (EES). These engineering codes use the mass and energy balance equations to analyze the performance of the four systems based on variable design data for steady-state operation. EES is used to conduct the analysis of absorption cycles and produce all of the presented results.

The EES has a built in procedure for thermodynamic properties of LiBr-H_2O solutions. Therefore, multiple iterations of the procedure are performed effectively to obtain the right solutions for the problem under analysis. The iterative loop is carried out by EES using the mass and energy balance equations to determine the enthalpy (h) and mass flow rate ($\dot{m}$) values for each of the thermodynamics states to analyze the performance and storage capacity of the four systems based on variable design data related to the components temperature, heat exchanger effectiveness and pump efficiency.

CHAPTER 8

UNSTEADY ANALYSIS FOR HYBIRD STORAGE DESIGNS

This chapter discusses the unsteady analysis for the hybrid storage design (cold plus refrigerant) for a continuous (24-hour a day) solar-powered LiBr-Water absorption air-conditioning systems. This chapter analyzes the impact of unsteady solar conditions on the operation parameters and the system performance of a hybrid storage LiBr-Water absorption air-conditioning chiller of 5 kW cooling power during a few representative days in summer and winter in Dhahran City, Saudi, Arabia. The system is designed to mainly cover summer peak load. The system consists of flat-plate collector and absorption chiller with hybrid storage tanks (cold and refrigerant) in addition to an excess heat storage tank that might be needed to prevent crystallization.

8.1 Hybrid Storage Design Description

Solar-powered LiBr-H_2O absorption air-conditioning system can meet continuous operation (daytime and nighttime) by using a hybrid cold and refrigerant storage system as shown in figure 8-1. The excess heat storage tank (EHST) shown in figure 8-1 is used to accommodate any extra heat (during solar insolation peak times) in order to avoid

crystallization due to the increase in the solution concentration above the allowable limit as a result of high generator temperature. The generator temperature might be more than the system requires for non-crystallization operation due to the increase in solar intensity and hence the collector output during peak solar insolation time. This excess heat can be utilized during hours of lower solar insolation and hence reduce the heat required to produce the refrigerant storage; which is another benefit of this excess heat storage tank. Moreover, the excess heat storage tank is used to supply hot water to the building heater.

Two temperature control valves (TCV1 and TCV2), one after the collector and the other after the excess heat storage tank (EHST), control and regulate the flow of the solar-collector fluid into the generator when the collector fluid temperature reaches its design limit (based on the generator working temperature range that prohibits crystallization). The temperature control valve (TCV1) directs the flow to the excess heat tank when the collector fluid temperature reaches 109 ºC. The second temperature control valve (TCV2) is used to regulate the temperature flow to supply the generator at 100 ºC. The flow to generator comes either from the collector directly or from the excess heat storage tank as one of the temperature control valves is closed when the other one is in the open mode, which means that both temperature control valves can't be in the open mode at the same time.

The heat rejection to the ambient can be by natural convection or forced fan. The total electricity requirement for the whole system is limited to that needed by the solution

pump. The valves: V1, V3, V4 and V5 are in open mode in the day operation and closed in night operation while valve V2, V6 and V7 are in close mode in the day operation and open in night operation.

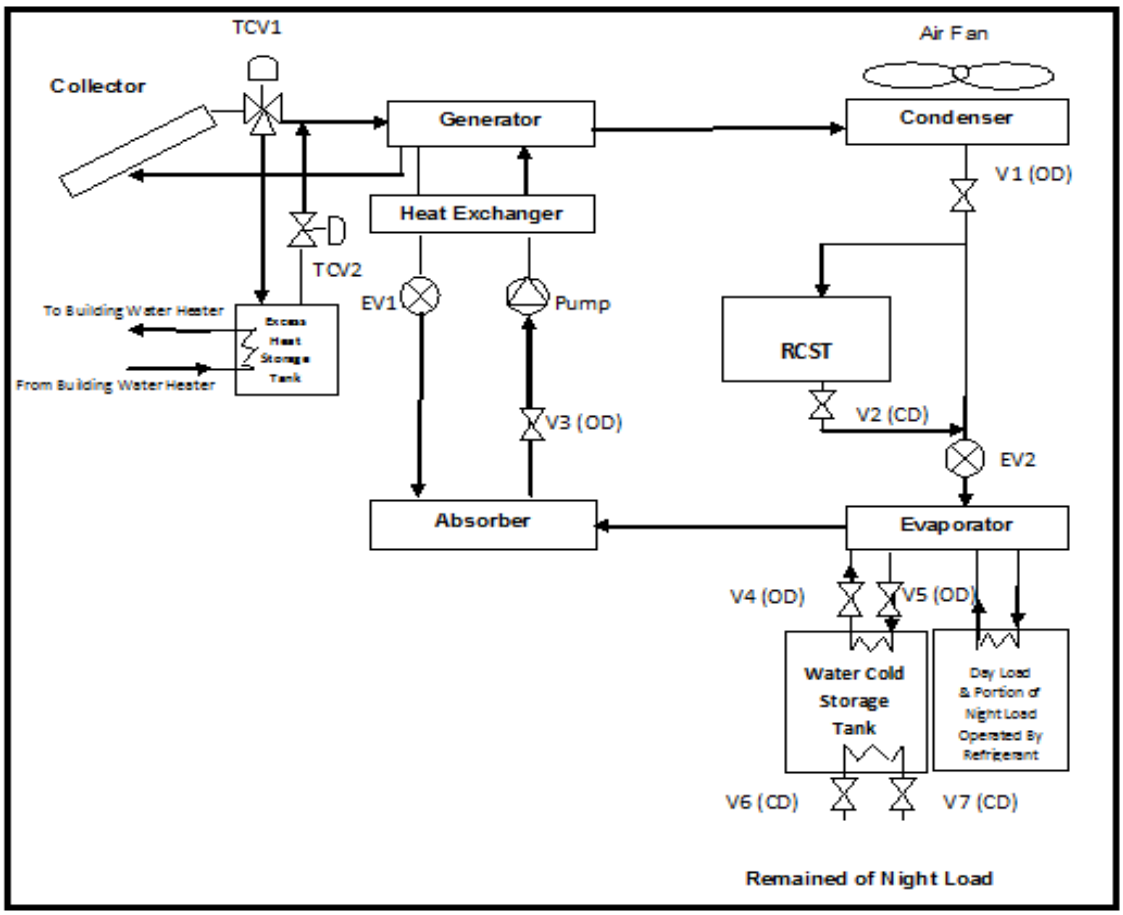

Figure 8-1 Continuously Operated Solar powered LiBr-Water Absorption Refrigeration System with Hybrid Cold and Refrigerant Storage.
(CD): Closed Daytime
(OD): Open Daytime
EV: Expansion Valve
RCST: Refrigerant-condensate (liquid-water) Storage Tank
TCV: Temperature Control Valve

The features of this system are:

- Continuous uninterrupted operation even if one of the storage tanks is in maintenance or taken away for repair which is not possible for other systems where only one type of storage tank is used.
- Crystallization prevention using excess heat storage tank and two temperature control valves
- The generator, condenser and absorber operate during daytime only.
- Less complexity in the control requirements due to less number of closing and opening daytime valves compared to hybrid heat and refrigerant storage system and hybrid heat and cold storage system.
- Assist building water heating system, the hot water can be supplied to the building from the excess heat storage tank.
- Refrigerant storage tank has thinner insulation compared to the cold and heat storage tanks.
- Cold and Refrigerant storage tanks sizes are smaller compared to the other hybrid storage systems such as hybrid heat and refrigerant storage system and hybrid heat and cold storage system.

8.2 Unsteady Enthalpy-Concentration Diagram

The thermodynamics state points (1-10) used in the analysis and simulation are shown in figure 7-1. For the sake of explanation, only three different time intervals (Δt) from morning till noon in the day period are shown in figure 8-2 as examples. The state points 1-10 represent the first time interval which starts when the generator temperature reaches its minimum required value to start the cycle operation. The second and the third time intervals are represented by the state points 1'-10' and 1''-10'', respectively.

The evaporator pressure (P_{low}) is constant with time based on a required constant cooling-effect temperature during the day and night time. However, the condenser pressure (P_{high}) varies and increases with time after sunrise based on the corresponding increase in solar intensity and ambient temperature. The mass concentrations of the solution in the generator and absorber also vary with time as shown in figure 8-2.

The maximum generator temperature can be one of the main causes of unacceptable level of the solution mass concentration, which leads to solution crystallization. The crystallization occurs when the concentration reaches high level [136]. Thus, the temperature control valves and the excess heat storage tank are used to control and regulate the flow of the solar collector fluid into the generator to avoid solution crystallization. Figure 8-2 shows that the weak and strong solution concentrations are increased with time due to the increase of generator maximum

temperature (from 8 to 8’ and then 8”) as the solar intensity and ambient temperature increase.

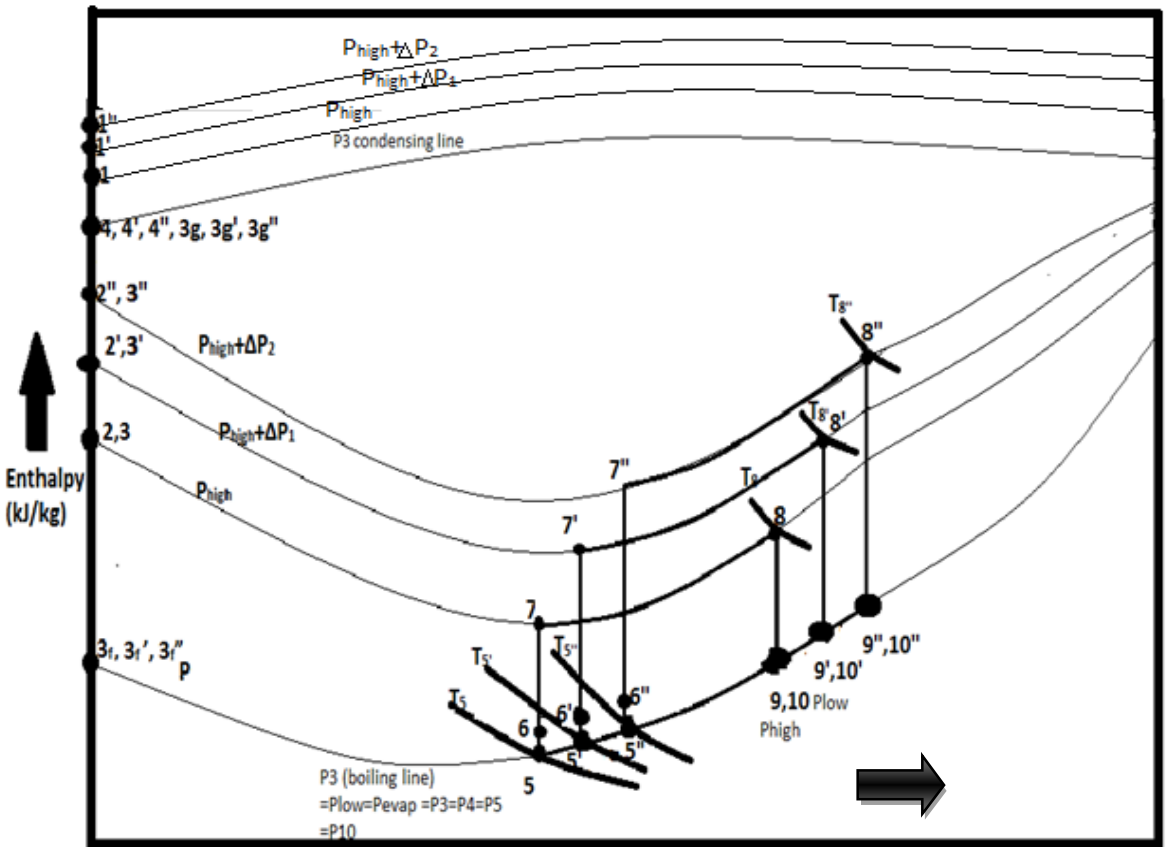

Pure Water **y, Concentration, kg Libr/ kg Solution = 1 - x**

y = 1

y = 0

x = 0

x =1

Figure 8-2 Enthalpy-Concentration Diagram of Unsteady LiBr-H_2O Absorption Cycle

8.3 Unsteady Thermodynamic Analysis

The analysis of this hybrid storage design has been developed to study the system performance and storage capacity based on estimated constant hourly cooling load of 5 kW for a period of 24 hours (day and night). This constant cooling power meets a total daily cooling load of 120 kWh. This assumption of a constant cooling load for day and night is acceptable in Dhahran (near Gulf) area since there is no great temperature difference between day and night ambient temperatures in such Gulf region. Such assumption might not be acceptable in Riyadh city where there is large variation between day and night ambient temperatures. The system is designed to meet this constant cooling load but it operates on an unsteady-state operation mode in accordance with the variable solar insolation and ambient temperature over the day. The collector and other components are designed to cover summer peak load. For each time interval Δt, the cycle is considered as a quasi-steady closed cycle in which the mass leaving a component is filled immediately by equivalent mass following it.

The operating parameters pertaining to generator, absorber and condenser temperatures, condenser pressure and enthalpies are dependent on the hourly variable ambient conditions. Accordingly the performance parameters of the system such as its COP vary throughout the day with the changes in ambient temperature and solar intensity. The plots for the unsteady energy analysis were developed by the EES Software at every one hour time-step interval.

During nighttime operation of this hybird-storage system, the refrigerant storage provides 50 % of the required amount of cooling effect and the remained 50 % are obtained by the cold storage. Selective-coated flat plate solar collector is used and the efficiency of the flat plate collector was assumed 42% [136]. The simulation is performed under Dhahran city ambient conditions. The condenser and absorber daytime operating temperatures are assumed at (T_{amb} + 5 ºC). The generator operating temperature is slected at (T_f - 3 ºC), where T_f is the solar collectors' working fuild exit temperature, and the evaporator operating temperature is selected as 7.5 °C (constant), which can be a suitable temperature for air-conditioning or some vegitables and fruits cooling applications. The minimum generator temperature required to operate the system in summer is 76 °C if the condenser temperature is above 35 °C. In winter, the minimum generator temperature required to operate the system is 55 °C if the condenser temperature is above 25 °C. In order to avoid crystallization, the maximum generator temperature should not exceed 109 °C in summer and 86 °C in winter. However, the generator temperature can reach in the present work 115 °C in summer and 94 °C in winter when the ambient temperature is above 38 °C (summer) and 20 °C (winter), respectively. This is because of the increases in the condenser temperature (hence pressure), which will decrease the possibility of crystallization. The following assumptions are made:

1. Only pure refrigerant (water) flows through the condenser and evaporator
2. Refrigerant exiting the condenser is saturated liquid
3. Refrigerant exiting the evaporator is saturated vapor
4. Pump efficiency is 75%
5. Heat exchanger effectiveness is 70%

The operating temperature of the generator depends on the temperature of the solar collectors' working fluid (T_f), which depends on the efficiency of the collector, ambient temperature (T_{amb}) and the solar intensity (I). The latter two parameters (T_{amb} and I) are taken from the hourly measured data for the city of Dhahran, Saudi Arabia by (the Research Institute at King Fahd University of Petroleum and Minerals, KFUPM). On the other hand, the area of the solar collectors' field depends on the thermal energy needed by the generator (Qg) to operate the system cycle for the given input conditions. The fluid temperature at the exit of the solar collector tubes (T_f) depends on the ambient temperature as well as the solar intensity based on the flat plate assumption (42% and flat-plate collector equation [136] as given by equation (1),

$$T_f = 0.098 * I + T_{amb} \tag{8.1}$$

The mass inside each component (control volume) of the cycle at the start of the time interval Δt is the same as that inside the same component at the end of that time interval Δt. Hence, there is no change in the mass inside the control volume.

$$m_f = m_i = m \tag{8.2}$$

$$\sum m_{in} = \sum m_{out} \tag{8.3}$$

where m_f is the final mass within boundaries of a system at end of a time interval (Δt), m_i is the initial mass within boundaries of a system at start of a time interval (Δt), m_{in} is the mass of fluid entering a system, m_{out} is the mass of fluid existing a system. However, for each component in the cycle under the unsteady working conditions, a generalized energy equation over each finite time duration (Δt), assuming uniform flow processes [138], can be written as:

$$Q - W = (\sum mh)_{out} - (\sum mh)_{in} + m\,(u_{f-}\,u_i)_{system} \qquad (8.4)$$

where Q and W are the net thermal and mechanical energies, m is the mass inside the control volume (CV) and ($u_{f-}\,u_i$) is the change in internal energy per unit mass inside the control volume during time Δt (u_f is the final internal energy per unit mass inside the CV at the end of the time step (Δt) while u_i is the initial value).

The mass flow rates of the weak and strong refrigerant-absorbent solutions for lithium bromide-water to avoid crystallization are based on the mass concentrations for weak and strong solutions as equations (7.5 and 7.6). By applying the energy balance for the solution; the generator and evaporator heat and pump work are given by equations (7.7, 7.8, 7.9 and 7.10) where the enthalpy $h_{(1\text{-}10)}$ is based on the thermodynamics state shown on figure 7-1 and Δt is one hour time-step interval.

The absorption system uses a heat exchanger between the generator and absorber to increase the coefficient of performance. The effectiveness of the heat exchanger is defined as the ratio of the actual heat transfer to the maximum possible heat transfer and is given by equation (7.14). The maximum heat transfer is the product of the minimum solution mass flow rate multiplied the enthalpy difference between the two heat exchanger inlet streams.

The COP of an absorption system and the collector area can be expressed as follows:

$$\text{COP} = \frac{Q\text{Ed}}{Q\text{G}+\text{Wp}} \tag{8.5}$$

Where Q_{Ed} is the evaporator heat during daytime operation which is required to fulfill the cooling requirements for daytime load as well the cold storage tank,

$$Q_{\text{Ed}} = \frac{Q\text{E}*24}{Effective\ Sunlight\ hours} \ * \text{RCECS} \tag{8.6}$$

RCECS is the ratio of cooling effect for nighttime by cold storage

$$\text{A}_\text{c} = \frac{\text{QG}}{\text{I} * \Delta\text{t} * \eta\text{c}} \tag{8.7}$$

The overall solar coefficient of performance that considers the solar energy as the input source can be obtained from the following equation:

$$COP_s = \frac{Q\mathrm{Ed}}{A * I * \Delta t} \quad (8.8)$$

In this hybrid storage system, 50% of the required amount of cooling effect for nighttime operation is stored in the cold storage tank (RCECS= 0.5, which is the ratio of cooling effect for nighttime by cold storage). The cold storage mass is obtained from the following equation:

$$m_{cs} = \frac{QCS.(24-\text{Hours Day}) . 3600}{h4 - h4f} \quad (8.9)$$

Where h_4 is the enthalpy of the vapor refrigerant (water) at the exit from the evaporator, h_{4f} is the enthalpy of the cold stored liquid refrigerant (water) in the cold storage tank and Q_{CS} is shown in the following equation:

$$Q_{CS} = Q_E . RCECS \quad (8.10)$$

The refrigerant storage mass for this system is obtained using equations (8.11, 8.12 and 8.13).

$$m_{rf} = \dot{m}_{rf}. 3600. \text{(24-Hours Day)} \quad (8.11)$$

$$\dot{m}_{rf} = \frac{\dot{Q}rf}{h4 - h3} \quad (8.12)$$

$$\dot{Q}_{rf} = \dot{Q}_{E} - \dot{Q}_{CS} - \dot{Q}_{hs} \quad (8.13)$$

The excess heat and mass storage are obtained by using the following equations:

$$Q_{hs} = \dot{m}_{r} * (h_{in} - h_{ex}) * \Delta t \quad (8.14)$$

h_{in} is the enthalpy at the inlet to the excess heat storage tank while h_{ex} is the enthalpy at the exit from the excess heat storage tank

$$m_{hs} = \dot{m}_{r} * 3600 \quad (8.15)$$

Engineering codes for this system has been developed by using the software, Engineering Equation Solver (EES). EES is used to conduct the analysis of absorption cycles and produce all of the presented results by using the mass and energy balance equations to analyze the performance of the system based on variable design data for quasi-state operation. The EES has a built in procedure for thermodynamic properties of LiBr-H_2O solutions. Therefore, multiple iterations of the procedure are performed effectively for providing the right solutions to the problem under analysis. The iterative loop is carried out by EES using the mass and energy balance equations to determine the enthalpy (h), mass flow rate ($\dot{m}$), maximum & minimum generator temperatures and concentration values for each of the thermodynamics state to analyze the performance and storage capacity of the system based on variable design data related to the components temperature, heat exchanger effectiveness and pump efficiency.

CHAPTER 9

RESULTS AND DISCUSSION

This chapter provides the detailed results and discussion for the techno-economic investigation for solar-assisted air-conditioning system for commercial building application in Saudi Arabia. Also, this chapter presents the detailed results and discussion for the simulation of the solar absorption (LiBr-water) of the continuous operation systems, the hybrid storage systems and the unsteady analysis of the hybrid storage (cold and refrigerant) system for residential building application in Saudi Arabia.

9.1 Techno-economic Results

9.1.1 Payback Period (PBP) Results

The economical results show that the payback periods for solar absorption system is 18.5 years while it is 23.9 years for PV system which demonstrate that solar absorption is more feasible than solar PV system at the rate of electricity ($0.0693/kWh). Table 9-1 summarizes the components cost, total investment cost and annual operation cost for the three systems.

The payback period results versus electricity rate range are investigated as shown in Table 9-2 and figure 9-1 illustrates that the payback periods decrease with the electricity rate increase for both systems. The solar absorption system is still more feasible for all ranges of electricity rate. Both systems have higher feasibility for larger commercial buildings than small commercial buildings that consume lower rate of electricity as shown in Table 9-2.

Figure 9-1 shows that the payback periods difference between the solar absorption system and solar PV-vapor compression system reduces as the electricity rate increases. Such payback periods difference becomes slight at very high electricity rates such as the international average electricity rate.

At the average international electricity rate of ($0.16/kWh [139]), the payback period for solar absorption system is 9 while it is 10 for PV system. This verifies that solar absorption system is more feasible when compared to PV system at the average international rate of electricity. Figure 9-2 shows that solar absorption system is still more feasible than solar PV system even for high electricity rate of $0.38/kWh, which is higher than the very expensive electricity rate, which is $0.373/kWh.

Table 9-1 PBP at Electricity Rate of $0.0693/kWh

E=$0.0693/kWh	Vapor Compression	PV-Vapor Compression	Solar Absorption
	Investment Cost		
VC Chiller	$600,000	$600,000	-
Absorption Chiller	-	-	$774,000
Solar Collectors	-	-	$1,058,000
Storage Tank	-	-	$184,000
PV System	-	$1,669,440	-
Total Investment Cost	**$600,000**	**$2,269,440**	**$2,016,000**
Cost Per kWc	**$638**	**$2,414**	**$2,145**
	Annual Operation Cost		
Electricity	$95,107	0	$9,502
Maintenance	$24,000	$24,000	$774
Total annual Cost	$119,107	$24,000	$10,276
Total Annual Saving	-	$95,107	$108,831
Payback Period PBP (Years)	-	**23.9**	**18.5**

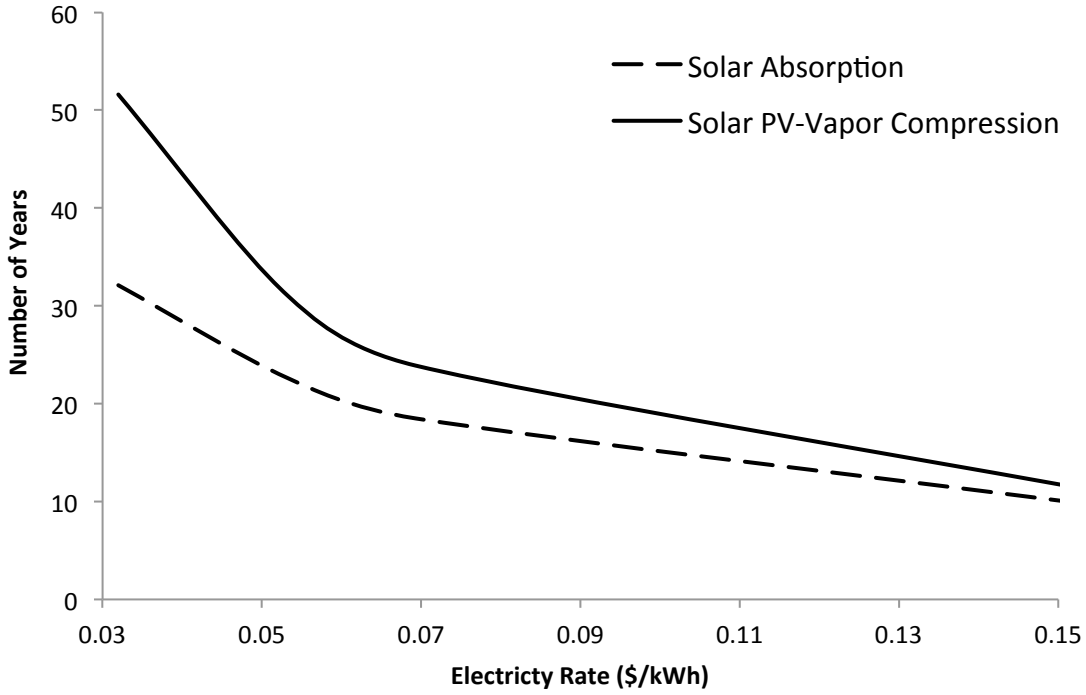

Figure 9-1 Payback Periods by Electricity Rate

Table 9-2 Payback Periods versus Electricity Rate Range

Electricity Rate ($/kWh)	PBP-Number of Years	
	Solar Absorption	Solar PV-VC
0.0320 (0- 4,000 kWh)	32.1	51.6
0.0533 (4,001-8,000 kWh)	22.6	31
0.0693 (More than 8,000 kWh)	18.5	23.9
0.16 (Average International)	9.1	10.3

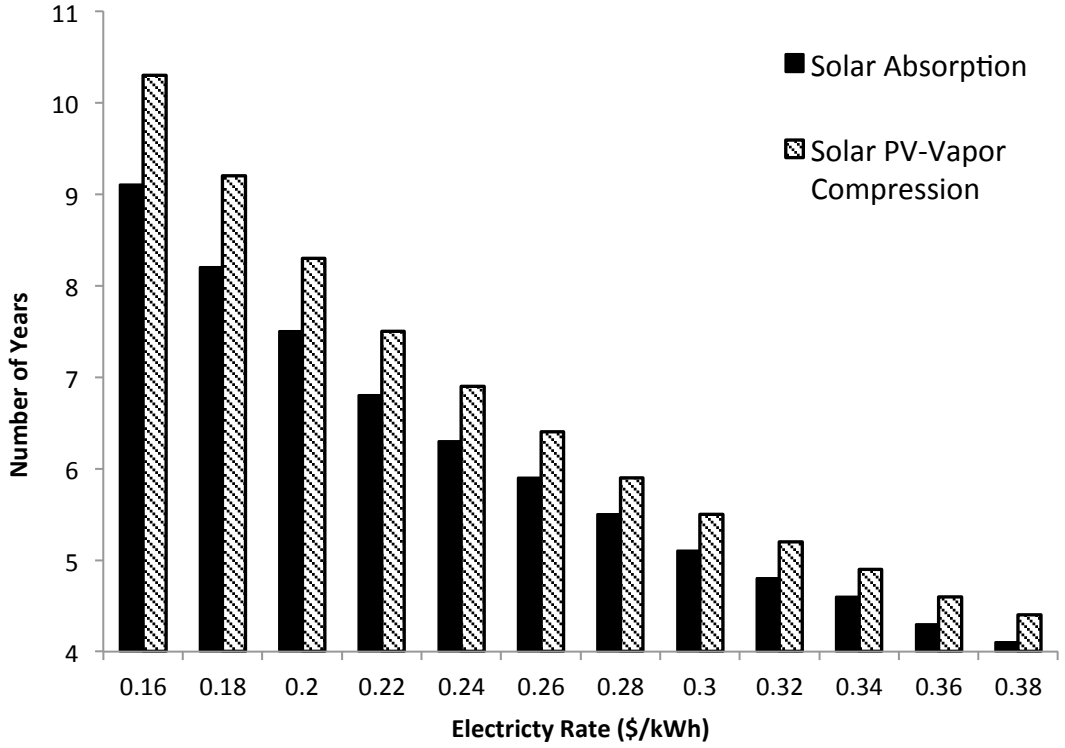

Figure 9-2 Payback Period for High Electricity Rate

In order to make both systems with more attractive feasibility, 50% government subsidy of the total investment shall reduce the payback period for both systems as shown in Table 9-3. The payback for solar absorption system reduced to 9 years at $0.0693/kWh electricity rate. For PV system, the payback decreased to 11 years at the same rate of electricity.

Thus, it is demonstrated that solar absorption system is the best economical choice for wider range of electricity rates in the eastern province of Saudi Arabia. Large buildings with high electricity consumption (above 8,000 kWh per month) are the most cost-effective option for solar absorption application.

Table 9-3 Payback Period versus electricity rate range with 50 % Government Subsidy

50 % Government Subsidy	**PBP-Number of Years**	
Electricity Rate ($/kWh)	**Solar Absorption**	**Solar PV-VC**
0.0320 (0- 4,000 kWh)	16.1	25.8
0.0533 (4,001-8,000 kWh)	11.3	15.5
0.0693 (More than 8,000 kWh)	9.2	11.9

9.1.2 Net Present Value (NPV) Results

The results of this type of analysis show that net present value for the solar absorption system is $701,512, indicating that solar absorption system is feasible at this rate of electricity. On the other hand, the PV system is not economic at the same rate of electricity as net present value is negative, -$13,327. The NPV detailed mathematical calculation at the electricity rate of $0.0693 is shown in APPENDIX 1 for solar absorption system and shown in APPENDIX 2 for PV-vapor compression system.

Table 9-4 and figure 9-3 show the net present value for both systems versus electricity rates. It demonstrates that the net present value for solar absorption system becomes positive "feasible" at the electricity rate of $0.0533/kWh while PV system is not feasible at all rates of electricity in Saudi Arabia. The net present value for PV system becomes positive "feasible" at the average international electricity rate, $2,154,209, which still has lower level of feasibility than solar absorption system, $2,652,143, at this rate. The net present value analysis indicates that the feasibility improves for higher electricity rates as shown in figure 9-3. Figure 9-4 shows the net present value for both systems versus electricity rates in the currency of Saudi Riyal.

Table 9-4 NPV Results

Electricity Rate ($/kWh)	NPV ($)	
	Solar Absorption	**Solar PV-VC**
0.0320	-11,036	-32,046
0.0533	18,052	-28,086
0.0693	701,512	-13,327
0.16 (Average International)	2,652,143	2,154,209

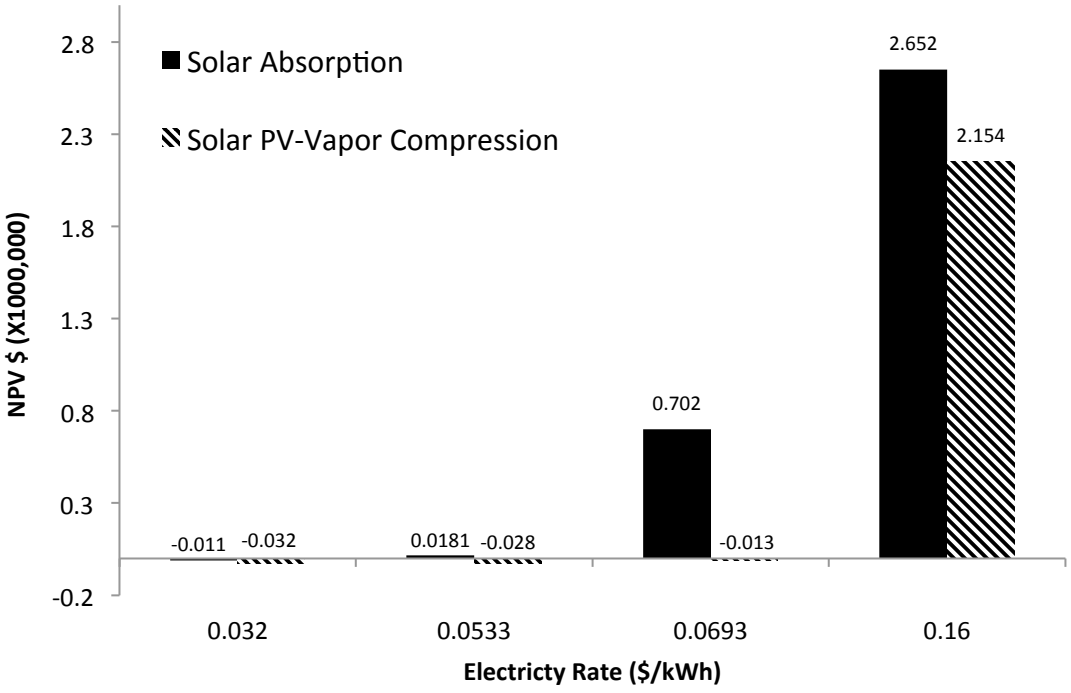

Figure 9-3 NPV by Electricity Rate in US Dollar

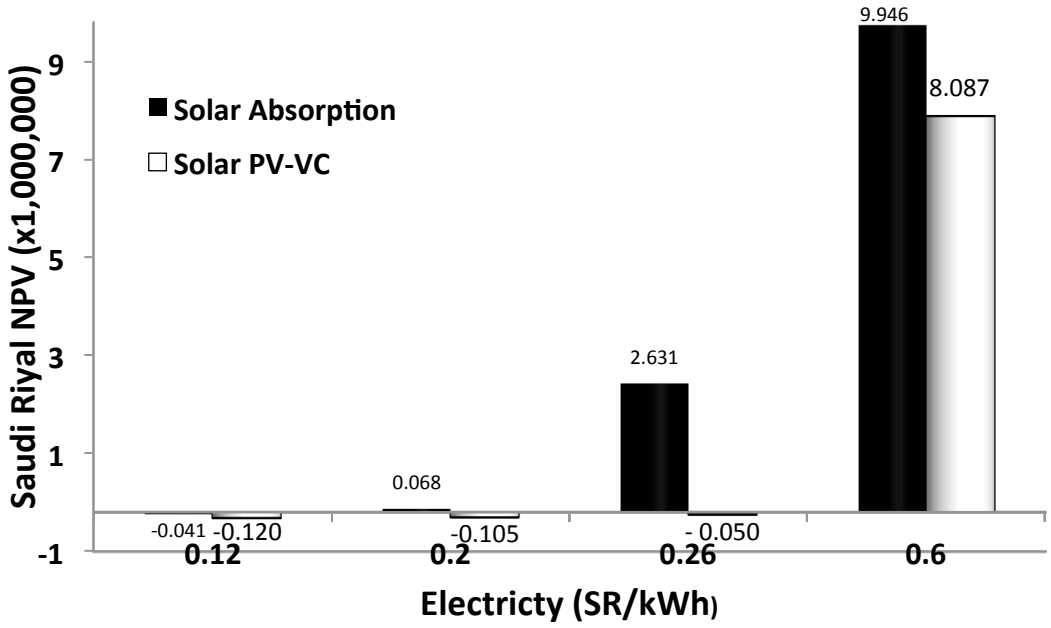

Figure 9-4 NPV by Electricity Rate in Saudi Riyal

The analysis of both methodologies shows that solar absorption system is more economic than PV system in the eastern province of Saudi Arabia. The feasibility improves at higher rate of electricity that is applicable for large commercial buildings consumes massive amount of electricity. Moreover, the feasibility is improved by applying government subsidy. According to the net present value methodology, the PV system is not feasible for eastern province of Saudi Arabia for all range of commercial buildings.

9.1.3 Economic Comparison Results

The economical results of the payback period PBP method has been compared with [14], HOTRES project which aimed the implementation for future massive applications of renewable energies. The comparison results showed that the feasibility of implementation of solar air-conditioning applications in Saudi Arabia is better than Europe for both PV system and solar thermal systems. Table 9-5 shows that the payback period for solar thermal in Saudi Arabia is 18.5 years while it is 19 years in France. Furthermore, the payback period for the PV system is lower in Saudi Arabia, 23.5 years compared to Greece, 43 years as shown in Table 9-6. The main factors of such results comparisons are the followings:

- Higher solar insolation in Saudi Arabia than Europe.
- Extreme cooling demand in Saudi Arabia during noon time

Table 9-5 Solar Thermal System PBP Comparison

Country	Number of Years
Saudi Arabia [Present Work]	18.5
France [14]	19

Table 9-6 Photovoltaic System PBP Comparison

Country	Number of Years
Saudi Arabia [Present Work]	23.9
Greece [14]	43

9.1.4 Technical Results

The pervious economical results were based on assumed COP and pump electrical consumption as the cost of the absorption chiller is based on such assumption. In this section, the results of the thermodynamic analysis are utilized to obtain the actual COP and pump electrical consumption in order to have more accurate economical results.

Applying the mass and energy equation, Table 9-7 shows the component thermodynamic results and the following are the main results:

- Q_G =1,962 kW
- Wp =0.0846 kW
- COP = 0.7644
- COP_{max} = 1.421
- η_{JI} = 0.538

Table 9-7 Solar Absorption Thermodynamics Properties Results

State	Enthalpy (kJ/kg)	Pressure (kPa)	Mass flow rate (kg/s)
1	2684	12.97	0.652
2	213.5	12.97	0.652
3	213.5	1.037	0.652
4	2514	1.037	0.652
5	138.67	1.037	8.48
6	138.7	12.97	8.48
7	222.3	12.97	8.48
8	268.2	12.97	7.82

The temperatures variables for the evaporator and condenser are studied to determine the optimum design temperatures and COP. The following five different evaporator temperatures are analyzed: T_e= 5 ºC, 7.5 ºC, 10 ºC, 12.5 ºC and 15 ºC. It found that COP increases with the increase of the evaporator temperature. The height COP reaches to 0.7687 when the evaporator temperature is 15 ºC.

The condenser temperatures are also investigated, the temperature is allowed to vary above the environment temperature with maximum temperature difference of 13ºC higher than the environment temperature. The following condenser temperatures are evaluated: T_c= 48 ºC, 49.5 ºC, 51 ºC, 52.5 ºC and 54 ºC. The results show that COP increases with the decrease of the condenser temperature. The highest COP reaches to 0.7683 when the condenser temperature is at the lowest temperature 48 ºC. This increase of COP will improve the system design and the economical feasibility in making the solar absorption more attractive for the development in Saudi Arabia. The design temperature variables can improve COP in order to make the solar absorption system more economically due to components sizing optimization and cost saving.

The calculated actual COP and pump consumption will provide enhanced assessment of the effect of COP on the economical results in term of PBP and NPV. The COP found 0.7644 and the pump consumption 0.0846 kW. Thus, the heating load is decreased to 1,230 kWh instead of 1,343kWh which resulted on system design optimization and cost saving by 8.4 % as shown in Table 9-8.

The actual annual pump consumption found 309 kWh, which achieve greater energy saving for the solar absorption system. The actual annual absorption electricity consumption cost is $21.4 rather than $9,502 making the solar absorption more feasible. Table 9-9 shows the economical results based on actual COP and pump consumption. For the actual COP, the payback for solar absorption is reduced to 16 years while it is 18 years for the assumed COP and pump consumption. The increase of COP from the assumed 0.7 to the actual 0.7641 resulted in two years reduction in PBP.

Table 9-8 Collector and Tank Cost (Assumed versus Actual COP)

Component	$ (Assumed COP)	$ (Actual COP)
Collector	1,058,000	968,617
Tank	184,000	164,455

Table 9-9 PBP at Electricity Rate of $0.0693/kWh and Actual COP and pump consumptions

	Vapor Compression	**Solar Absorption**
	Investment Cost	
VC Chiller	600,000	-
Absorption Chiller	-	774,000
Solar Collectors	-	968,617
Storage Tank	-	164,455
PV System	-	-
Total Investment Cost	**$600,000**	**$1,907,072**
	Annual Operation Cost	
Electricity	$95,107	$21.4
Maintenance	$24,000	$774
Total annual Cost	$119,107	$795
Total Annual Saving	-	$118,312
Payback Period PBP (years)	-	**16.1**

The economical results indicate that for actual COP and pump consumption, the NPV is increased to $975,527 compared to NPV at the assumed COP and pump consumption $701,512 by the rate of 39%. From both methodologies, COP improvement has major and direct impact on the economical results making the solar absorption more attractive for implementation. This type of analysis shall assist the designers and engineers to select the optimum design temperatures to develop improved economical system.

9.2 Continuous Operation Designs

A comprehensive comparative analysis is summarized in Table 9-10 after conducting a thorough thermodynamic analysis for all the three design alternatives. This forms the basis for selecting the optimum design. As indicated by Table 9-10, the heat capacity of the generator for the heat storage system is the lowest during nighttime operation and highest for the cold storage system during daytime operation. Since the heat capacity of the condenser is directly proportional to the heat capacity of the generator, the heat capacity of condenser for heat storage system during nighttime operation is the lowest. The heat capacity of the evaporator for the cold storage systems is in general higher than in the refrigerant system or heat storage system.

Additionally, the refrigerant storage systems require a practically smaller collector area. Table 9-10 also indicates that the system mass and collector area are large for heat storage system (1896 kg and 62.8 m^2, respectively), as shown in figure 9-5 and Table 9-8. Hence, the heat storage system is an unsuitable selection.

Figure 9-5 shows the storage mass for all the three designs. It shows that heat storage system has the highest storage capacity (1,896 kg) where the cold and refrigerant systems have the lowest storage capacity (101.5 kg and 108.5 kg, respectively), with slight difference between the two.

Table 9-10 Thermodynamic Analysis for the three continuous operation systems

Parameter	Unit	Designs		
		Heat Storage	**Cold Storage**	**Refrigerant Storage**
COPs		0.327	0.324	0.775
Storage	Mass (kg)	1896	101.5	108.5
Generator	Heat (kW)	6.374	15.58	6.491
Condenser	Heat (kW)	5.309	12.83	5.348
Evaporator	Heat (kW)	5	12	5
Absorber	Heat (kW)	6.066	14.74	6.143
Pump	Work (kW)	0.0001208	0.0004763	0.0001985
Heat Exchanger	Heat (kW)	2.349	5.638	2.349
Flat Plate Collector	m^2	62.8	63.5	26.5

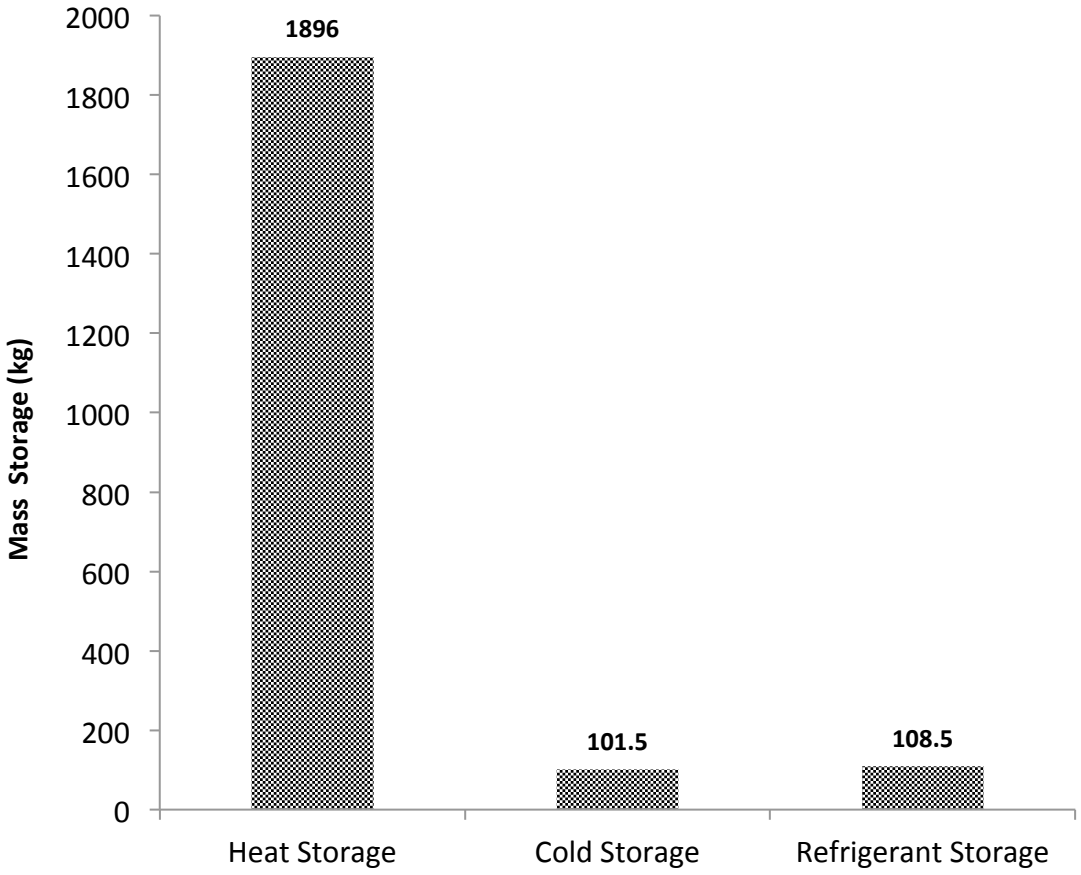

Figure 9-5 Mass Storage for the Three Systems

The cost of each component relies on the heat-capacity of that component. The lower heat-capacity corresponds to lower heat exchange area required for each component. Thus, this further depends on a lower cost for the component. The cold storage system has the lowest storage capacity. However, this system has large collector area, hence; it is not the optimum design. Table 9-11 shows the cost for the collector for the three designs. The rate of the flat plate collector is \$230/ m^2 [125]. For the evacuated tube collector, the rate is \$551 /m^2 [20].

Table 9-11 Collector Cost for the Alternative Designs

Parameter	**Alternative Designs**		
	Heat Storage	**Cold Storage**	**Refrigerant Storage**
Collector ($)	26,151	14,605	6,095

From the above results, the refrigerant storage system is found most candidate choice in terms of system performance, storage capacity and collector cost as indicated by Table 9-10 and 9-11 and Figure 9-5. Additionally, the refrigerant storage system has no complexity in design where the size and mass are acceptable. Moreover, this system doesn't require insulation. Thus, the refrigerant storage system is the greatest selection among the analyzed designs to provide continuous operation of cooling for solar absorption LiBr-water system.

Figure 9-6 shows the effect of evaporator temperature on the mass storage for the refrigerant storage system. The mass storage decreases for higher evaporator temperatures. This means that increasing the evaporator temperature will result in cost savings due to the reduction in storage tank. Similarly, figure 9-7 compares the mass storage for the refrigerant storage system against condenser temperatures. It shows that the mass storage increases as the condenser temperature increases.

Figure 9-8 shows that as the solar available time for the refrigerant storage system increases, which is applicable for summer, the mass storage capacity decreases. This indicates that a location featuring longer solar availability is highly suitable for this system. For locations where the solar available time is 14.5, the storage capacity is decreased to less than 75 kg.

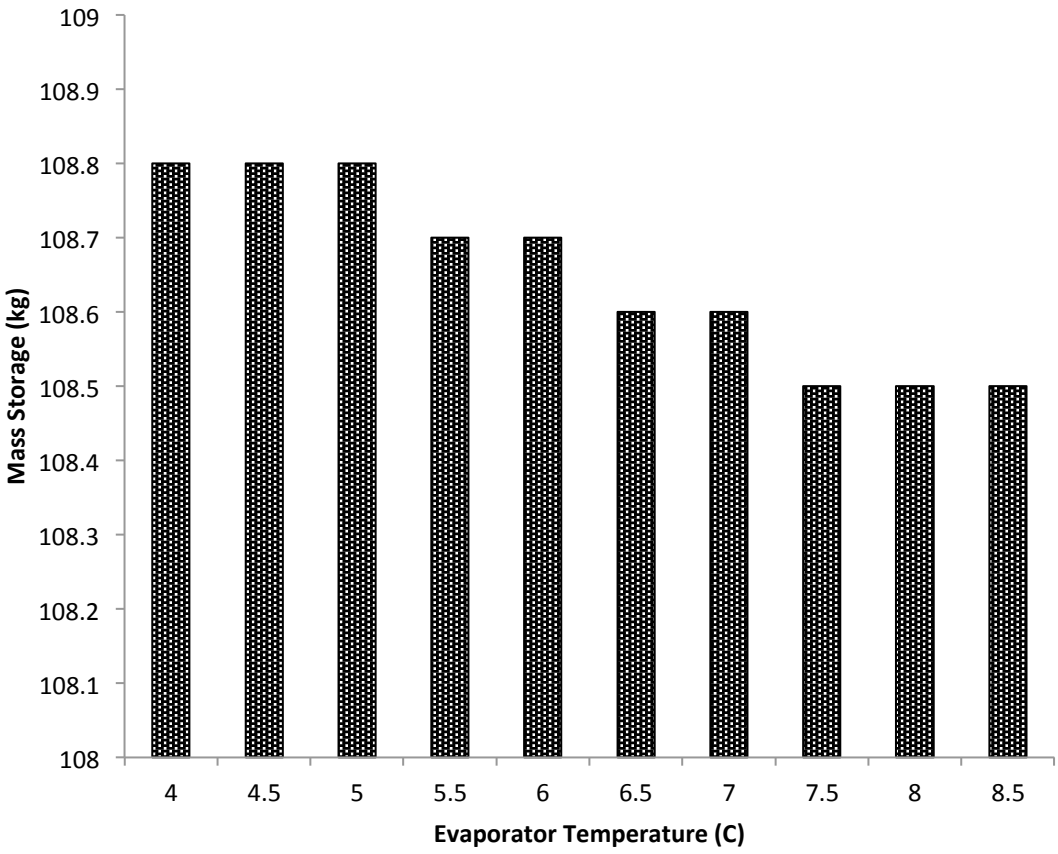

Figure 9-6 Evaporator Temperature Variation versus Mass Storage for Refrigerant Storage System

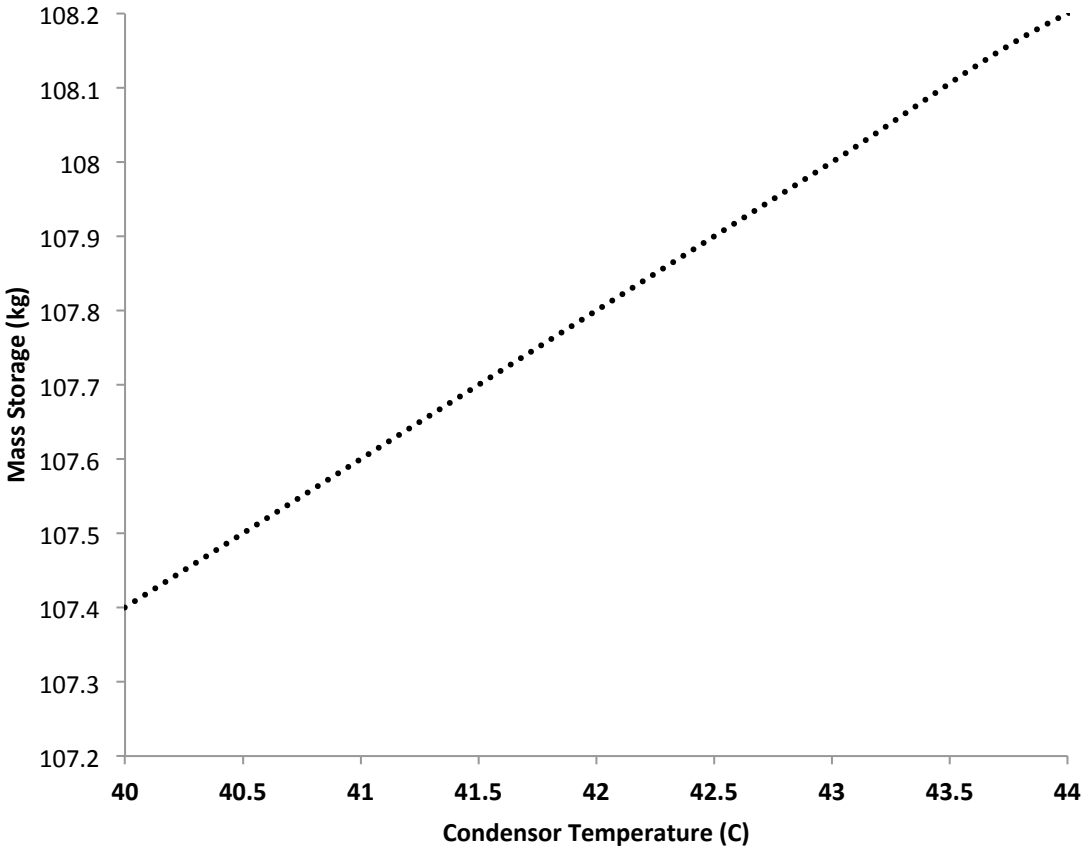

Figure 9-7 Condenser Temperature Variation versus Mass Storage for Refrigerant Storage System

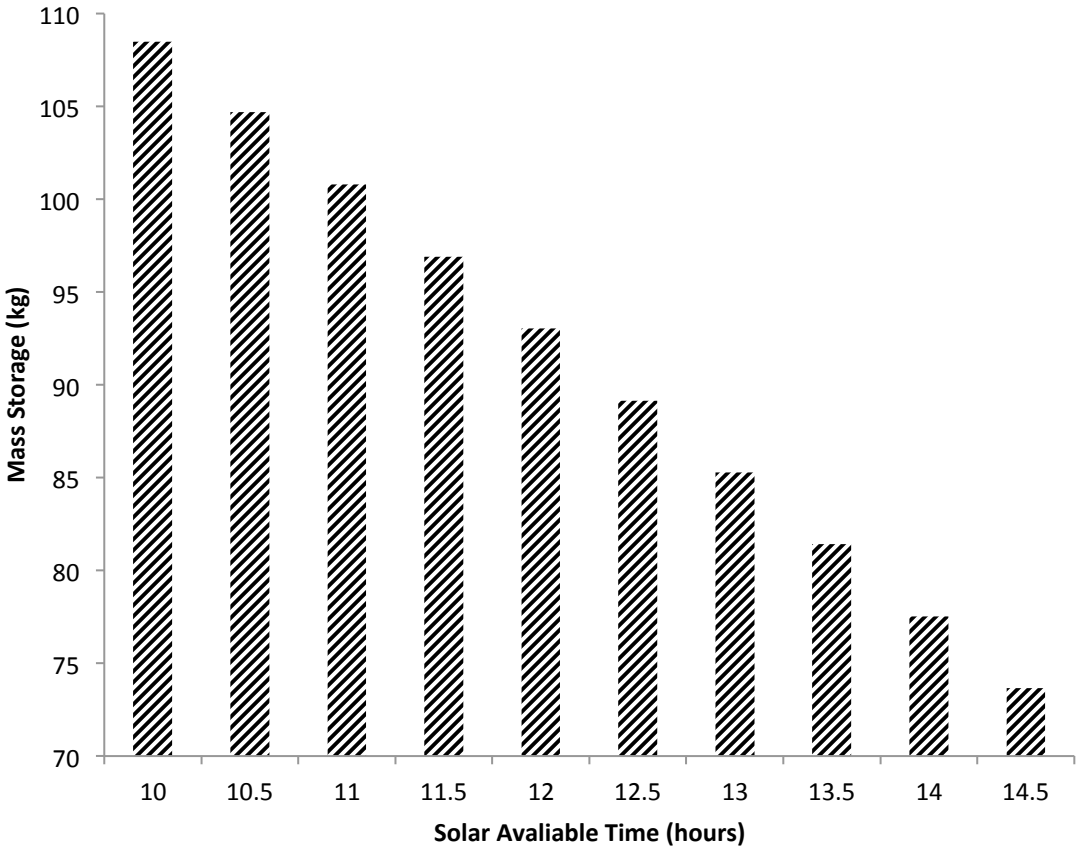

Figure 9-8 Solar Time by Mass Storage for Refrigerant Storage System

During the whole day (24-hour) for the three systems, the only electrical energy used is the pump consumption which is less than 0.01% of the total energy produced by electricity. Table 9-10 shows the amount of energy saved using solar air-conditioning with three systems. It indicates that for one building, 56.3 MWh of electrical energy can be saved in annual bases.

For 5 kW cooling power, solar air-conditioning through the three design systems can reduce large amount of CO_2 emission as shown in Table 9-11.

Table 9-12 Energy Saving

Period	Energy Saving
Hourly	6.43 kWh
Daily	154.2 kWh
Annually	56.3 MWh

Table 9-13 CO_2 Emission Saving

Period	CO_2 Emission Saving
Hourly	2.544 kg of CO_2
Daily	61 kg of CO_2
Annually	22,289.5 kg (22 ton) of CO_2

9.3 Hybrid Storage Designs

A complete comparative analysis is summarized in Table 9-14 after conducting thorough thermodynamic analysis for all the four hybrid storage designs which forms the basis for selecting the optimum design. As indicated in the table, the generator heat capacity is the lowest for heat, cold and refrigerant hybrid storage system during nighttime operation and highest for the cold and refrigerant hybrid storage system and heat and cold hybrid storage system during daytime operation. As the heat capacity of the condenser is directly proportional to the heat capacity of the generator, the heat capacity of the condenser for the heat, cold and refrigerant hybrid storage system during nighttime operation is the lowest. The heat capacity of the evaporator for cold and refrigerant hybrid storage system and heat and cold hybrid storage system is generally high compared to the other systems. Table 9-14 also indicates that COP_s is the highest for heat, cold and refrigerant hybrid storage system and the lowest for heat and cold hybrid storage system.

Heat, cold and refrigerant hybrid storage system requires a reasonably small collector area for operation and highest COP_s. However, the mass storage of this system for the three tanks is large especially for the heat storage (473.9 kg). Hence, this system is an unsuitable selection. Table 9-14 shows that the heat and refrigerant hybrid storage system has the highest storage capacity while cold and refrigerant hybrid storage system has the lowest storage capacity accompanied with second highest COP_s.

Table 9-14 Thermodynamics Analysis Results for the four hybrid designs

Parameter	Unit	Hybrid Storage Designs			
		Heat-Refrigerant	**Cold-Refrigerant**	**Heat-Cold**	**Heat-Cold-Refrigerant**
COP_s		0.521	0.701	0.497	0.765
Heat Storage	Mass (kg)	947.8	-	947.8	473.9
Cold Storage	Mass (kg)	-	50.75	50.75	25.37
Refrigerant Storage	Mass (kg)	54.27	54.27	-	54.27
$Generator_{day}$	Heat (kW)	6.491	7.789	7.789	3.894
$Generator_{night}$	Heat (kW)	3.187	-	3.187	1.594
$Condenser_{day}$	Heat (kW)	5.348	6.417	6.417	3.209
$Condenser_{night}$	Heat (kW)	2.654	-	2.654	1.327
$Evaporator_{day}$	Heat (kW)	5	6	6	3
$Evaporator_{night}$	Heat (kW)	5	5	5	5
$Absorber_{day}$	Heat (kW)	6.143	7.372	7.372	3.686
$Absorber_{night}$	Heat (kW)	3.033	-	3.033	1.516
$Pump_{day}$	Work (kW)	0.0001985	0.0002381	0.0002381	0.0001191
$Pump_{night}$	Work (kW)	0.0000604	-	0.0000604	0.0000302
Heat $Exchanger_{day}$	Heat (kW)	2.349	2.819	2.819	1.409
Heat $Exchanger_{night}$	Heat (kW)	1.132	-	1.132	0.5658
Flat Plate Collector	Area (m^2)	39.46	31.76	44.75	22.37

From the above results, the cold and refrigerant hybrid storage system appears to be the most candidate system in terms of performance, storage capacity and collector size, as indicated by Table 9-14. Additionally, this system has no complexity and simple in design and this system size and mass are acceptable. Hence, the cold and refrigerant hybrid storage system is the best choice of the investigated systems to provide for the continuous operation of cooling effect for solar absorption LiBr-water system.

The most suitable hybrid system (cold and refrigerant storage system) is compared with the most suitable system for continuous operation design (the refrigerant storage system) which discussed in section 9.2 as shown in Table 9-15. The COPs for refrigerant storage system is higher due to smaller collector area as shown in Table 9-15 based on smaller evaporator and generator sizes as there is no cold storage operation requirements. However, the storage size compared to the hybrid cold and refrigerant storage system is larger by 3 %. It shows that the storage capacity for cold and refrigerant hybrid storage system reduction is one of the major features of hybrid cold and refrigerant storage system. Also, the cold and refrigerant hybrid storage system continues uninterrupted operation even if one the storage tanks need maintenance/shutdown which is not possible in refrigerant storage system.

Table 9-15 Comparison between Refrigerant Storage [**9.2**] and Hybrid Cold and Refrigerant Storage Systems

Parameter	**Unit**	**System**	
		Refrigerant Storage [9.2]	**Hybrid Cold & Refrigerant Storage**
COP_s		0.775	0.701
Storage	Mass (kg)	108.5	105.02
Generator	Heat (kW)	6.491	7.789
Condenser	Heat (kW)	5.348	6.417
Evaporator	Heat (kW)	5	6
Absorber	Heat (kW)	6.143	7.372
Pump	Work (kW)	0.0001985	0.0002381
Heat Exchanger	Heat (kW)	2.349	2.819
Collector	Area (m^2)	26.5	31.76

The share of each storage tank towards the cooling effect supply has major effects on the mass storage and the system design improvement. Table 9-16 shows such type of effects for the heat, cold and refrigerant hybrid storage system. It can be seen from the table that the heat and cold mass storages decrease and the refrigerant mass storage increases when RCEHS and RCECS decrease. Also, the table indicates that the optimum selection of storage sizes based on RCEHS and RCECS values which occur when they are equal to 0.05 and 0.75, respectively. Figure 9-9 shows the storage capacity by RCEHS and RCECS variation for the heat, cold and refrigerant hybrid storage system when RCEHS = RCECS. As RCEHS & RCECS increase, the heat and cold mass storages increase while the refrigerant mass storage decreases. It shows that the mass storage for the three tanks is feasible when RCECS & RCEHS are low. Table 9-17 shows the effect of RCEHS and RCECS variation on the collector size for the heat, cold and refrigerant hybrid storage system. It shows that the collector area decreases as the RCEHS and RCECS decrease. The table indicates that the collector area reaches its smallest value (4.475 m^2) when RCEHS and RCECS are both equal to 0.05.

Table 9-16 Storage capacity by RCEHS and RCECS variation for the Heat, Cold and Refrigerant Hybrid Storage System

RCEHS %	RCECS %	Cold Storage Mass (Kg)	Heat Storage Mass (Kg)	Refrigerant Storage Mass (Kg)
0.05	0.05	5.075	94.78	97.69
0.15	0.15	15.22	284.3	75.98
0.25	0.25	25.37	473.9	54.27
0.35	0.35	35.52	663.5	32.56
0.45	0.45	45.67	853	10.85
0.45	0.05	5.075	853	54.27
0.35	0.15	15.22	663.5	54.27
0.25	0.25	25.37	473.9	54.27
0.15	0.35	35.52	284.3	54.27
0.05	0.45	45.67	94.78	54.27
0.75	0.05	5.075	1422	21.71
0.65	0.15	15.22	1232	21.71
0.55	0.25	25.37	1043	21.71
0.45	0.35	35.52	853	21.71
0.35	0.45	45.67	663.5	21.71
0.25	0.55	55.82	473.9	21.71
0.15	0.65	65.97	284.3	21.71
0.05	0.75	76.12	94.78	21.71

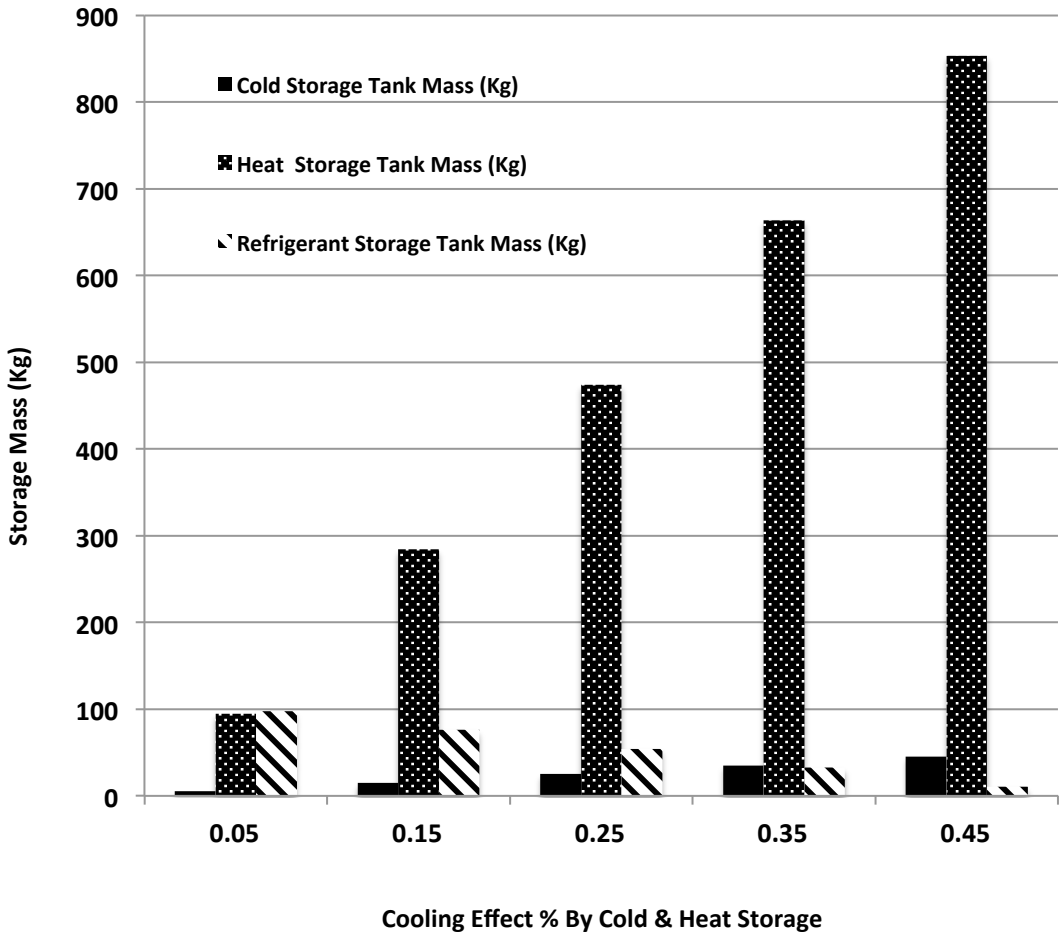

Figure 9-9 Storage capacity by RCECS and RCEHS variation for Heat, Cold and Refrigerant Hybrid Storage System

Table 9-17 Collector size by RCEHS and RCECS variation for the Heat, Cold and Refrigerant Hybrid Storage System

RCECS %	RCEHS %	Collector Area (m2)
0.05	0.05	4.475
0.15	0.15	13.42
0.25	0.25	22.37
0.35	0.35	31.32
0.45	0.45	40.27
0.05	0.45	14.87
0.15	0.35	18.62
0.25	0.25	22.37
0.35	0.15	26.13
0.45	0.05	29.88
0.05	0.75	22.67
0.15	0.65	26.42
0.25	0.55	30.17
0.35	0.45	33.92
0.45	0.35	37.68
0.55	0.25	41.43
0.65	0.15	45.18
0.75	0.05	48.93

Figure 9-10 shows the effect of RCEHS variation on the mass storages for the heat and refrigerant hybrid storage system. The refrigerant mass storage decreases slightly for higher RCEHS. However, the heat mass storage increases as RCEHS increases which means that decreasing RCEHS will result on cost saving due to heat storage tank major reduction and refrigerant storage tank low cost. Similarly, figure 9-11 shows the mass storages for the cold and refrigerant hybrid storage system against RCECS variation. It shows that the refrigerant mass storage decreases while cold mass storage increases with the increase of RCECS.

Figure 9-12 shows that as RCECS for the heat and cold hybrid storage system increases, the heat mass storage capacity decreases and cold mass storage increases slightly. When RCECS is 0.95, both heat and cold storage will have the same storage capacity. The effect of RCEHS and RCECS on the collector area for the hybrid storage systems (heat and refrigerant, cold and refrigerant, & heat, cold and refrigerant) is shown in figure 9-13. It shows that as RCEHS and RCECS increase, the collector area increases. The smallest collector area occurs for cold and refrigerant hybrid system when RCECS is small. However, the largest collector area occurs for heat and cold hybrid storage system and cold and refrigerant hybrid storage system when RCEHS and RCECS become larger.

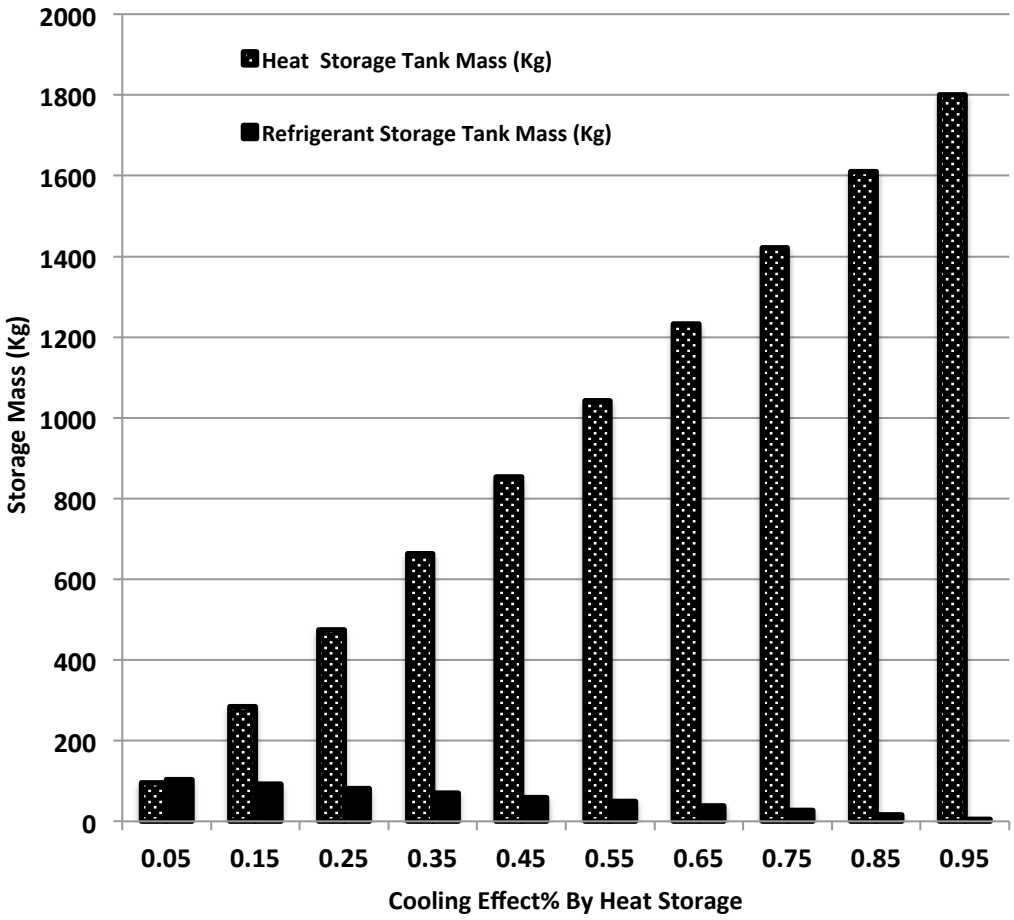

Figure 9-10 RCEHS variation for Heat and Refrigerant Hybrid Storage System

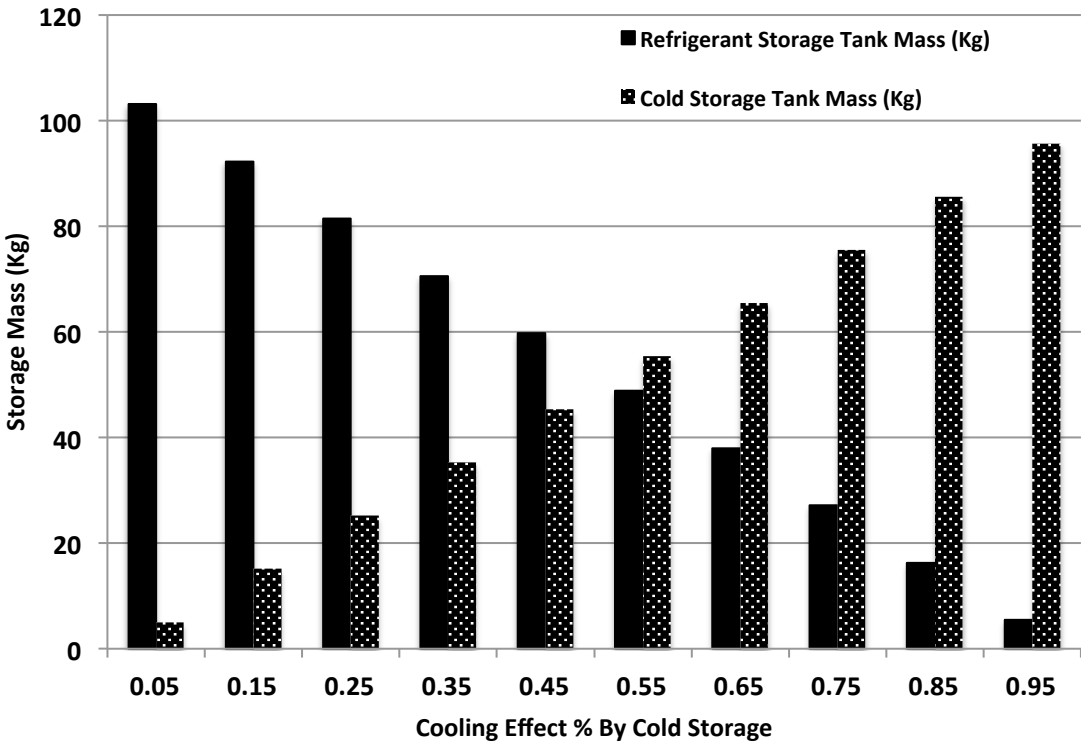

Figure 9-11 RCECS variation for Cold and Refrigerant Hybrid Storage System

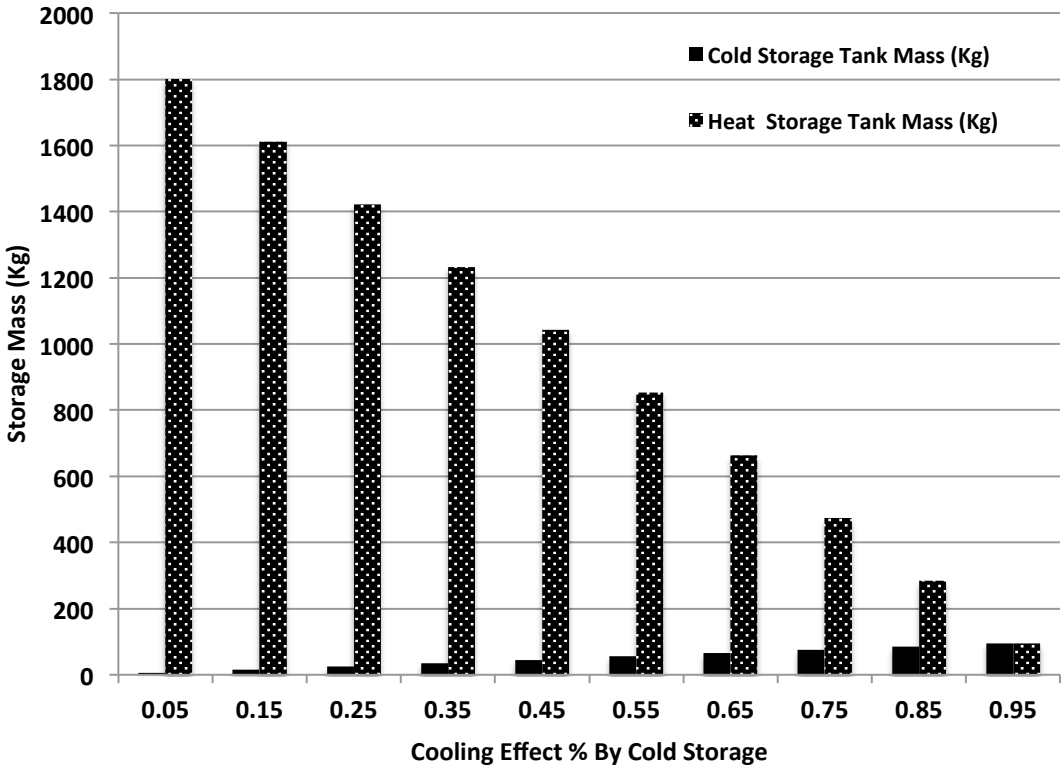

Figure 9-12 RCECS variation for Heat and Cold Hybrid Storage System

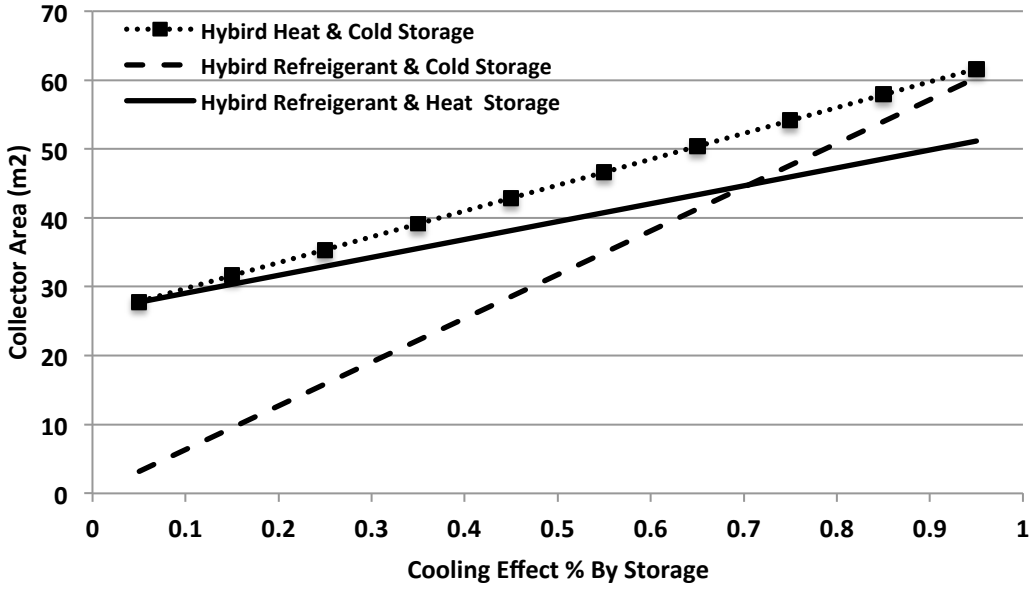

Figure 9-13 Collector area for Three Hybrid Storage Systems

Since the cold and refrigerant hybrid storage system is the most suitable system, the solar available time effect on the mass storage capacity and collector area was investigated as shown in figures 9-14 and 9-15. The cold and refrigerant mass storages capacities and collector area decrease as the solar available time increases. This indicates that a location featuring longer solar availability is highly suitable for this system. Also, it indicates that the feasibility of this system is higher in summer time where the solar availability increases.

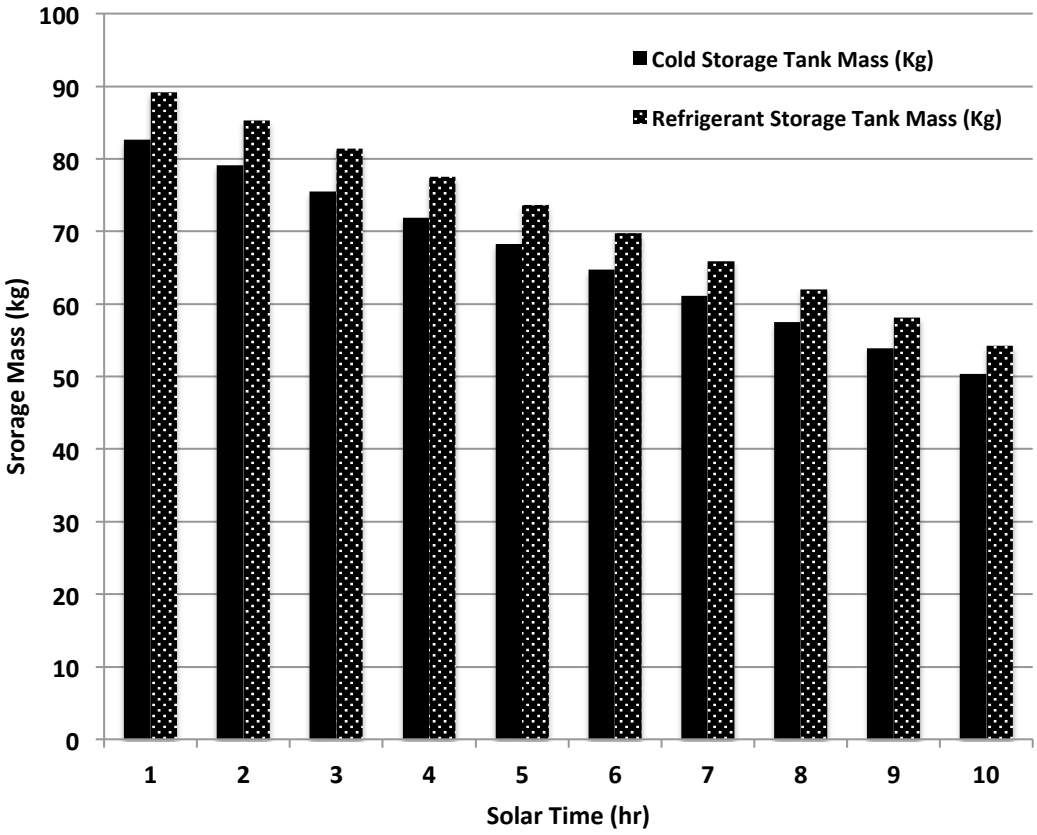

Figure 9-14 Solar Available Times versus Mass Storage for Cold-Refrigerant Hybrid Storage System

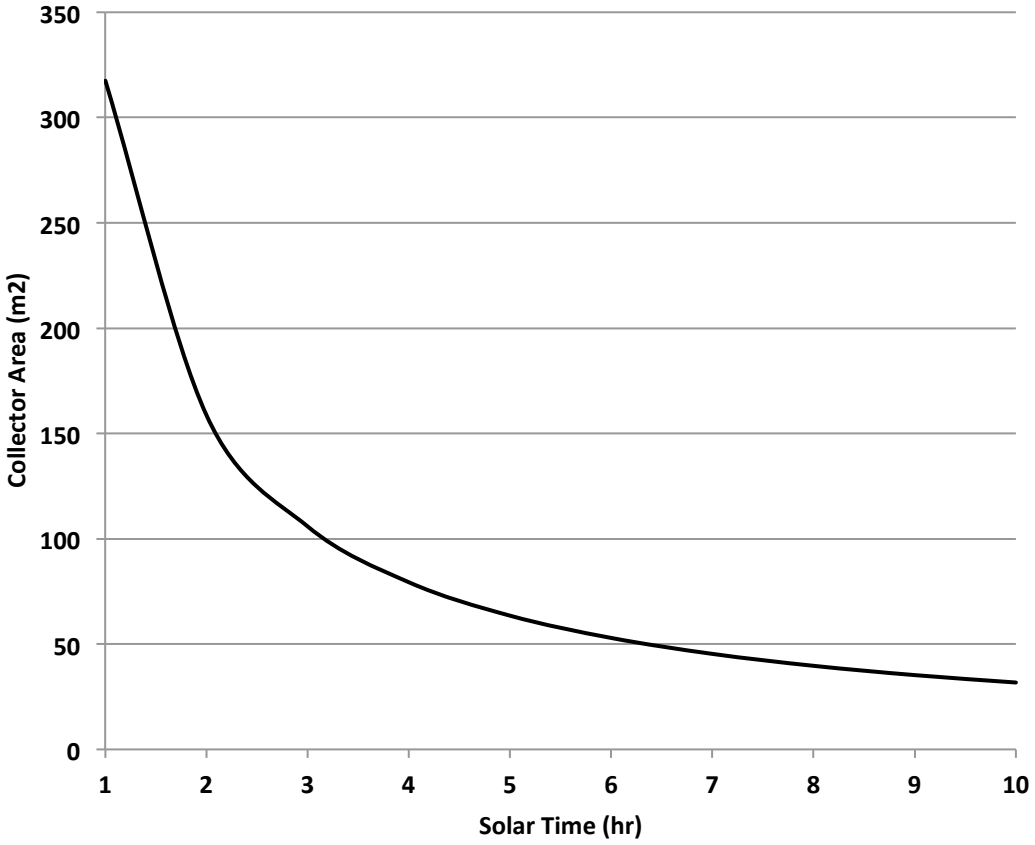

Figure 9-15 Solar Available Times versus Collector Area for Cold-Refrigerant Hybrid Storage System

9.4 Unsteady Analysis of Hybrid Storage Design

The data of the monthly average daily solar radiation and ambient temperature for Dhahran city, which have been obtain from King Abdullah City for Atomic and Renewable Energy [140], are shown in figure 9-16. It shows that the maximum solar radiation and ambient temperature occur in May, June and July while the minimum take place in November, December and January. Nine representative days for three months in summer and eight representative days for three months in winter are shown in figures 9-17 and 9-18. The data of the representative days are obtained from the Research Institute at King Fahd University of Petroleum and Minerals, KFUPM [141].

It can be seen from figures 9-17 and 9-18 that the solar intensity and ambient temperature increased and reached the peak values during noon time. Also, figures 9-17 and 9-18 show that the summer time has higher solar intensity and ambient temperature than winter time. The peak time for solar intensity is from 11:00 to 13:00 while the peak time for ambient temperature is from 12:00 to 14:00 for both winter and summer. In winter, the ambient temperature is higher in November while solar intensity is higher in January as shown in figure 9-17. Figure 9-18 shows that the ambient temperature is increased in July; however, the solar intensity is higher and reached to its peak values in June. The main energy and capacity input in summer are summarized in Table 9-18.

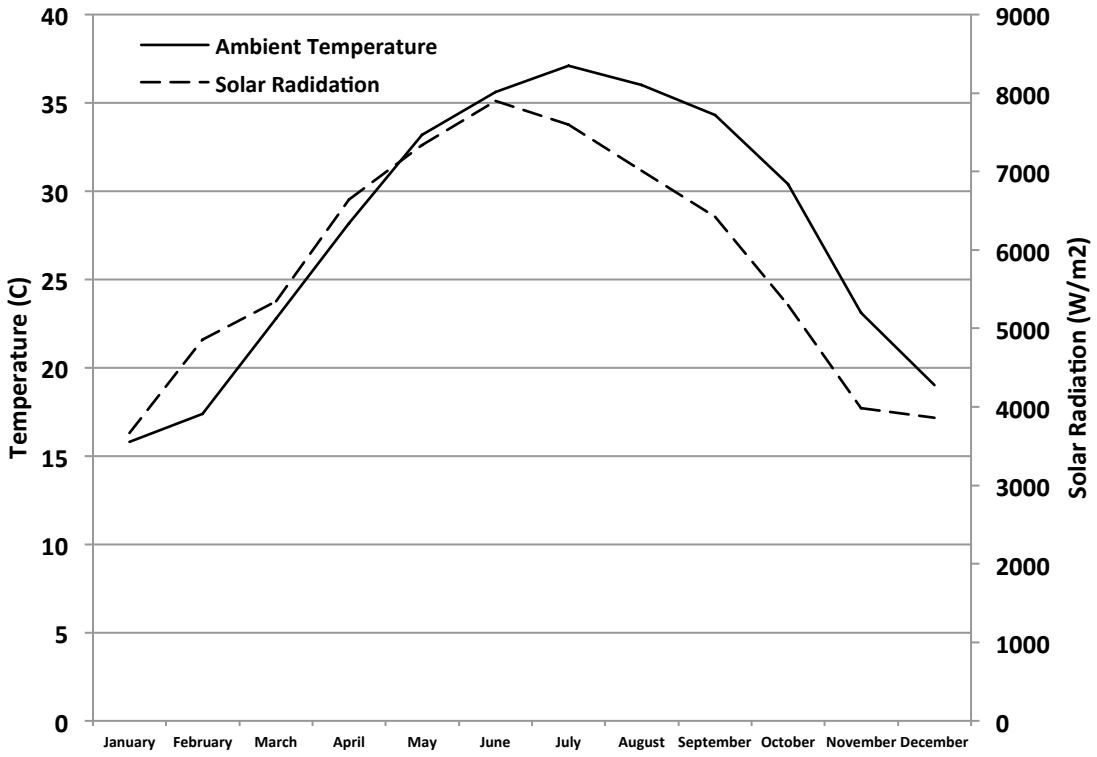

Figure 9-16 Monthly Average Daily Solar Radiation and Ambient Temperature during the year 2014.

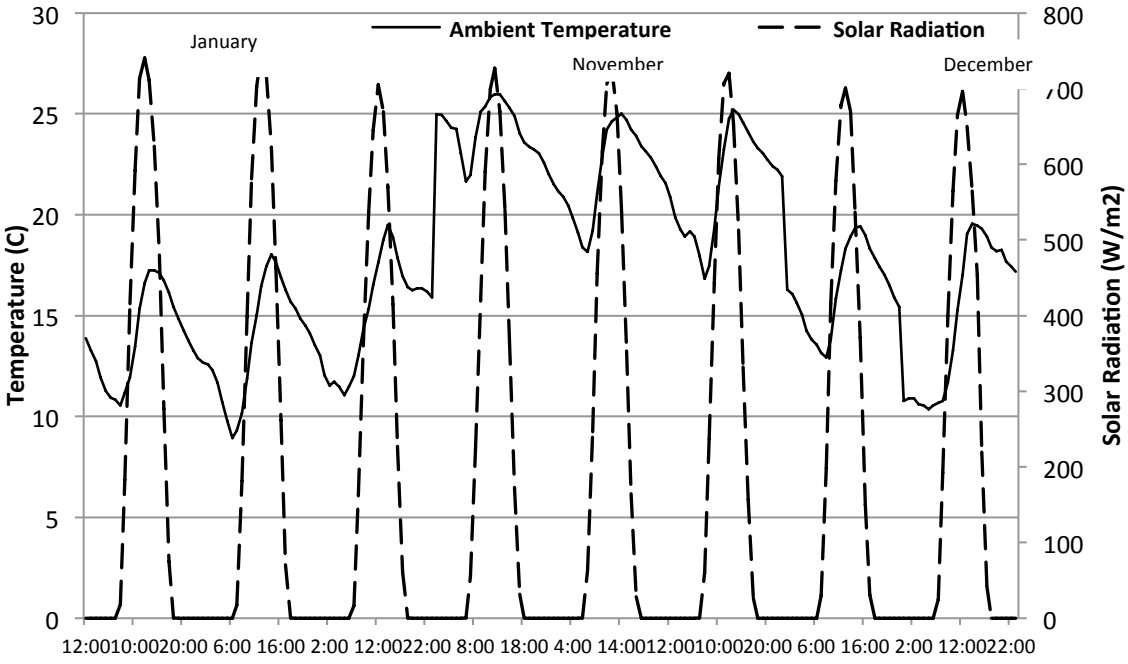

Figure 9-17 Daily variation of solar radiation and ambient temperature in winter.

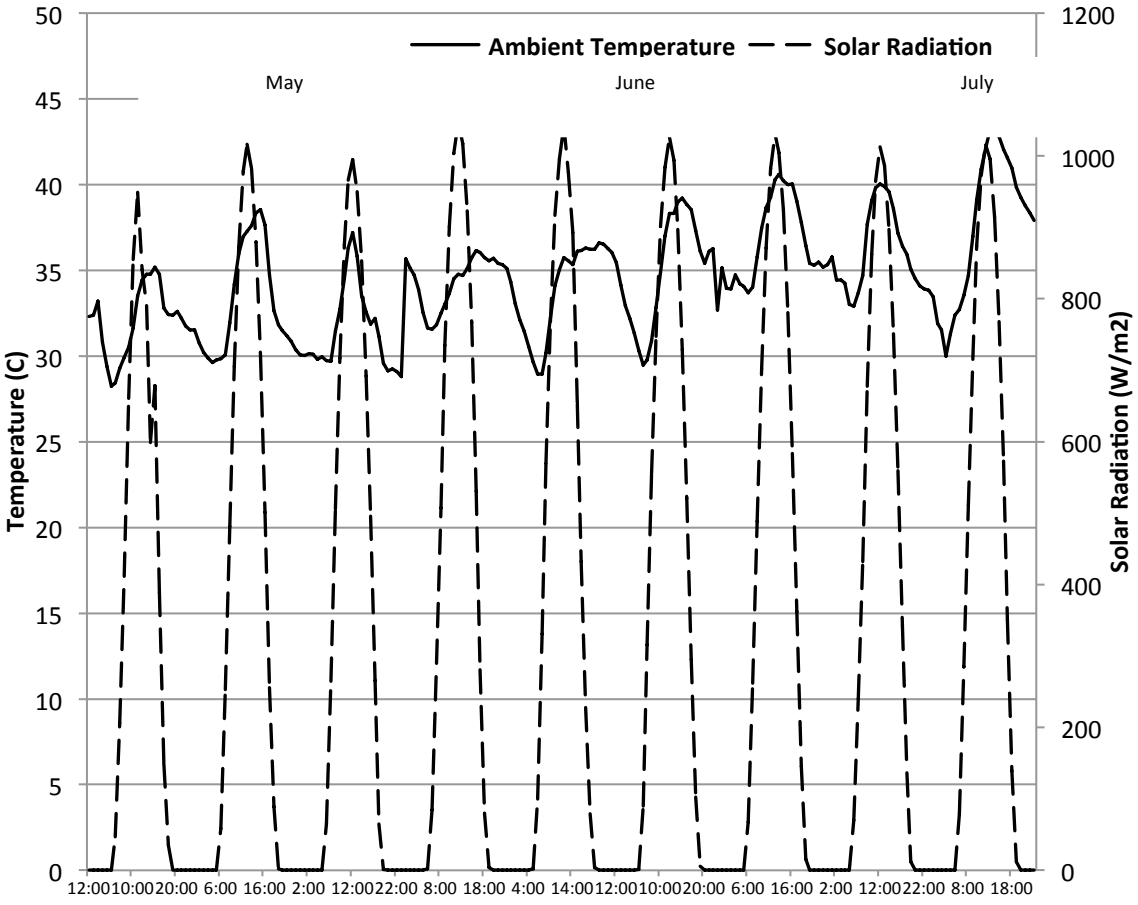

Figure 9-18 Daily variation of solar radiation and ambient temperature in summer.

Table 9-18 Energy and Storage Capacity Inputs in summer

Parameter	Unit	Value
Effective Sunlight Hours	Hour	**9**
Nighttime Cooling Hours	Hour	**15**
Hourly Cooling Energy	kWh	**5**
Daily Cooling Load	kWh	**120**
Qcold storage	kWh	**37.5**
Cold Storage Size	kg	**54.37**

The energy for generator, condenser and absorber during the representative days of summer is shown in figure 9-19. The generator has the highest energy values while the condenser has the lowest energy values. Figure 9-19 shows that the daily variation with time in summer of the required generator energy to satisfy the constant load constraint and the obtained absorber energy. It is noticeable that these two energies have their highest daily values at the start and the end of the effective sunlight hours (around 8:00 AM and 16:00 PM). This is due to the low solar energy intensity at 8:00 AM and 16:00 PM and the high ambient temperature around 16:00 PM. These ambient conditions and the constraint of constant cooling load all over the 24 hours of the day require high enthalpy difference between the generator inlet and exit around 8:00 AM and 16:00 PM, which will increase the required generator and the obtained absorber energies at the start and the end of the effective sunlight hours. In the representative summer day of May and June and at the end of the effective sunlight hour, the generator and absorber energy reaches the peak values (22.38 kWh and 22 kWh, respectively) as a result of extremely low solar intensity and high ambient temperature. The condenser energy does not show any major change since it depends on the condenser temperature which shows slight variation. In summer, the daily average generator, absorber and condenser energy are 8.82, 8.38 and 7.11, respectively.

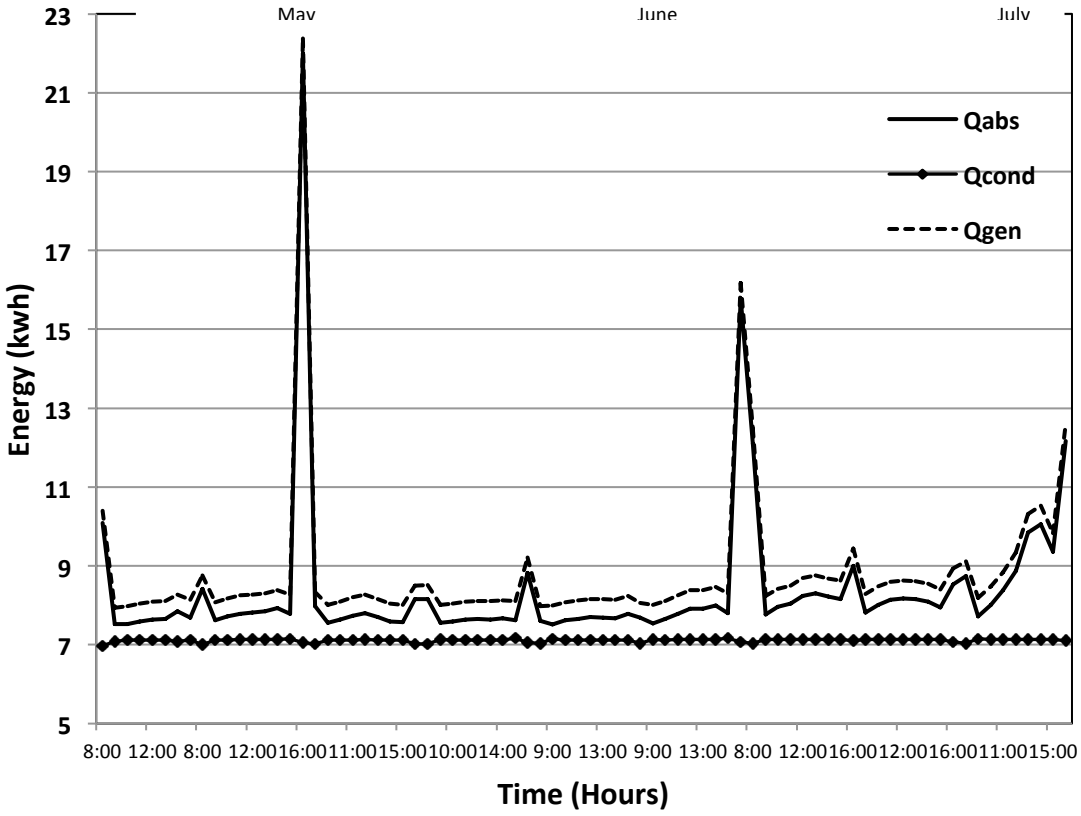

Figure 9-19 Components Hourly Energy for representative days of summer

Figures 9-20 and 9-21 show the absorber temperature and solution concentration at the exit of the absorber (strong refrigerant solution concentration, X_{ss}) for representative days of summer and winter. The absorber concentration depends on the ambient temperature (absorber temperature) as shown in figures 9-20 and 9-21. The absorber concentration is higher in summer than in winter as indicated in figure 9-20. The maximum absorber concentration in summer is in July while it reaches its peak value in winter in November.

The coefficient of performance (COP) for the representative days of summer is shown in figure 9-22. The coefficient of performance (COP) decreases at the start and the end of the effective sunlight due to the high generator heat energy at this time. COP reaches to its peak values (0.84) at noon time in summer and the daily average COP is (0.775).

Table 9-19 shows the variation range of the solar coefficient of performance (COPs) for the representative days of summer.

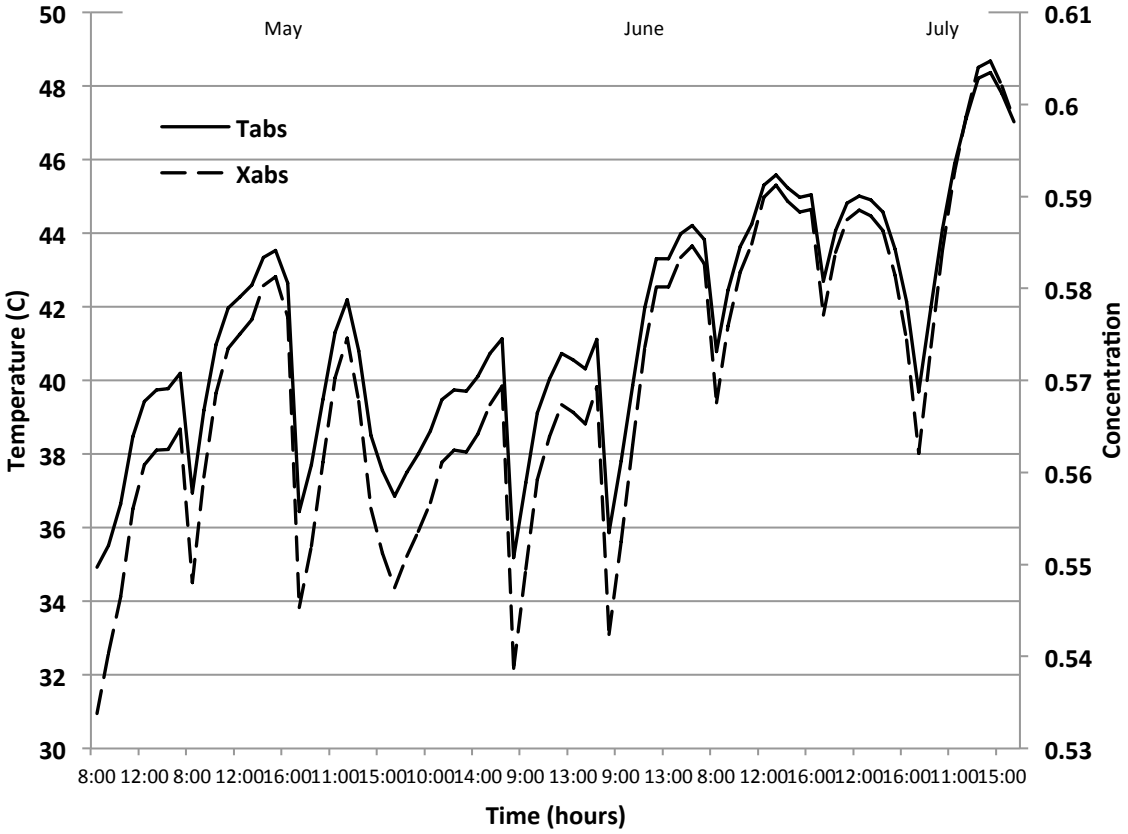

Figure 9-20 Time Variation of Absorber Temperature and Concentration for representative days of summer

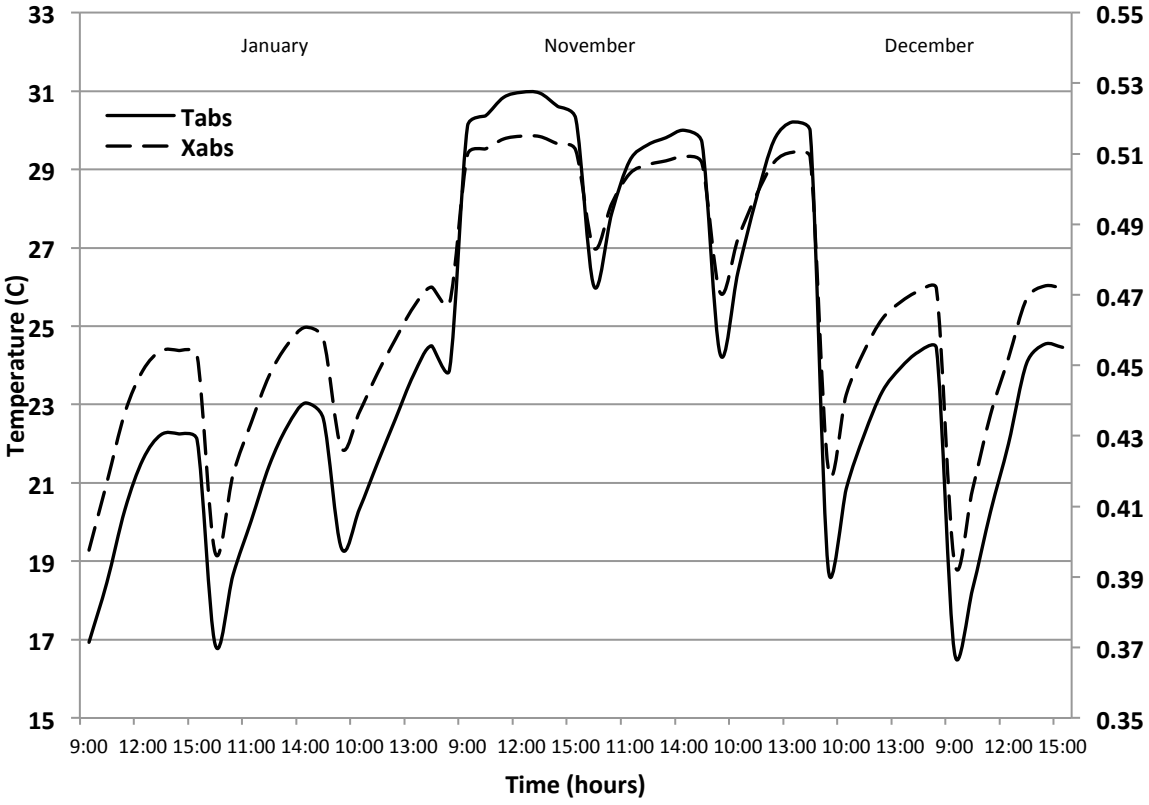

Figure 9-21 Time Variation of Absorber Temperature and Concentration for representative days of winter

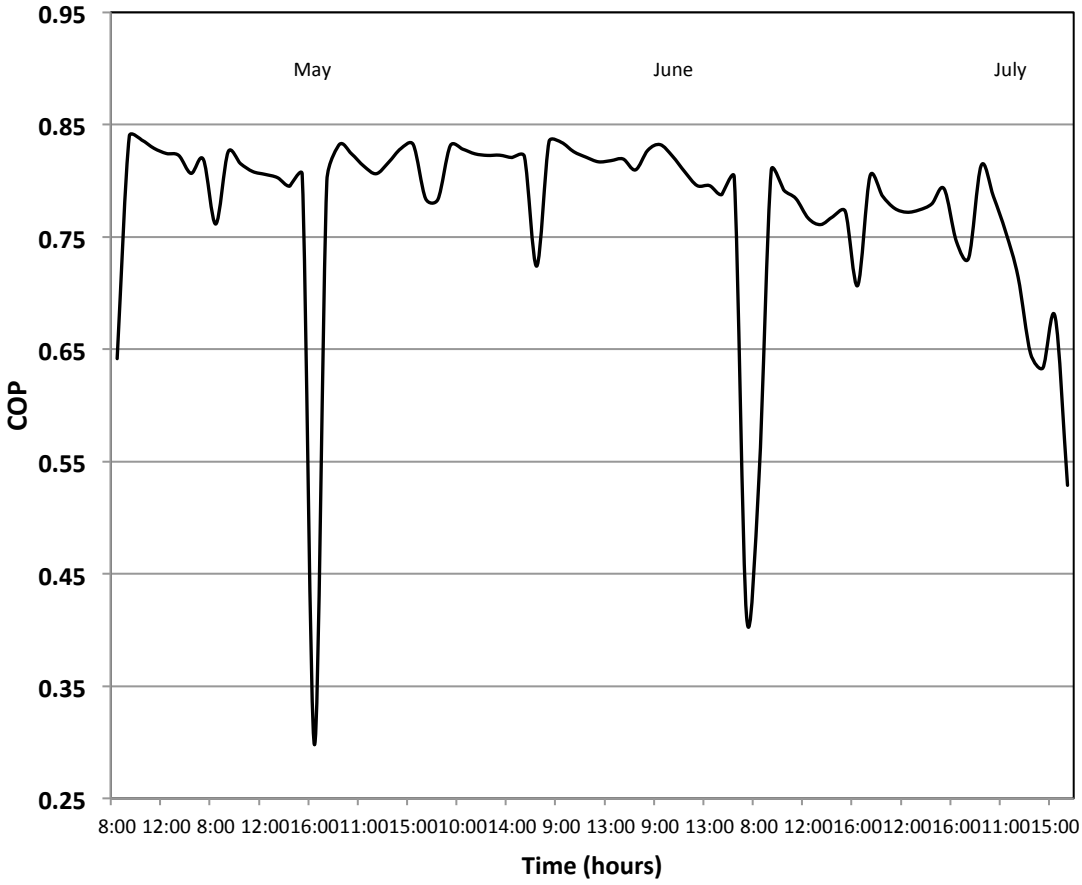

Figure 9-22 Coefficient of Performance (COP) for representative days of summer

Table 9-19 COPs Variation in summer

Parameter	**Range**
COPs	**0.125-0.353**

Figure 9-23 show the collector area for the representative days of summer. The collector area for summer reaches its highest size at the start and the end of the effective sunlight due to the required high generator heat energy (due to the assumption of constant cooling load and low solar intensity). On the other hand, the collector area has its minimum value at noon time. The daily average collector area is 28.3 m^2.

The refrigerant storage tank size for the representative days of summer is shown in figure 9-24. The refrigerant storage tank size increases and reaches its peak values at the start and the end of the effective sunlight in summer due to the lower contribution of the heat storage tank supply as a result of low solar intensity. The minimum refrigerant storage tank size occurs in the noon time. The daily average refrigerant storage tank size is 53.3 kg.

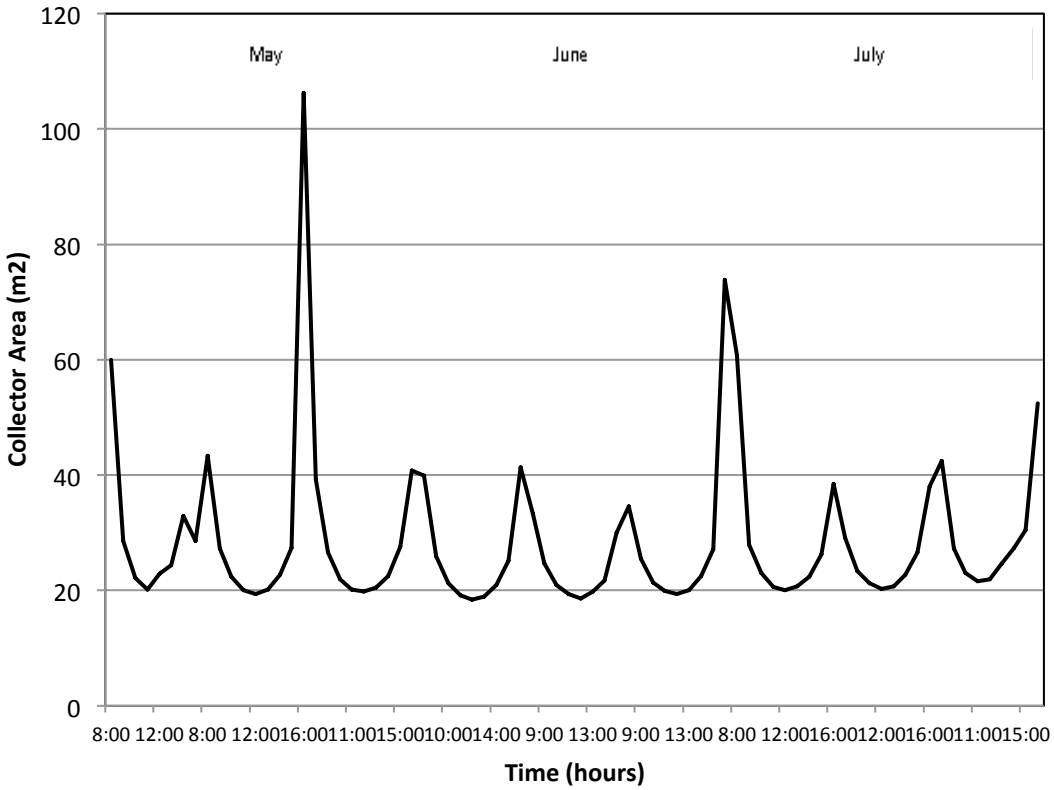

Figure 9-23 Collector Area for representative days of summer

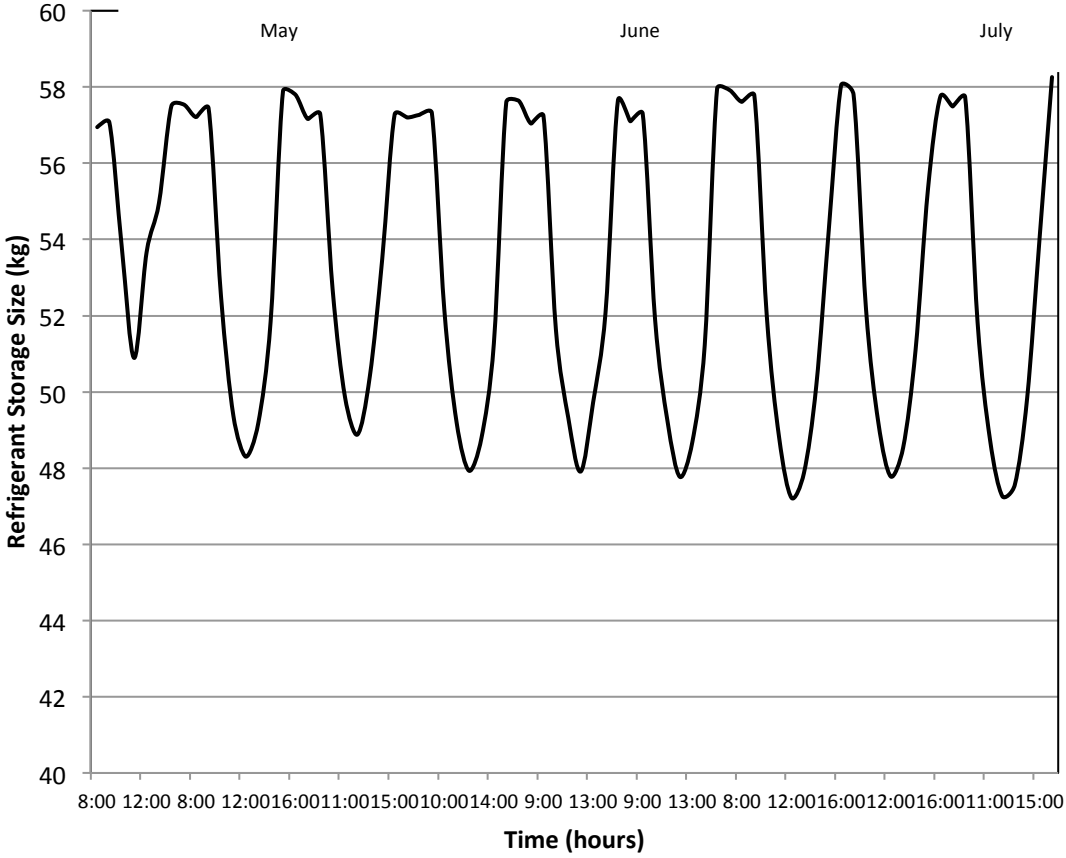

Figure 9-24 Refrigerant Storage Size for representative days of summer

CHAPTER 10

VALIDATION

This chapter provides the validation of the simulation carried out. The system modeling of LiBr-water absorption, single-effect, air-cooled system with flat plate collector is validated against the results of experiments carried out in Madrid during summer 2010 [95].

For the sake of the comparison with the experimental work, the following are the main input parameters used in the present work simulation which were used in the experimental work [95]: cooling power = 4.5 kW, generator temperature = 95 °C, condenser temperature = 47 °C, absorber temperature = 42 °C, evaporator temperature = 10 °C and heat exchanger effectiveness = 0.88. In this comparison, the storage tank used is the heat storage tank as per the experimental work storage method. The comparison shows that the results of the maximum heat rates of generator and absorber, COP, storage mass and collector area are acceptable. The comparison in Table 10-1 shows a maximum percentage difference of 5.7% in COP.

Table 10-1 Comparison between present study and experimental work results

Parameter	Present Study (EES)	Experimental Results	Percentage Difference (%)
COP	**0.8488**	**0.90**	**5.7**
Generator (kW)	**5.301**	**5.5**	**3.62**
Absorber (kW)	**5.004**	**5**	**0.08**
Hot Storage Mass (kg)	**1509**	**1500**	**0.6**
Collector Area (m2)	**46.26**	**48**	**3.625**

The system modeling in this study using (EES) is also validated by published work results using TRNSYS program [84] feeding same cooling capacity of 11 kW and operating conditions (Tg = 84.6 °C, Te=4.4°C, Tc=38 °C, Ta=36.2° C, ε_{HE}=0.6, Xss = 0.561, Xws = 0.613. The same results were obtained from the two programs for the heat rates of condenser and the COP as presented in Table 7.2. The corresponding results for refrigerant, weak and strong solutions mass flow rates from TRNSYS software are also presented in Table 10-2 for the sake of comparison. The maximum percentage difference between the two programs simulations results was 3.3% for COP.

Table 10-2 Comparison between present study (EES) and published (TRNSYS) software results

Parameter	Present Study (EES)	Published Results (TRNSYS)	Percentage Difference (%)
COP	**0.7647**	**0.74**	**3.3**
Condenser (kW)	**11.67**	**11.89**	**1.8**
Refrigerant Mass Flow Rate (kg/s)	**0.004682**	**0.0048**	**2.4**
Weak Solution Mass Flow Rate (kg/s)	**0.05051**	**0.0512**	**1.3**
Strange Solution Mass Flow Rate (kg/s)	**0.05519**	**0.056**	**1.4**

CHAPTER 11

CONCLUSIONS AND RECOMMENDATIONS

The development of a solar air-conditioning system that will meet a 24-hour uninterrupted daily cooling load in buildings in Saudi Arabia is presented. The development includes an in-depth review of novel alternative solar-powered LiBr-water absorption designs of three storage systems and four hybrid storage systems. Also, the impact of unsteady analysis of hybrid storage (cold plus refrigerant) design system on the operation and performance parameters of absorption chiller of 5 kW cooling power with hybrid storage system is discussed. Moreover, the techno-economic analysis and feasibility for three systems: conventional vapor-compression system, solar absorption system and solar photovoltaic vapor-compression system is presented. Based on the analysis of the results; the following can be concluded:

1- The economical analysis using payback period (PBP) and net present value (NPV) methods revealed that solar LiBr-H_2O absorption system and solar photovoltaic vapor-compression systems can be economically feasible in the eastern province of Saudi Arabia for large commercial buildings that consume large amount of electrical energy (more than 8000 kWh per month). However, the results show that solar absorption systems are more feasible than solar photovoltaic vapor-compression

systems. The results indicate that the increase in the COP reduces the payback period (PBP) and increases the net present value (NPV) of the system.

2- The results for the continuous operation designs analysis show that the cold storage system has the lowest mass requirement and has the highest collector area. Although the heat storage system has the highest COP during nighttime operation, its mass requirement is the highest. The analysis revealed that the best-suited alternative design is that with refrigerant storage for a solar LiBr-H_2O absorption system because the collector size is smaller than to the other alternates designs. Additionally, the refrigerant storage system requires non-insulated storage tank. These two features confirm that the cost of the refrigerant storage system is lowest compared to the alternatives designs.

3- The results for the hybrid storage designs analysis show that heat, cold and refrigerant hybrid storage system require smaller collector area (22.37 m^2), however, has a high storage capacity especially for heat storage tank (473.9 kg). Although, the heat, cold and refrigerant hybrid storage system has high COP_s (0.765), the mass requirement for this system is very high. The analysis revealed that hybrid storage design with cold and refrigerant storage for solar LiBr-H_2O absorption systems is the best suitable design since the collector size is comparatively smaller (31.76 m^2) than to the heat and refrigerant hybrid storage and the heat and cold hybrid storage systems. The mass storage capacities of this system will be the lowest (cold storage tank: 50.32 kg and refrigerant storage tank: 54.27 kg). Also, this system is simple in

design due less complexity in the control requirements compared to other systems. These three features do confirm that the cost of the cold-refrigerant hybrid storage system is lower than to the other systems. The improvement of the mass storage and collector area by increasing the solar availability time shall have positive effect on the design parameter, size and system selection.

4- The results for unsteady behavior of the hybrid refrigerant and cold storage tanks design show that the coefficient of performance (COP) in summer decreases at the start and the end of the effective sunlight due to the high generator heat energy at this time. COP reaches to its peak values (0.84) at noon time in summer and the daily average COP is (0.775).

Based on the results of the present dissertation analysis, it is recommended to consider the following in the future:

1) Study the implementation options (new buildings or existing buildings) of solar absorption air-conditioning system for the implementation in commercial and residential buildings in Saudi Arabia.
2) Analyze the feasibility of concentrator photovoltaic (CPV) for Air-conditioning application in Saudi Arabia.
3) Study the performance of the continuous operation and hybrid storage designs when using the double-effect and triple-effect absorption systems.
4) Conduct techno-economic analysis for other sectors and small-scale systems.

APPENDICES

APPENDIX 1 (NPV detailed mathematical calculation for solar absorption system at the electricity rate of $0.0693)

Year	Initial Cost	Electricity Cost for Non-Solar System	Electricity Cost for Solar System	Maintenance Cost for Non-Solar System	Maintenance Cost for Solar System	Annual Cost Saving	Present Value
0	**-$1,416,000**	-	-	-	-	-1416000	- 1,416,000.00
1		$95,107.00	$9,502.00	$24,000.00	$774.00	$108,831	$105,661.17
2		$95,107.00	$9,502.00	$24,960.00	$804.96	$109,760	$103,459.36
3		$95,107.00	$9,502.00	$25,958.40	$837.16	$110,726	$101,330.20
4		$95,107.00	$9,502.00	$26,996.74	$870.64	$111,731	$99,271.63
5		$95,107.00	$9,502.00	$28,076.61	$905.47	$112,776	$97,281.68
6		$95,107.00	$9,502.00	$29,199.67	$941.69	$113,863	$95,358.45
7		$95,107.00	$9,502.00	$30,367.66	$979.36	$114,993	$93,500.08
8		$95,107.00	$9,502.00	$31,582.36	$1,018.53	$116,169	$91,704.75
9		$95,107.00	$9,502.00	$32,845.66	$1,059.27	$117,391	$89,970.72
10		$95,107.00	$9,502.00	$34,159.48	$1,101.64	$118,663	$88,296.30
11		$95,107.00	$9,502.00	$35,525.86	$1,145.71	$119,985	$86,679.83
12	**$600,000.00**	$95,107.00	$9,502.00	$36,946.90	$1,191.54	$721,360	$505,947.64
13		$95,107.00	$9,502.00	$38,424.77	$1,239.20	$122,791	$83,614.41
14		$95,107.00	$9,502.00	$39,961.76	$1,288.77	$124,278	$82,162.40
15		$95,107.00	$9,502.00	$41,560.23	$1,340.32	$125,825	$80,762.23
16		$95,107.00	$9,502.00	$43,222.64	$1,393.93	$127,434	$79,412.48
17		$95,107.00	$9,502.00	$44,951.55	$1,449.69	$129,107	$78,111.78
18		$95,107.00	$9,502.00	$46,749.61	$1,507.67	$130,847	$76,858.79
19		$95,107.00	$9,502.00	$48,619.60	$1,567.98	$132,657	$75,652.21
20	- **$774,000.00**	$95,107.00	$9,502.00	$50,564.38	$1,630.70	-$639,461	- $354,054.23
21		$95,107.00	$9,502.00	$52,586.96	$1,695.93	$136,496	$73,373.34
22		$95,107.00	$9,502.00	$54,690.43	$1,763.77	$138,532	$72,298.64
23		$95,107.00	$9,502.00	$56,878.05	$1,834.32	$140,649	$71,265.55
24		$95,107.00	$9,502.00	$59,153.17	$1,907.69	$142,850	$70,272.97
25		$95,107.00	$9,502.00	$61,519.30	$1,984.00	$145,140	$69,319.82
Total							**701,512.18**

APPENDIX 2 (NPV detailed mathematical calculation for PV-vapor compression system at the electricity rate of $0.0693)

Year	Initial Cost	Electricity Cost for Non-Solar System	Electricity Cost for Solar System	Annual Cost Saving	Present Value
0	-$1,669,440	-	-	-1669440	-1,669,440.00
1		$95,107	$0	$95,107	$92,336.89
2		$95,107	$0	$95,107	$89,647.47
3		$95,107	$0	$95,107	$87,036.38
4		$95,107	$0	$95,107	$84,501.34
5		$95,107	$0	$95,107	$82,040.13
6		$95,107	$0	$95,107	$79,650.62
7		$95,107	$0	$95,107	$77,330.69
8		$95,107	$0	$95,107	$75,078.34
9		$95,107	$0	$95,107	$72,891.60
10		$95,107	$0	$95,107	$70,768.54
11		$95,107	$0	$95,107	$68,707.32
12		$95,107	$0	$95,107	$66,706.14
13		$95,107	$0	$95,107	$64,763.24
14		$95,107	$0	$95,107	$62,876.93
15		$95,107	$0	$95,107	$61,045.56
16		$95,107	$0	$95,107	$59,267.54
17		$95,107	$0	$95,107	$57,541.30
18		$95,107	$0	$95,107	$55,865.34
19		$95,107	$0	$95,107	$54,238.19
20		$95,107	$0	$95,107	$52,658.44
21		$95,107	$0	$95,107	$51,124.70
22		$95,107	$0	$95,107	$49,635.63
23		$95,107	$0	$95,107	$48,189.93
24		$95,107	$0	$95,107	$46,786.34
25		$95,107	$0	$95,107	$45,423.63
Total					**-13,327.76**

References

[1] Syed A.M. Said, Kadry HM, Ismail BI. Climatic conditions for Saudi Arabia. ASHRAE Trans 1996; 102 (1):37–44.

[2] Saudi Electricity Company. Annual report 2014. https://www.se.com.sa/en-us/Lists/AnnualReports/Attachments/14/AnnualReport2014En.pdf.

[3] Ministry of Industry and Electricity. Electricity in the Kingdom of Saudi Arabia: Growth and Development. Annual Report (in Arabic). Riyadh, Saudi Arabia.

[4] King Abdullah City for Atomic and Renewable Energy, Towards Sustainable Energy Mix for Saudi Arabia. 3rdSaudi Solar Forum, Riyadh, Saudi Arabia, April, 17th, 2011.

[5] http://data.worldbank.org/indicator/EN.ATM.CO2E.KT/countries. last accessed May 2015.

[6] http://data.worldbank.org/indicator/EN.ATM.CO2E.PC/countries. last accessed May 2015.

[7] Sam Friggens. How much Carbon Dioxide do solar panels save. http://blog.abundancegeneration.com/2013/08/how-much-carbon-dioxide-do-solar-panels-save. Last accessed May 2015.

[8] Balaras CA, Grossman G, Henning HM, Infante-Ferreira CA, Podesser E, Wang L, Wiemken E. Solar air conditioning in Europe — an overview. Renewable and Sustainable Energy Reviews 2007; 11: 299–314.

[9] Solanki CS. Solar Photovoltaic Technology and Systems. 2013; 1: 23-24.

[10] THE annual solar energy conference and accelerator for solar business development in Saudi Arabia. 2013. http://desertsolarsaudiarabia.com/top-10-solar-projects-ksa/#. Last accessed December 2015.

[11] Z.F. Li, K. Sumathy. Technology development in the solar absorption air-conditioning systems. Renewable and Sustainable Energy Reviews 4 (2000) 267-293.

[12] Henning, H.-M. Solar assisted air conditioning of buildings – an overview. Applied Thermal Engineering, (2007) 1734-1749.

[13] O. Enibe, Solar Refrigeration for Rural Applications. Renewable Energy12, (1997) 157-167.

[14] K.F. Fong, T.T. Chow, C.K. Lee, Z. Lin, L.S. Chan. Comparative study of different solar cooling systems for buildings in subtropical city. Solar Energy, 84 (2010) 227-244.

[15] Michaelis Karagiorgas, Theocharis Tsoutsos, Vassiliki Drosou, Stephane Pouffary, Tulio Pagano, German Lopez Lara, Jose´ Manuel Melim Mendes, HOTRES: renewable energies in the hotels. An extensive technical tool for the hotel industry. Renewable and Sustainable Energy Reviews 10 (2006) 198–224.

[16] D.S. Kim, C.A. Infante Ferreira. Solar refrigeration options – a state-of-the-art review. International Journal of Refrigeration 31 (2008) 3–15.

[17] Marwan Mokhtar, Muhammad Tauha Ali, Simon Bräuniger, Afshin Afshari, Sgouris Sgouridis, Peter Armstrong, Matteo Chiesa. Systematic

comprehensive techno-economic assessment of solar cooling technologies using location-specific climate data. Applied Energy 87 (2010) 3766–3778.

[18] P. Kohlenbach, M. Dennis. Solar Cooling in Australia: The Future of Air-conditioning?. 9th IIR Gustav Lorentzen Conference, Sydney, Australia 2010.

[19] N. Hartmann, C. Glueck, F.P. Schmidt. Solar cooling for small office buildings: Comparison of solar thermal and photovoltaic options for two different European climates. Renewable Energy 36 (2011) 1329-1338.

[20] Hector D. Arias-Varela, Wilfredo Soto-Gomez and Oscar Castillo-Lopez. Thermodynamic Design of A Solar Refrigerator To Preserve Sea Products.

[21] G.A. Florides, S.A. Kalogirou, S.A. Tassou, L.C. Wrobel. Modeling, simulation and warming impact assessment of a domestic-size absorption solar cooling system.Applied Thermal Engineering 22 (2002) 1313–1325.

[22] Nick Zettel. Solar-Assisted Absorption Chilling for Commercial HVAC Systems Technology Application for Public Power Utilities. Redding Electric Utility (2005).

[23] M. Shekarchiana, M. Moghavvemib, F. Motasemic, T.M.I. Mahliaa. Energy savings and cost–benefit analysis of using compression and absorption chillers for air conditioners in Iran. Renewable and Sustainable Energy 15 (2011) 1950-1960.

[24] Dirk Pietruschka, UliJakob, Ursula Eicker. Solar Cooling Technologies for Southern Climates - A System Comparison. Proceedings of 4th Solar Air Conditioning Conference (2011).

[25] Daniel Chemisana, Jesus Lopez-Villada, Alberto Coronas, Joan Ignasi Rosell. Building integration of concentrating systems for solar cooling applications. Applied Thermal Engineering (2012) 1-8.

[26] Todd Otanicar, Robert A. Taylor, Patrick E. Phelan. A Prospects for solar cooling – An economic and environmental assessment, Solar Energy (2012).

[27] K.F. Fong, C.K. Lee, T.T. Chow, Comparative study of solar cooling systems with building-integrated solar collectors for use in sub-tropical regions like Hong Kong. Applied Energy 90 (2012) 189–195.

[28] F. Asdrubali, G. Baldinelli, A. Presciutti, M. Caporali. Solar Cooling: State Of The Art, Technical Analysis and Firsts Applications.

[29] J. M. Abdulateef, M. Y. Sulaiman, Baharudinali, M. A. Alghoul. An economic viability analysis and optimization of solar cooling system. Proceedings of the 4th ASME/ WSEAS International Conference on ENERGY & ENVIRONMENT (2009).

[30] Sebastien Thomas, Philippe Andre. Dynamic Simulation of a Complete Solar Assisted Conditioning System in an Office Building Using TRNSYS.

[31] Xavier Casals. Solar absorption cooling in Spain: Perspectives and outcomes from the simulation of recent installations. Renewable Energy 31 (2006) 1371–1389.

[32] Tamer Shahin. Lessons learnt in Saudi Arabia with Solar PV system performance under desert conditions. Desert Solar Saudi Arabia, 17-18 September 2014, Riyadh.

[33] Green Riho Energy. Concentrating Photovoltaics (CPV). http://www.greenrhinoenergy.com/solar/technologies/pv_concentration.php

[34] Dr. Simon P. Philipps, Dr. Andreas W. Bett. CURRENT STATUS OF CONCENTRATOR PHOTOVOLTAIC (CPV) TECHNOLOGY. FRAUNHOFER INSTITUTE FOR SOLAR ENERGY SYSTEMS ISE NATIONAL RENEWABLE ENERGY LABORATORY NREL. Version 1.1, September 2015.

[35] Theocharis Tsoutsos, Joanna Anagnostou, Colin Pritchard, Michalis Karagiorgas, Dimosthenis Agoris. Solar cooling technologies in Greece. An economic viability analysis. Applied Thermal Engineering 23 (2003) 1427–1439.

[36] R. Younes, H. Zeidan, H. Harb, A. Ghaddar. Optimal Design and Economical Study for Solar Air-Conditioning By Absorption Chillers. International IIR conference on latest developments in refrigerated storage, transportation and display of food products (2005).

[37] F. Calise. Thermo-economic analysis and optimization of high efficiency solar heating and cooling systems for different Italian school buildings and climates. Energy and Buildings 42 (2010) 992–1003.

[38] Tommy Cleveland, Thomas Pash, Henry Tsai, Laurel Varnado. Optimizing Solar Thermal Resource Use At Commercial Buildings. First published in the SOLAR 2010 Conference Proceedings.

[39] T. Tsoutsos , E. Aloumpi, Z. Gkouskos, M. Karagiorgas. Design of a solar absorption cooling system in a Greek hospital. Energy and Buildings 42 (2010) 265–272.

[40] Koroneos C, Nanaki E, Xydis G. Solar air conditioning systems and their applicability-an exergy approach. Resources, Conservation and Recycling 2010; 55: 74–82.

[41] Yin Hang, Ming Qu, Fu Zhao. Economical and environmental assessment of an optimized solar cooling system for a medium-sized benchmark office building in Los Angeles, California. Renewable Energy 36 (2011) 648-658.

[42] A. Al-Alili, M.D. Islam, I. Kubo, Y. Hwang, R. Radermacher. Modeling of a solar powered absorption cycle for Abu Dhabi. Applied Energy 93 (2012) 160–167.

[43] Ursula Eicker, Dirk Pietruschka, Design and performance of solar powered absorption cooling systems in office buildings. Energy and Buildings 41 (2009) 81–91.

[44] GA Florides, SA Kalogirou, SA Tassou, LC Wrobel. Modeling and simulation of an absorption cooling system for Cyprus. Solar Energy 2002; 72(1): 43-51.

[45] Georgios A. Florides and Soteris A. Kalogirou. Optimization and Cost Analysis of a Lithium Bromide Absorption Solar Cooling System. Proceedings of Clima 2007 Well Being Indoors.

[46] A. Gomez Moreno, J.M. Palomar Carnicero, F. Cruz Peragon, Simulation of a solar cooling system. International Conference on Renewable Energies and Power Quality (2010).

[47] F. Calise, M. Dentice d'Accadia, L. Vanoli. Thermo-economic optimization of Solar Heating and Cooling systems. Energy Conversion and Management 52 (2011) 1562–1573.

[48] M. Moya, J.C. Bruno, P. Eguia, E. Torres, I. Zamora, A. Coronas. Performance analysis of a tri-generation system based on a micro gas turbine and an air-cooled, indirect fired, ammonia-water absorption chiller. Applied Energy 88 (2011) 4424–4440.

[49] K. Sumayth, Z. C. Huang and Z. F. Li. Solar absorption cooling with low grade heat source- A strategy of development in South China. Solar Energy 72 (2002), 155-165.

[50] K. Edem N'Tsoukpoe, Hui Liu, Nolwenn Le Pierres, Lingai Luo. A review on long-term sorption solar energy storage. Renewable and Sustainable Energy Reviews 13 (2009) 2385–2396.

[51] O. Kızılkan, A. Sencan, S. A. Kalogirou. Thermo-economic optimization of a LiBr absorption refrigeration system. Chemical Engineering. Process 46 (2007), 1376–1384.

[52] M. A. Rosen. A Concise Review of Exergy-Based Economic Methods. 3rd ASME/WSEAS International Conference on Energy Environ., pp. 23-25, 2008.

[53] Farshi LG, Mahmoudi SMS, Rosen MA, Yari M, Amidpour M. Exergoeconomic analysis of double effect absorption refrigeration systems. Energy Conversion and Management 2013; 65: 13–25.

[54] M. D. d'Accadia, F. Rossi. Thermo-economic optimization of a refrigeration plant. International Journal of Refrigeration 21 (1998), 42-54.

[55] Jerko M. LABUS, Joan Carles BRUNO, Alberto CORONAS. REVIEW ON ABSORPTION TECHNOLOGY WITH EMPHASIS ON SMALL CAPACITY ABSORPTION MACHINES. THERMAL SCIENCE: 2013, Vol. 17, No. 3, pp. 739-762.

[56] Chung R, Duffie JA, Lof, GOG. A study of a solar air-conditioner. Mechanical Engineer 1963; 85(31).

[57] R.Z. Wang, T.S. Ge, C.J. Chen, Q. Ma and Z.Q. Xiong. Solar sorption cooling systems for residential applications: Options and guidelines, International Journal of Refrigeration 32 (2009) 638-660.

[58] K.R. Ullah, R.Saidur, H.W.Ping, R.K.Akikur, N.H.Shuvo. A review of solar thermal refrigeration and cooling methods. Renewable and Sustainable Energy Reviews 24 (2013) 499–513.

[59] X.Q. Zhai, M. Qu, Yue. Li, R.Z. Wang. A review for research and new design options of solar absorption cooling systems. Renewable and Sustainable Energy Reviews 15 (2011) 4416– 4423.

[60] I. Shwartz, and A. Shitzer. Solar Absorption System for Space Cooling & Heating. ASHRAE Journal, 19, (11), 1977, 51-54.

[61] D.W. Sun. Thermodynamic Design Data an Optimum Design Maps for Absorption Refrigeration Systems. Applied Thermal Engineering, 17, (3), 1996, 211-221.

[62] Antonio J. Bula, Luis F. Navarro, Diane L. Herrera, Lesme A. Corredor. Thermodynamic Simulation of A Solar Absorption Refrigeration System Generator-Heat Exchanger. Ed 1 (May 1987); p.12

[63] M.I. Karamangil, S. Coskun, O. Kaynakli, N. Yamankaradeniz. A simulation study of performance evaluation of single-stage absorption refrigeration system using conventional working fluids and alternatives. Renewable and Sustainable Energy Reviews 14 (2010) 1969–1978.

[64] Rabah Gomri. Investigation of the potential of application of single effect and multiple effect absorption cooling systems. Energy Conversion and Management 51 (2010) 1629-1638.

[65] Kaushik SC, Arora A. Energy and exergy analysis of single effect and series flow double effect water–lithium bromide absorption refrigeration systems. International Journal of Refrigeration 2009; 32: 1247-1258.

[66] Kilic M, Kaynakli O. Second law-based thermodynamic analysis of water lithium bromide absorption refrigeration system. Energy 2007; 32: 1505–1512.

[67] Rosiek S, Batlles FJ. Integration of the solar thermal energy in the construction: analysis of the solar-assisted air-conditioning system installed in CIESOL building. Renewable Energy 2009;34(6):1423–31.

[68] Pongsid Srikhirin, S. Aphornratana, S. Chungpaibulpatana. A review of absorption refrigeration Technologies. Renewable and Sustainable Energy Reviews, vol. 5, pp. 343-372, 2001.

[69] Gomri R. Second law comparison of single effect and double effect vapour absorption refrigeration systems. Energy Conversion and Management 2009; 50: 1279–1287.

[70] S. Alizadeh. Multi-pressure absorption cycles in solar refrigeration: A technical and economical study. Solar Energy, vol. 69, pp. 37–44, 2000.

[71] M. Balghouthi, M.H. Chahbani, A. Guizani. Investigation of a solar cooling installation in Tunisia. Applied Energy 98 (2012) 138–148.

[72] A. Lecuona, R. Ventas, M. Venegas, A. Zacarıas, R. Salgado. Optimum hot water temperature for absorption solar cooling. Solar Energy 83 (2009) 1806–1814.

[73] D.S. Kim, C.A. Infante Ferreira. Air-cooled LiBr–water absorption chillers for solar air conditioning in extremely hot weathers. Energy Conversion and Management 50 (2009) 1018–1025.

[74] J.M. Gordon, K.C. Ng, High-efficiency solar cooling. Solar Energy 68 (2000) (1), 23‑31.

[75] B. H. Gebreslassie, M. Medrano, D. Boer. Exergy analysis of multi-effect water–LiBr absorption systems: From half to triple effect. Renewable Energy, vol.35, pp. 1773–1782, 2010.

[76] B. H. Gebreslassie, M. Medrano, F. Mendes, D. Boer. Optimum heat exchanger area estimation using coefficients of structural bonds: Application to an absorption chiller. International Journal of Refrigeration, vol. 33, pp. 529 – 537, 2010.

[77] B. H. Gebreslassie, G. G. Gosálbez, L. Jiménez, D. Boer. Design of environmentally conscious absorption cooling systems via multi-objective optimization and life cycle assessment. Applied Energy, vol. 86, pp. 1712–1722, 2009.

[78] Kaynakli O, Kilic M. Theoretical study on the effect of operating conditions on performance of absorption refrigeration system. Energy Conversion and Management 2007; 48: 599–607.

[79] Kundu B, Mondal PK, Datta SP, Wongwises S. Operating design conditions of a solar-powered vapor absorption cooling system with an absorber plate having different profiles: An analytical study. International Communications in Heat and Mass Transfer 2010; 37: 1238–1245.

[80] R.U. Yang, P. Wang. Simulation study of performance evaluation of single-glazed and double-glazed collectors/regenerators for an open-cycle absorption solar cooling system. Solar Energy 71 (2001) (4), 263‑268.

[81] N Tubb. The commercialisation of Solar Powered Transport Refrigeration. Energy Design Limited (2001).

[82] Atmaca I, Yigit A. Simulation of solar-powered absorption cooling system. Renew Energy 2003; 28(8):1277–93.

[83] Joudi, Qussai J. Abdul-Ghafour. Development of design charts for solar cooling systems. Part I: computer simulation for a solar cooling system and development of solar cooling design charts. Energy Conversion and Management 44 (2003) 313–339.

[84] M. Balghouthi, M.H. Chahbanib, A. Guizania. Feasibility of solar absorption air conditioning in Tunisia. Building and Environment 43 (2008) 1459–1470.

[85] Ming Qu, Hongxi Yin, David H. Archer. A solar thermal cooling and heating system for a building: Experimental and model based performance analysis and design. Solar Energy 84(2010) 166-182.

[86] Praene JP, Marc O, Lucas F, Miranville F. Simulation and experimental investigation of solar absorption cooling system in Reunion Island. Applied Energy 2011; 88: 831–839.

[87] N. Molero-Villar, J.M. Cejudo-Lopez, F. Domı´nguez-Munoz, A. Carrillo-Andres. A comparison of solar absorption system configurations. Solar Energy 86 (2012) 242–252.

[88] Onan C, Ozkan DB, Erdem S. Exergy analysis of a solar assisted absorption cooling system on an hourly basis in villa applications. Energy 2010; 35: 5277-5285.

[89] Hong DL, Chen GM, Tang LM, He YJ. Simulation research on an EAX (Evaporator-Absorber-Exchange) absorption refrigeration cycle. Energy 2011; 36: 94-98.

[90] Somers C, Mortazavi A, Hwang Y, Radermacher R, Rodgers P, Al-Hashimi S. Modeling water/lithium bromide absorption chillers in ASPEN Plus. Applied Energy 2011; 88: 4197–4205.

[91] Cascales JRG, García FV, Izquierdo JMC, Marín JPD, Sánchez RM. Modeling an absorption system assisted by solar energy. Applied Thermal Engineering 2011; 31: 112-118.

[92] F. Calise, M. Dentice d'Accadia, A. Palombo, Transient analysis and energy optimization of solar heating and cooling systems in various configurations. Solar Energy 84 (2010) 432-449

[93] Ortiz M, Barsun H, He H, Vorobieff P, Mammoli A. Modeling of a solar assisted HVAC system with thermal storage. Energy and Buildings 2010; 42: 500–509.

[94] Eicker U, Pietruschka D, Pesch R. Heat rejection and primary energy efficiency of solar driven absorption cooling systems. International Journal of Refrigeration 2012; 35: 729-738.

[95] A. González-Gil, M. Izquierdo, J.D. Marcos E. Palacios. Experimental evaluation of a direct air-cooled lithium bromide-water absorption prototype for solar air conditioning. Applied Thermal Engineering 31 (2011) 3358-3368.

[96] B. Zalba, J. Marın, L. F. Cabeza, H. Mehling. Review on thermal energy storage with phase change: materials, heat transfer analysis and applications. Applied Thermal Engineering, vol.23, pp. 251–283, 2003.

[97] A. Koca, H. F. Oztopb, T. Koyunc, Y. Varola. Energy and exergy analysis of a latent heat storage system with phase change material for a solar collector. Renewable Energy, vol. 33, pp. 567 – 574, 2008.

[98] P. Patrice, A.C. Cynthia, B.M. Ian, W. Adam. A review of available methods for seasonal storage of solar thermal energy in residential applications. Renewable Sustainable Energy Reviews 15 (2011), 3341-3359.

[99] L.A. Chidambaram, A.S. Ramana, G. Kamaraj, R. Velraj. Review of solar cooling methods and thermal storage options. Renewable and Sustainable Energy Reviews 15 (2011) 3220– 3228.

[100] Li ZF, Sumathy K. Experimental studies on a solar powered air conditioning system with partitioned hot water storage tank. Sol Energy 2001; 71(5):285–97.

[101] R. Salgado, P. Rodríguez, M. Venegas, A. Lecuona, M.C. Rodríguez. Optimized Design of Hot Water Storage in Solar Thermal Cooling Facilities. 5th European Thermal-Sciences Conference, the Netherlands, 2008.

[102] Ching-Jen Tang, William Gerstler, A Lithium Bromide Absorption Chiller with Cold Storage. Proceedings of the 11th International Sorption Heat Pump Conference (ISHPC11) held in Padua, Italy, on April 6-8, 2011 http://www.iifiir.org/.

[103] Renato M. Lazzarin, Solar Cooling Plants: How to Arrange Solar Collectors, Absorption Chillers and the Load. 61st ATI National Congress –International Session "Solar Heating and Cooling.

[104] Ahmed Hamza H. Ali, Peter Noeres, Clemens Pollerberg. Performance assessment of an integrated free cooling and solar powered single-effect lithium bromide-water absorption chiller. Solar Energy 82 (2008) 1021–1030.

[105] Syed A.M. Said, Maged A.I. El-Shaarawi, Muhammad U. Siddiqui. Alternative designs for a 24-h operating solar-powered absorption refrigeration technology. International Journal of Refrigeration 35 (2012) 1967-1977.

[106] A.A. Al-Ugla, M.A.I. El-Shaarawi, S.A.M. Said. Alternative Designs for a 24-Hours Operating Solar-Powered LiBr-Water Absorption Air-conditioning Technology. International Journal of Refrigeration (2015), 90-100.

[107] M.A.I. El-Shaarawi, S.A.M. Said, F.R. Siddiqui. Hybrid storage absorption refrigeration system. US Patent # US 8,881,539 BI (2014).

[108] M.A.I. El-Shaarawi, S.A.M. Said, F.R. Siddiqui. Unsteady thermodynamics analysis for a solar driven dual storage absorption refrigeration cycle in Saudi Arabia. Solar Energy 110 (2014), 268-302.

[109] Adnan Sozen, Duran Altıparmak, Huseyin Usta. Development and testing of a prototype of absorption heat pump system operated by solar energy. Applied Thermal Engineering 22 (2002) 1847–1859.

[110] A. Pongtornkulpanich, S. Thepa, M. Amornkitbamrung, C. Butcher. Experience with fully operational solar-driven 10-ton LiBr/H_2O single-effect absorption cooling system in Thailand. Renewable Energy 33 (2008) 943–949.

[111] Sumathy K, Huang ZC, Li ZF. Solar absorption cooling with low grade heat source - A strategy of development in south china. Solar Energy 2002; 72(2):155-165.

[112] A. Syed, M. Izquierdo, P. Rodrı´guez, G. Maidment, J. Missenden, A. Lecuona, R. Tozer. A novel experimental investigation of a solar cooling system in Madrid. International Journal of Refrigeration 28 (2005) 859-871.

[113] M. Izquierdo, R. Lizarte, J.D. Marcos, G. Gutierrez. Air conditioning using an air-cooled single effect lithium bromide absorption chiller: Results of a trial

conducted in Madrid in August 2005. Applied Thermal Engineering 28 (2008) 1074–1081.

[114] Agyenim F, Knight I, Rhodes M. Design and experimental testing of the performance of an outdoor LiBr/H_2O solar thermal absorption cooling system with a cold store. Solar Energy 2010; 84 (5):735–44.

[115] T. Berlitz, N. Lemke, P. Satzger and F. Ziegler. Cooling Machine with Integrated Cold Storage. International Journal of Refrigeration 21:2 (98) 157-161.

[116] Hu JS, Chao CYH. Study of a micro absorption heat pump system. International Journal of Refrigeration 2008; 31: 1198-1206.

[117] Bermejo P, Pino FJ, Rosa F. Solar absorption cooling plant in Seville. Solar Energy 2010; 84: 1503–1512.

[118] M.C. Rodrı´guez Hidalgo, P. Rodrı´guez Aumente, M. Izquierdo Milla´n, A. Lecuona Neumann, R. Salgado Mangual. Energy and carbon emission savings in Spanish housing air-conditioning using solar driven absorption system. Applied Thermal Engineering 28 (2008) 1734–1744

[119] R. Salgado Mangual, P. Rodriguez Aumente, M. Izquierdo Millán, A. Lecuona Nuemann. Experimental Analysis of Thermal Storage Tank Configuration in a Solar Cooling Installation with an Absorption Chiller. 61st ATI National Congress –International Session “Solar Heating and Cooling”.

[120] Sabina Rosiek, Francisco Javier Batlles Garrido. Performance evaluation of solar-assisted air-conditioning system with chilled water storage (CIESOL building). Energy Conversion and Management 55 (2012) 81–92.

[121] Darkwa J, Fraser S, Chow DHC. Theoretical and practical analysis of an integrated solar hot water-powered absorption cooling system. Energy 2012; 39: 395-402.

[122] J.D. Marcos, M. Izquierdo, D. Parra. Solar space heating and cooling for Spanish housing: Potential energy savings and emissions reduction, Solar Energy 85 (2011) 2622-2641.

[123] Jafaar Awni Hajibrahim, Load and Energy Analysis of a Commercial Building. Master Thesis 2012, King Fahad University of Petroleum & Minerals (KFUPM), Dhahran, Saudi Arabia.

[124] S.M. Shaahid, M.A. Elhadidy. Technical and economic assessment of grid-independent hybrid photovoltaic-diesel-battery power systems for commercial loads in desert Environments. Renew. Sustain. Energy Rev. 11 (2007), 1794-1810.

[125] Intelligent Energy-Europe IEE program. Solar Cooling Overview and Recommendations. www.solcoproject.net.

[126] F. A. Al-Sulaiman and B. Ismail. Estimation of monthly average daily and hourly solar radiation impinging on a sloped surface using the isotropic sky model for Dhahran, Saudi Arabia, Renewable Energy, Vol. 11, No. 2, pp. 257 262, 1997.

[127] Maged A.I. El-Shaarawi, Hussain Al Awjan1, Dawood Al Ramadhan, Mustafa Hussain. Effect of thermodynamic limitations on PV initial cost estimations for solar-powered RO desalination. Desalination 276 (2011) 28–37.

[128] Alantech Solar. www.atlantechsolar.com/sizing_photovoltaic_solar_power_system_array.html Last accessed May 2014.

[129] John A. Duffie, William A. Beckman. Solar Engineering of Thermal Process Textbook-Chapter 11, Third Edition, 2006.

[130] Electricity & Cogeneration Regulatory Authority. Approved Electricity Tariff (ECRA Board of Directors Decision (1/22/31) dated 01/06/1431 AH).www.ecra.gov.sa, Last accessed May 2014.

[131] www.solarwirtschaft.de/fileadmin/media/pdf/BSW_facts_solarpower_en.pdf. Last accessed May 2014.

[132] Saudi Arabia Economy Profile 2012. www.indexmundi.com/saudi_arabia/economy _profile. Last accessed May 2014.

[133] http://www.tradingeconomics.com/saudi-arabia/inflation-cpi. Last accessed May 2014.

[134] SACE. Solar Air Conditioning in Europe: Final Report. EC project (2003) NNE5/2001/25.

[135] S.L. Grassie, N.R. Sheridan. Modeling of a solar-powered absorption air-conditioning system with refrigerant storage. Solar Energy 19 (1997), 691-700.

[136] W. F. Stoecker, J. W. Jones. Refrigeration and Air Conditioning. McGraw-Hill Book Company, (1982) Second Edition.

[137] M.M. Talbi, B. Agnew, "Exergy analysis: an absorption refrigerator using lithium bromide and water as the working fluids," Applied Thermal Engineering, Volume 20, Issue 7, May 2000, Pages 619-630.

[138] Y.A. Cengel, M.A. Boles. Thermodynamics: An Engineering Approach. McGraw-Hill. (2006) Fifth Edition.

[139] Electricity & Cogeneration Regulatory Authority, Activities and Achievements of the Authority 2009.www.ecra.gov.sa, Last accessed May 2014.

[140] King Abdullah City for Atomic and Renewable Energy, As part of the Renewable Resource Monitoring and Mapping (RRMM) Program, 2014. http://rratlas.kacare.gov.sa.

[141] Center for Engineering Research, Research Institute, King Fahd University of Petroleum and Minerals (KFUPM), 2012.

Vitae

Name	Ali Abdulaziz Al-Ugla
Nationality	Saudi Arabia
Date of Birth	September 8, 1976
Email	ali.ugla@aramco.com
Address	PO 13133, Dhahran 31311, Saudi Arabia
Academic Background	MS Mechanical Engineering (2007) KFUPM - Saudi Arabia
	BS Mechanical Engineering (1999) KFUPM - Saudi Arabia

Publications

1. M. A. I. El-Shaarawi ***and A. A. Al-Ugla***. Transient Moment to Rotate Inner Walls of Vertical Concentric Annuli in the Natural Convection Regime. International Journal of Numerical Methods for Heat and Fluid Flow 2009, 19 (2), 201 - 222.
2. ***A. A. Al-Ugla,*** Maged A. I. El-Shaarawi, Syed Mohammad Said. Alternative Designs for a 24-Hours Operating Solar-Powered LiBr-Water Absorption Air-conditioning Technology. International Journal of Refrigeration 2015 (53), 90-100.
3. ***A. A. Al-Ugla,*** M. A. I. El-Shaarawi, S. A. M. Said, A. M. Al-Qutub. Techno-economic Analysis of Solar-Assisted Air-conditioning Systems for Commercial Buildings in Saudi Arabia. Renewable and Sustainable Energy Reviews Journal 2016, 1301-1310.

4. M. A. I. El-Shaarawi ***and A. A. Al-Ugla***. Hybrid Storage Designs for Continuous Operation of Solar-Powered LiBr-Water Absorption Air-conditioning. Accepted for publication in International Journal of Energy Research.
5. ***A. A. Al-Ugla*** and Maged A. I. El-Shaarawi. Solar Air-conditioning Designs for Residential Buildings in Saudi Arabia. Journal of Energy Challenges and Machines. Accepted for publication based on the conference paper.
6. M. A. I. El-Shaarawi ***and A. A. Al-Ugla***. Unsteady Analysis for Solar-Powered Hybrid Storage LiBr-Water Absorption Air-conditioning. Submitted in Solar Energy Journal.

Conference

1. ***A. A. Al-Ugla*** and Maged A. I. El-Shaarawi. Solar Air-conditioning Designs for Residential Buildings in Saudi Arabia. Delivered a Speech in the 3rd International Symposium on Energy Challenges and Mechanics (ECM3) - towards a big picture, July7-9, 2015, Aberdeen, UK.

Patent

1. M. A. I. El-Shaarawi, Syed Mohammad Said, ***A. A. Al-Ugla***. SYSTEM AND METHOD FOR CONTINUOUSLY OPERATING A SOLAR-POWERED AIR CONDITIONER. Accepted for USPO filing.
2. M. A. I. El-Shaarawi ***and A. A. Al-Ugla***. SOLAR-POWERED LIBR-WATER ABSORPTION AIR CONDITIONING SYSTEM USING HYBRID STORAGE. Accepted for USPO filing.

3. M. A. I. El-Shaarawi and ***A. A. Al-Ugla.*** Crystallization Prevention in Continuous Operation of Solar Cooling System. Submitted for KFUPM Intellectual Asset Office processing.